



THE ENCOUNTER BAY GRANITES, SOUTH AUSTRALIA,
AND THEIR ENVIRONMENT

by

ANTHONY RICHARD MILNES

B.Sc.(Hons) Adelaide

Submitted for Ph.D.

in the

Department of Geology and Mineralogy

at

The University of Adelaide,

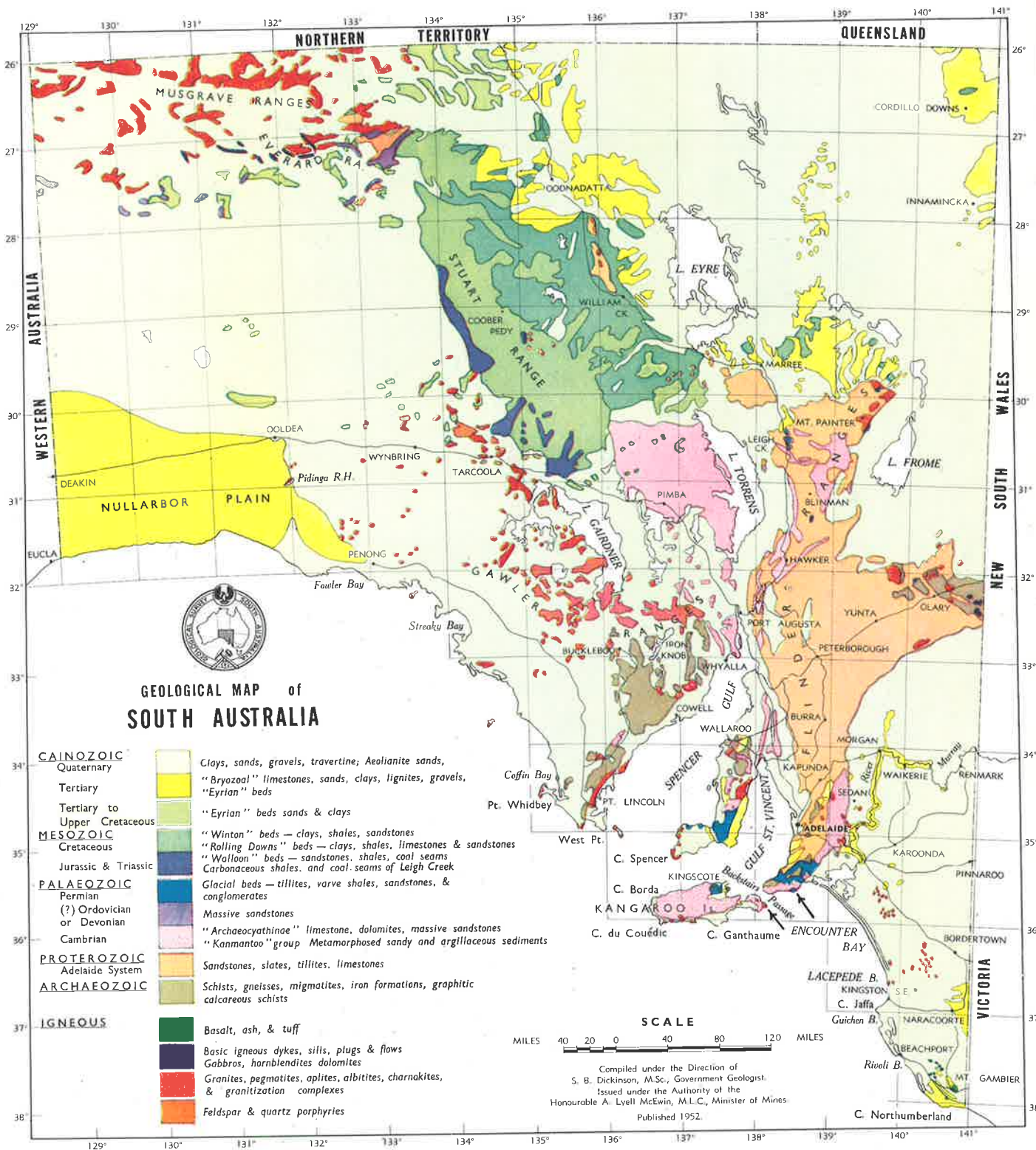
South Australia

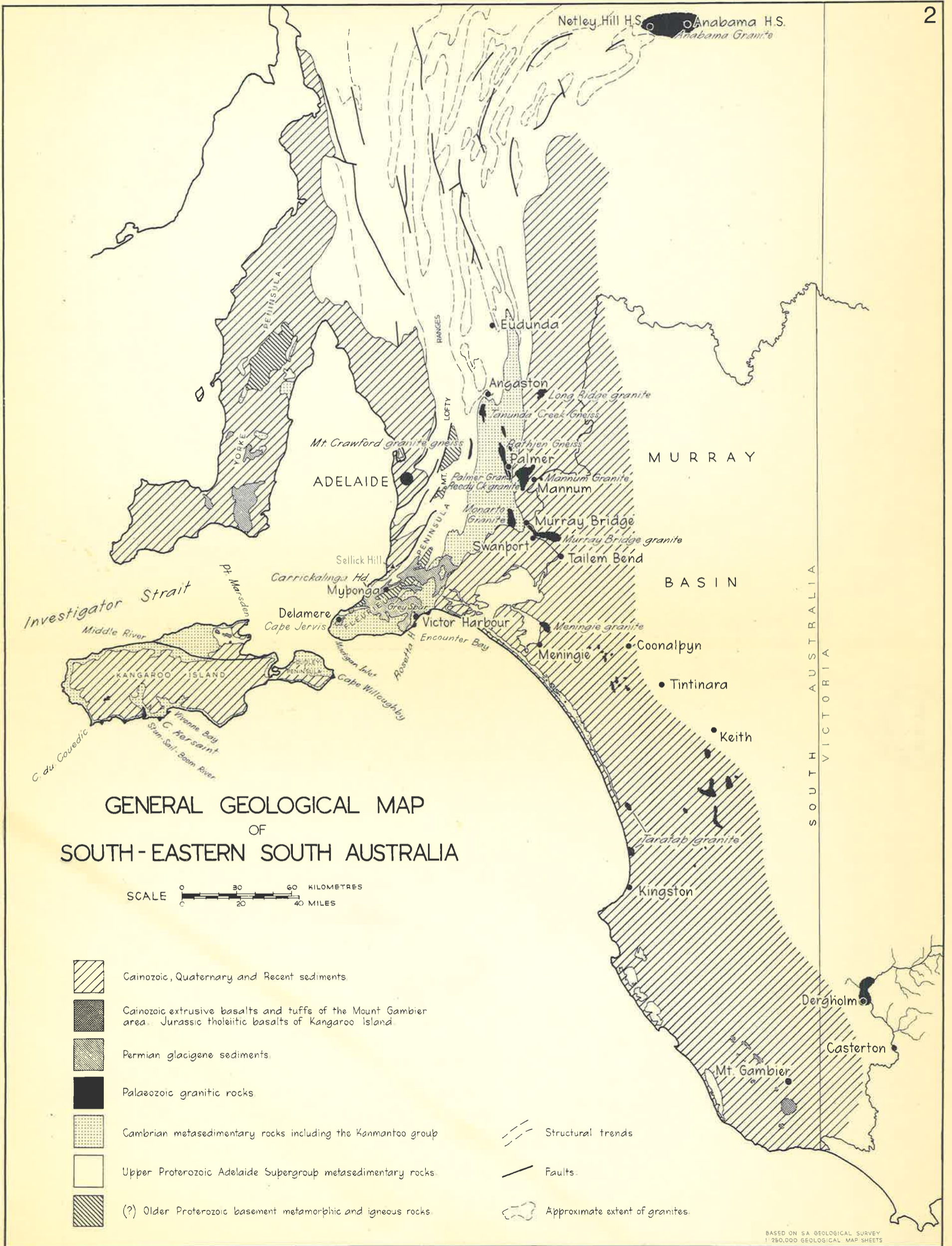
April, 1973

FIGURES

FIGURE 1

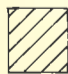
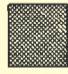


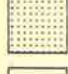
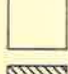

Simplified geological map of South Australia.








GENERAL GEOLOGICAL MAP
OF
SOUTH-EASTERN SOUTH AUSTRALIA

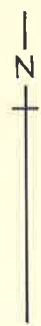
SCALE 0 30 60 KILOMETRES
0 20 40 MILES

-  Cainozoic, Quaternary and Recent sediments
-  Cainozoic extrusive basalts and tuffs of the Mount Gambier area. Jurassic tholeiitic basalts of Kangaroo Island
-  Permian glaciogene sediments
-  Palaeozoic granitic rocks
-  Cambrian metasedimentary rocks including the Kanmantoo group
-  Upper Proterozoic Adelaide Supergroup metasedimentary rocks
-  (?) Older Proterozoic basement metamorphic and igneous rocks

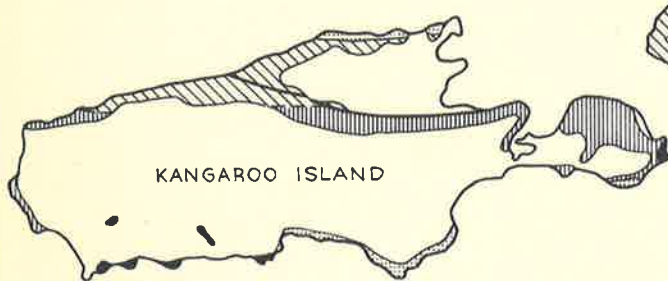
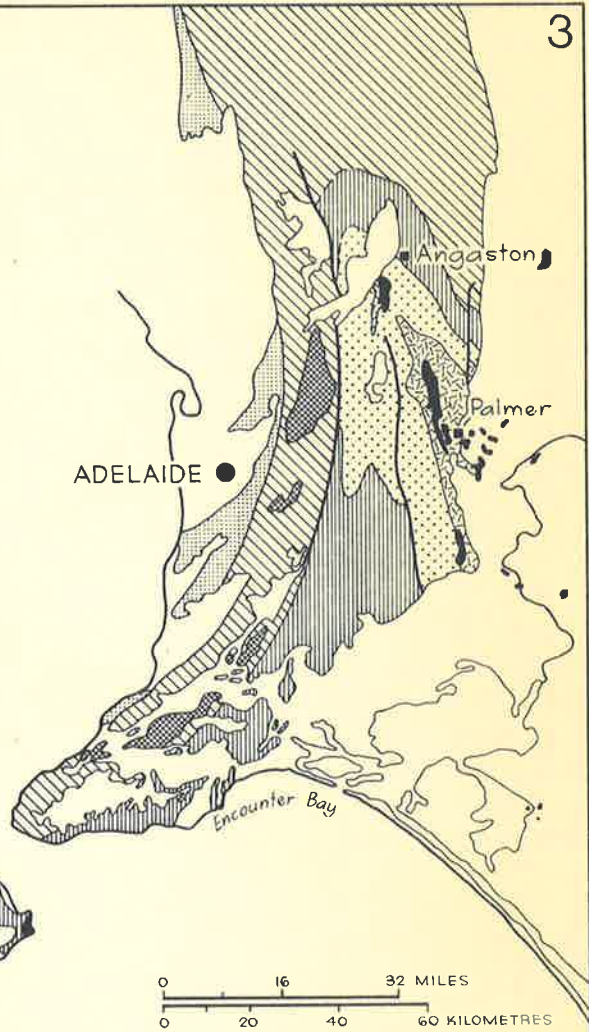
-  Structural trends
-  Faults
-  Approximate extent of granites

BASED ON SA GEOLOGICAL SURVEY
1:250,000 GEOLOGICAL MAP SHEETS

-  CHLORITE ZONE
-  BIOTITE ZONE
-  ANDALUSITE - STAUROLITE ZONE
-  SILLIMANITE ZONE
-  MIGMATITE
-  GRANITE, GRANITE GNEISS
-  L. PRECAMBRIAN



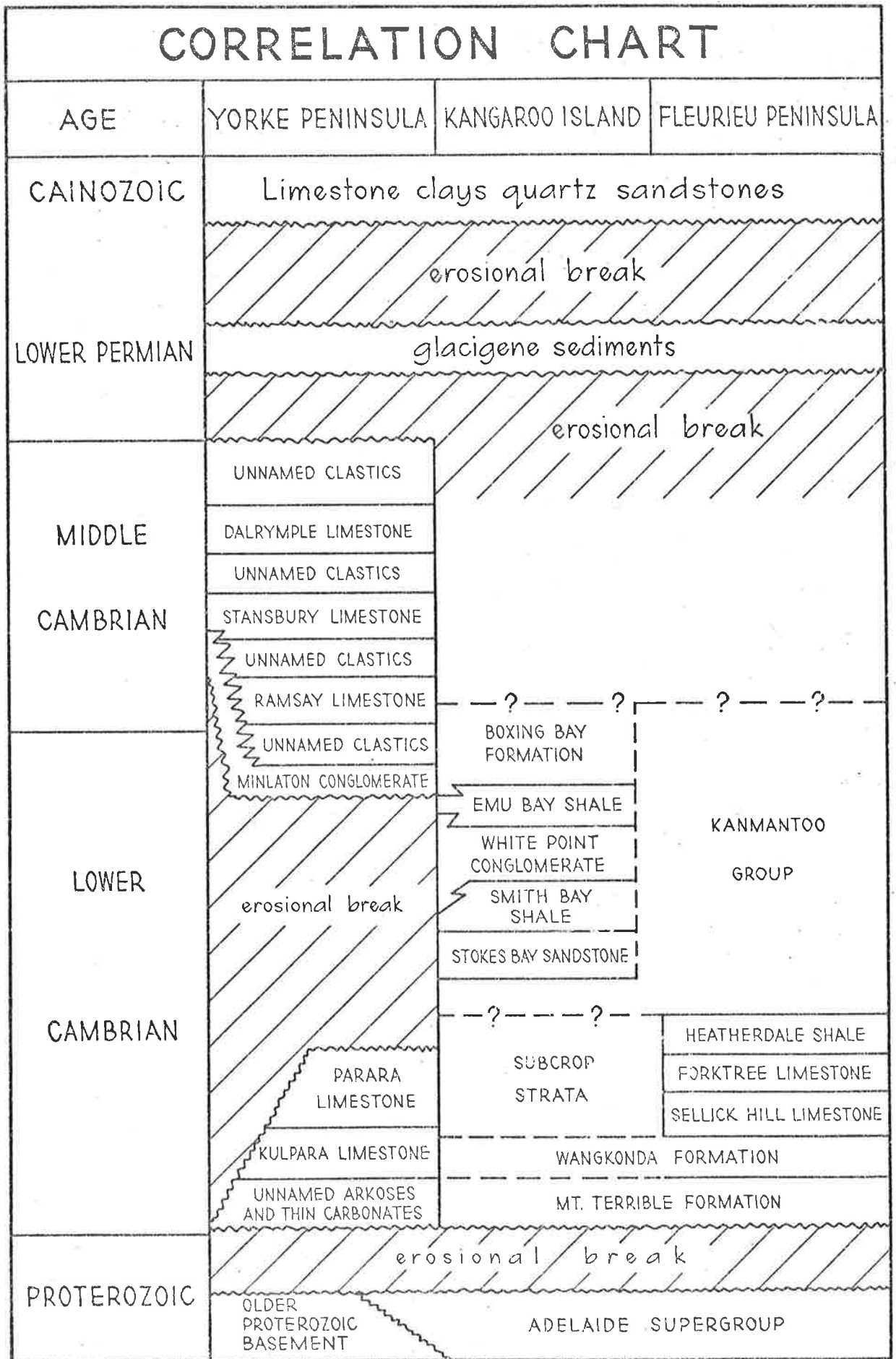
METAMORPHIC ZONES IN THE MOUNT LOFTY RANGES



AFTER OFFLER AND FLEMING (1968)

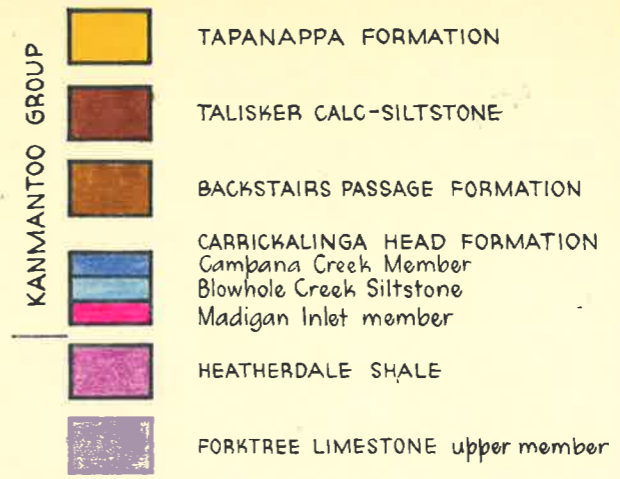
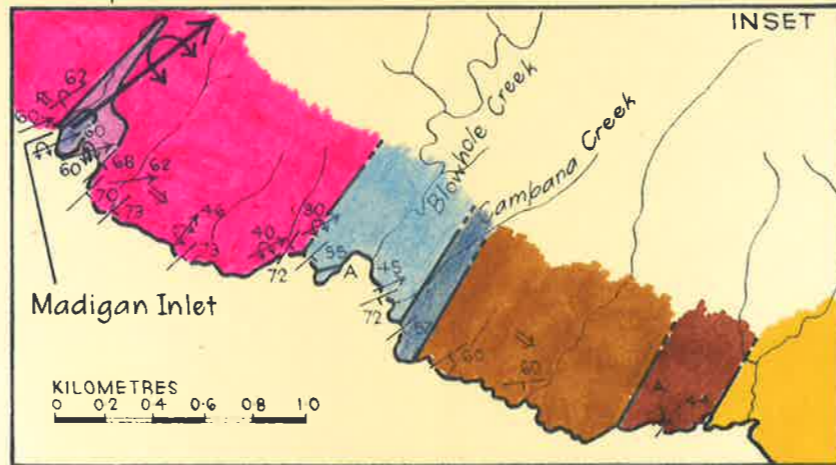
FIGURE 4

Chart showing the stratigraphic relationships of Cambrian sequences on Fleurieu Peninsula, Kangaroo Island, and Yorke Peninsula (after Stuart and von Sanden, 1972).



AFTER STUART AND VON SANDEN (1972)

GEOLOGY OF THE SOUTHERN COAST OF FLEURIEU PENINSULA CAMPBELL CREEK TO TUNKALILLA BEACH



- L₁ Lineation L₁' Lineation
- Fold axis - only anticlinal axes shown.
- Bedding
- Facing
- Amphibolite dyke
- Conglomerates

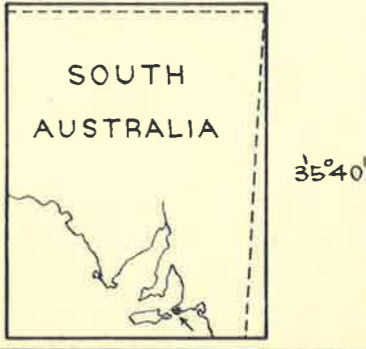
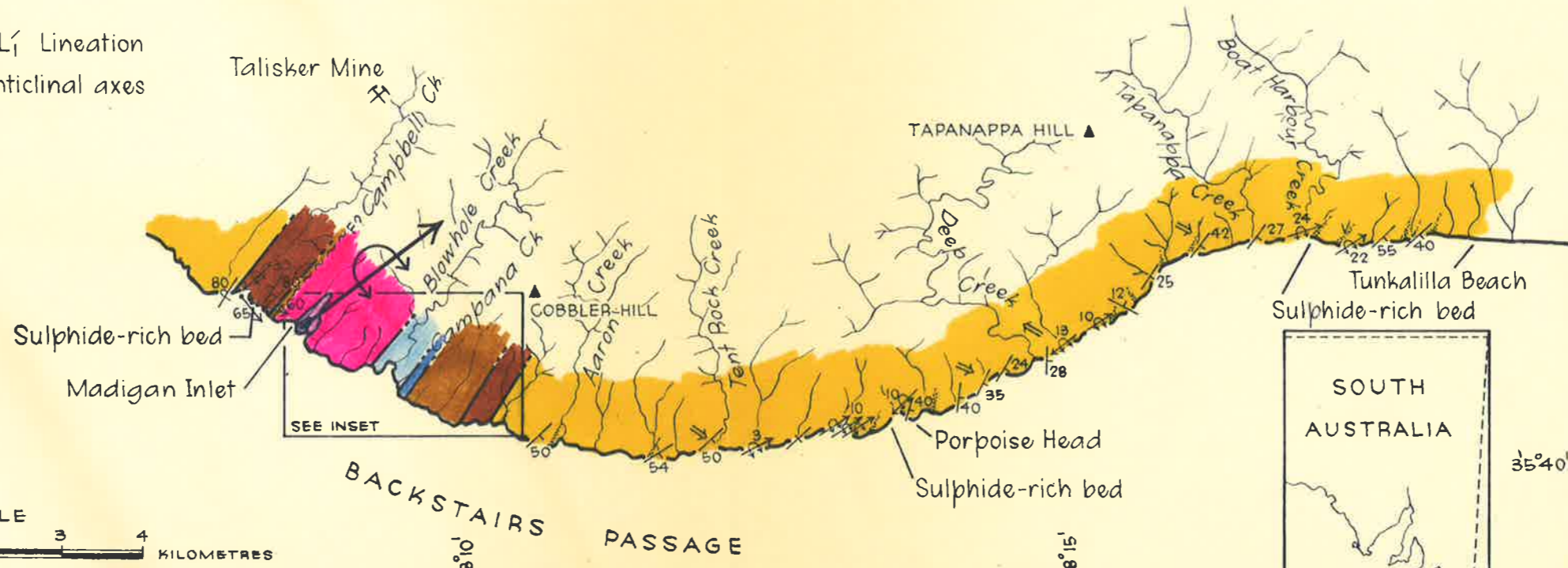


FIGURE 5

Based on JERVIS 1:63,360 sheet, Geological Surv S. Aust.

138°15'

138°20'

138°25'

GEOLOGY

OF THE

SOUTHERN COAST

OF

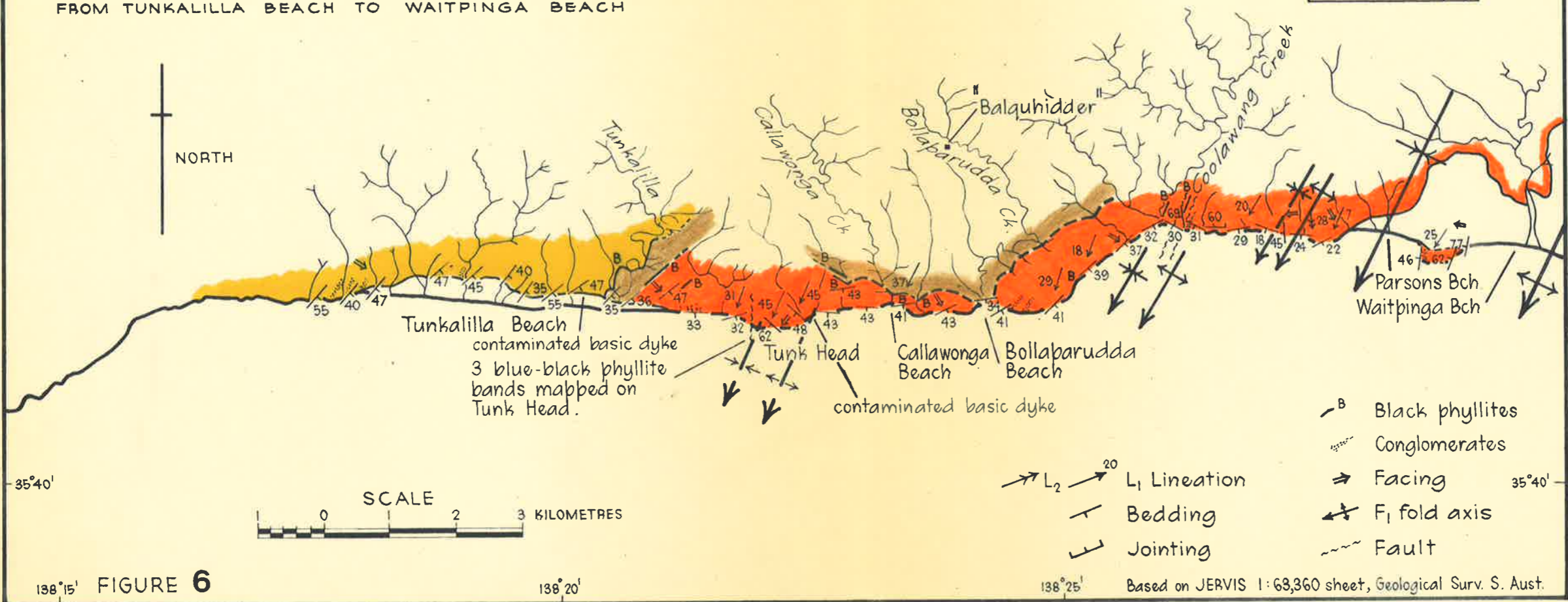
FLEURIEU PENINSULA

FROM TUNKALILLA BEACH TO WAITPINGA BEACH

KANMANTOO GROUP
INMAN HILL
SUB-GROUP



BALQUHIDDER FORMATION
TUNKALILLA FORMATION
TAPANAPPA FORMATION



Tunkalilla Beach
contaminated basic dyke
3 blue-black phyllite
bands mapped on
Tunk Head.

contaminated basic dyke

B Black phyllites

Conglomerates

Facing

F₁ fold axis

Fault

L₂ L₁ Lineation

Bedding

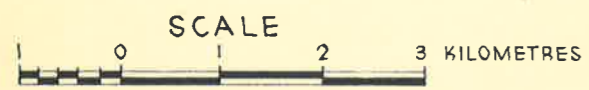
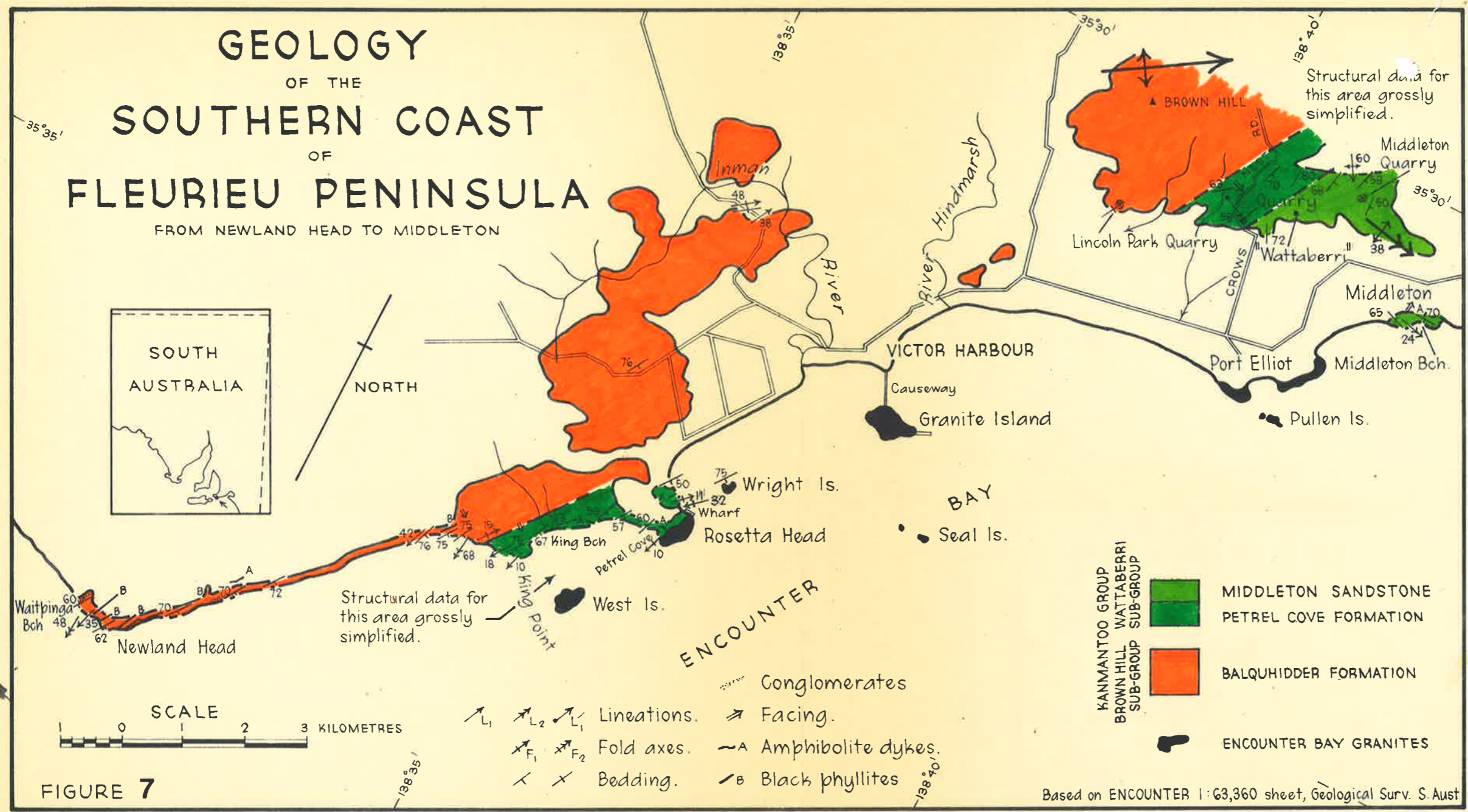
Jointing

SCALE
0 1 2 3 KILOMETRES

FIGURE 6

Based on JERVIS 1:63,360 sheet, Geological Surv. S. Aust.

GEOLOGY OF THE SOUTHERN COAST OF FLEURIEU PENINSULA FROM NEWLAND HEAD TO MIDDLETON



- L_1 L_2 L_1 Lineations.
- F_1 F_2 Fold axes.
- \times \times Bedding.
- \Rightarrow Facing.
- $-A$ Amphibolite dykes.
- $-B$ Black phyllites
- \dots Conglomerates

- KANMANTOO GROUP
- BROWN HILL WATABERRI SUB-GROUP
- MIDDLETON SANDSTONE
- PETREL COVE FORMATION
- BALQUHIDDER FORMATION
- ENCOUNTER BAY GRANITES

FIGURE 7

Based on ENCOUNTER 1:63,360 sheet, Geological Surv. S. Aust

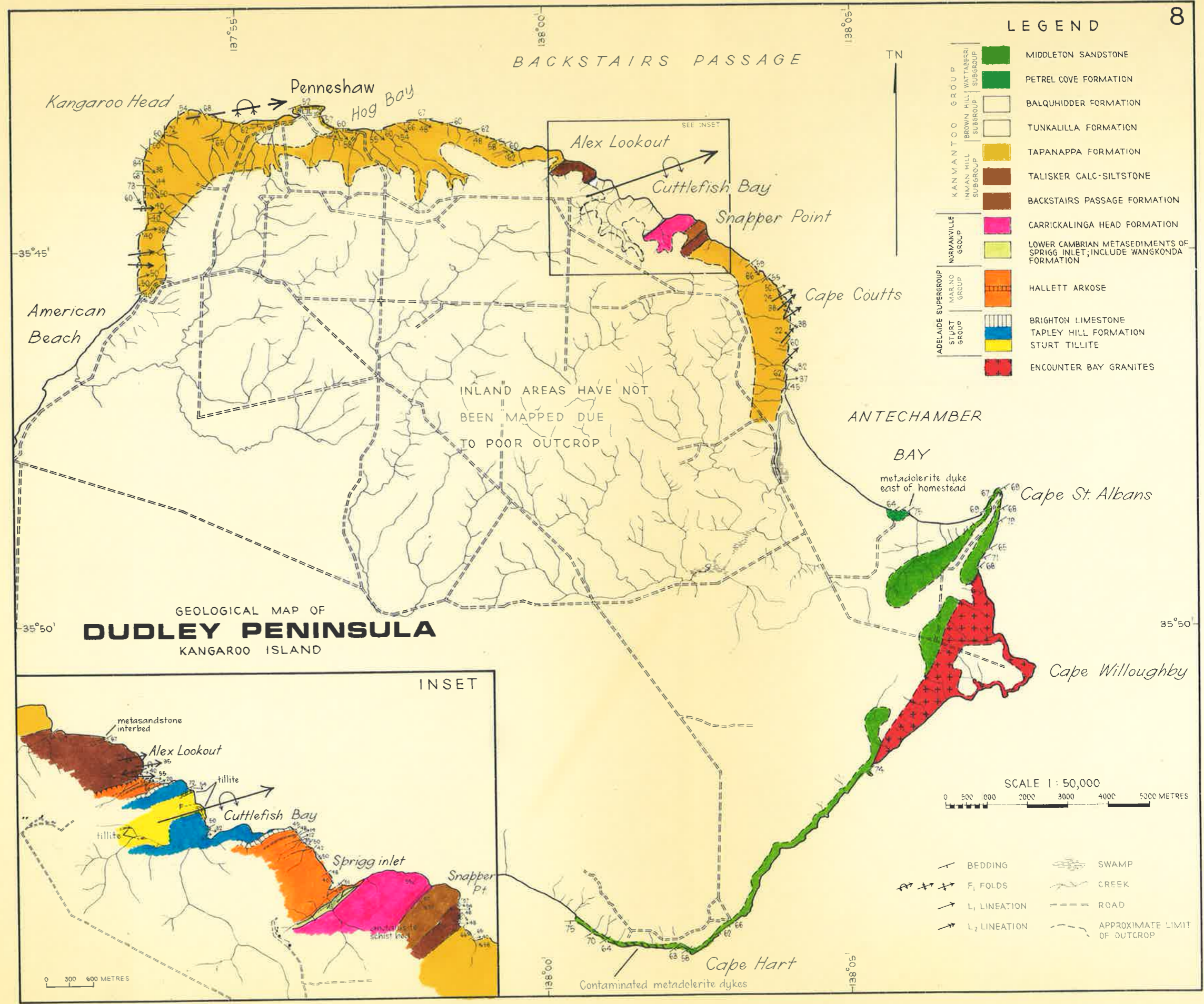
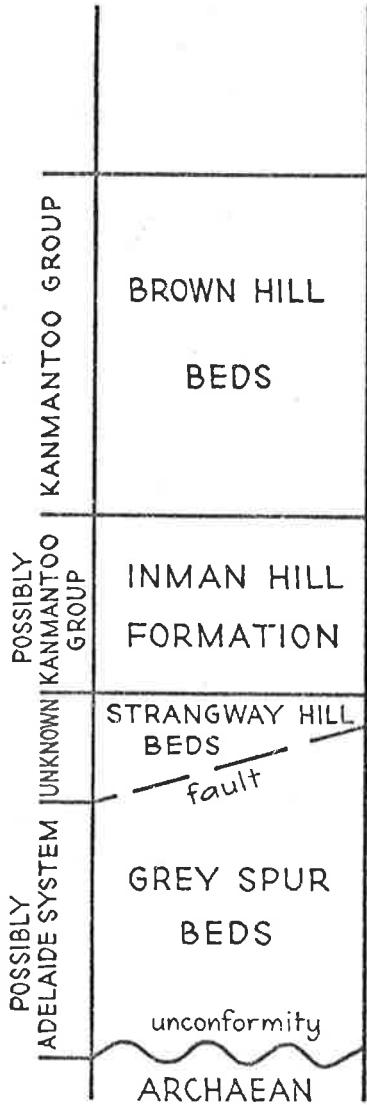


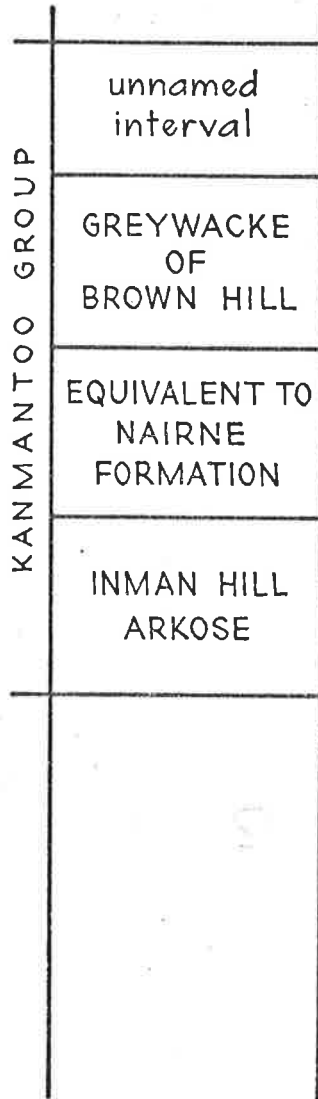
FIGURE 9

Chart showing the schemes of stratigraphic nomenclature applied to the Kanmantoo Group in its type section along the southern coastline of Fleurieu Peninsula.

FORBES
(1957)
Section from Grey
Spur to Port Elliot



CRAWFORD & THOMSON
(1959)
ENCOUNTER 1:63,000
Geological sheet



THOMSON & HORWITZ
(1962)
BARKER 1:250,000
Geological sheet

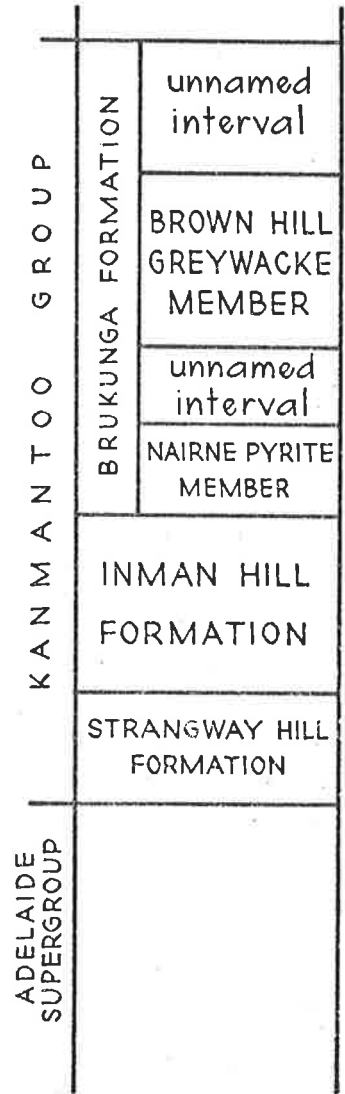
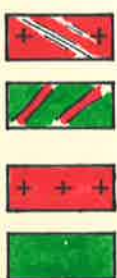
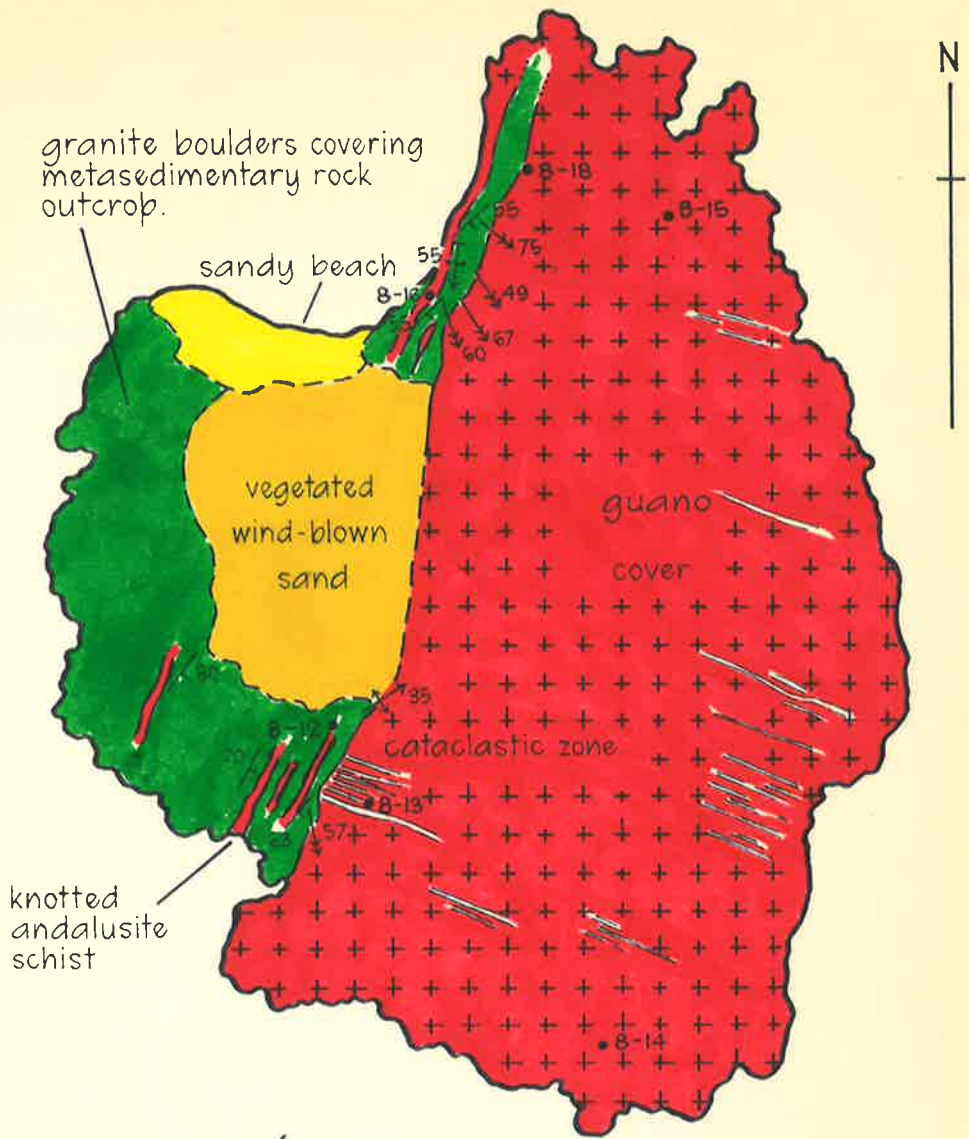


FIGURE 10

Chart showing the stratigraphic subdivision of the Kamantoo Group proposed by Daily and Milnes (1972b).

K A N M A N T O O G R O U P	WATTABERRI SUBGROUP	MIDDLETON SANDSTONE
		PETREL COVE FORMATION
	BROWN HILL SUBGROUP	BALQUHIDDER FORMATION
		TUNKALILLA FORMATION
	INMAN HILL SUBGROUP	TAPANAPPA FORMATION
		TALISKER CALC - SILTSTONE
		BACKSTAIRS PASSAGE FORMATION
	CARRICKALINGA HEAD FORMATION	Cambana Creek Member
		Blowhole Creek Siltstone Member
		Madigan Inlet Member
	HEATHERDALE SHALE	unnamed upper member
		unnamed lower member
	FORKTREE LIMESTONE	unnamed upper member

GEOLOGICAL MAP OF
WRIGHT ISLAND
 ENCOUNTER BAY



ALBITISED MEGACRYSTIC GRANITE.

MEGACRYSTIC GRANITE SHEETS BROADLY CONCORDANT WITH BEDDING IN METASEDIMENTS.

MAIN MASS OF BORDER FACIES MEGACRYSTIC GRANITE.

PETREL COVE FORMATION METASEDIMENTS.

• 8-12 SAMPLE LOCALITY

F₁ FOLD

FOLD OF UNKNOWN AGE

BEDDING

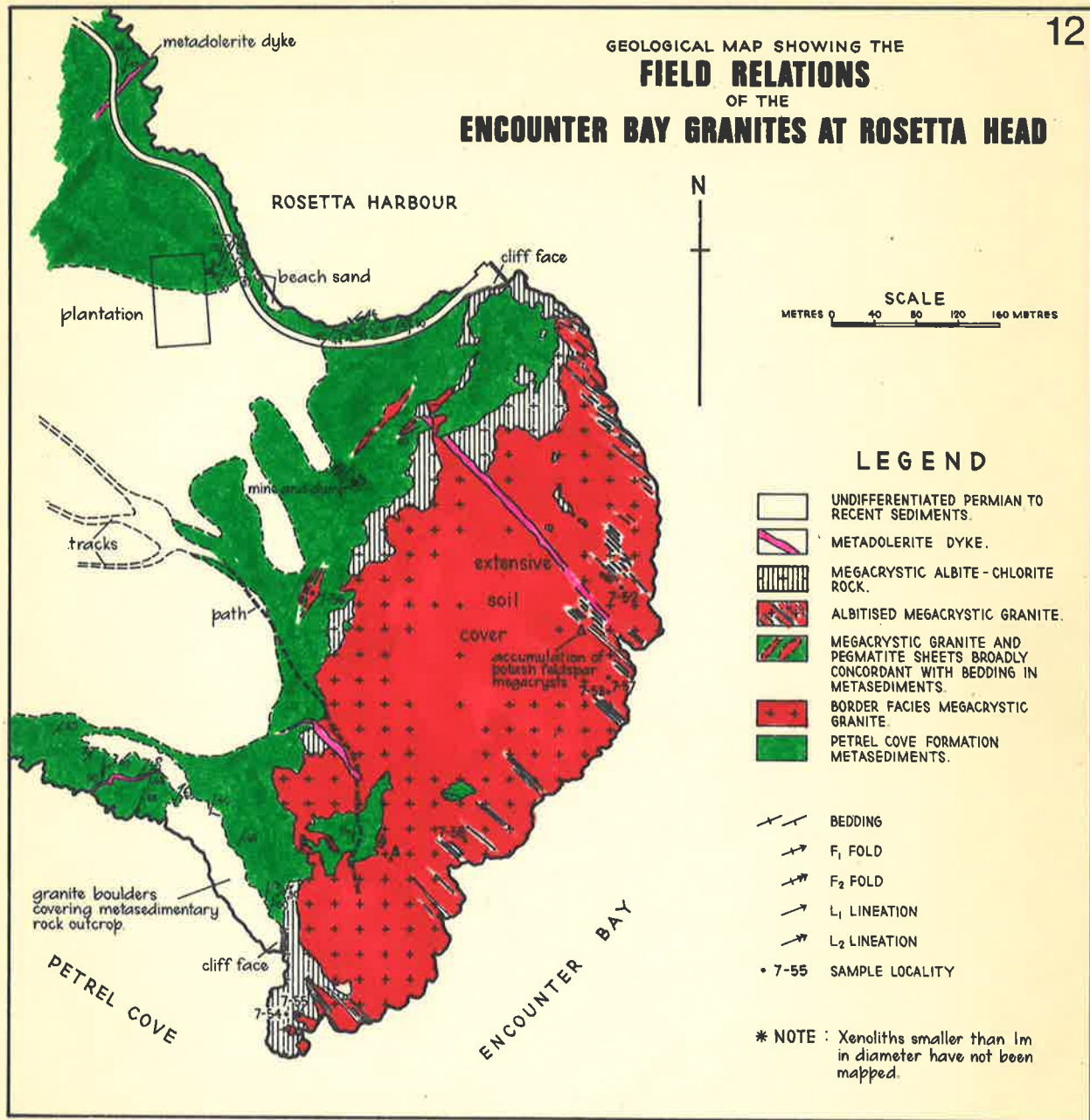
L₁ LINEATION

L₂ LINEATION

* NOTE : XENOLITHS IN THE BORDER FACIES MEGACRYSTIC GRANITE ARE LESS THAN 1m IN DIAMETER AND HAVE NOT BEEN MAPPED.



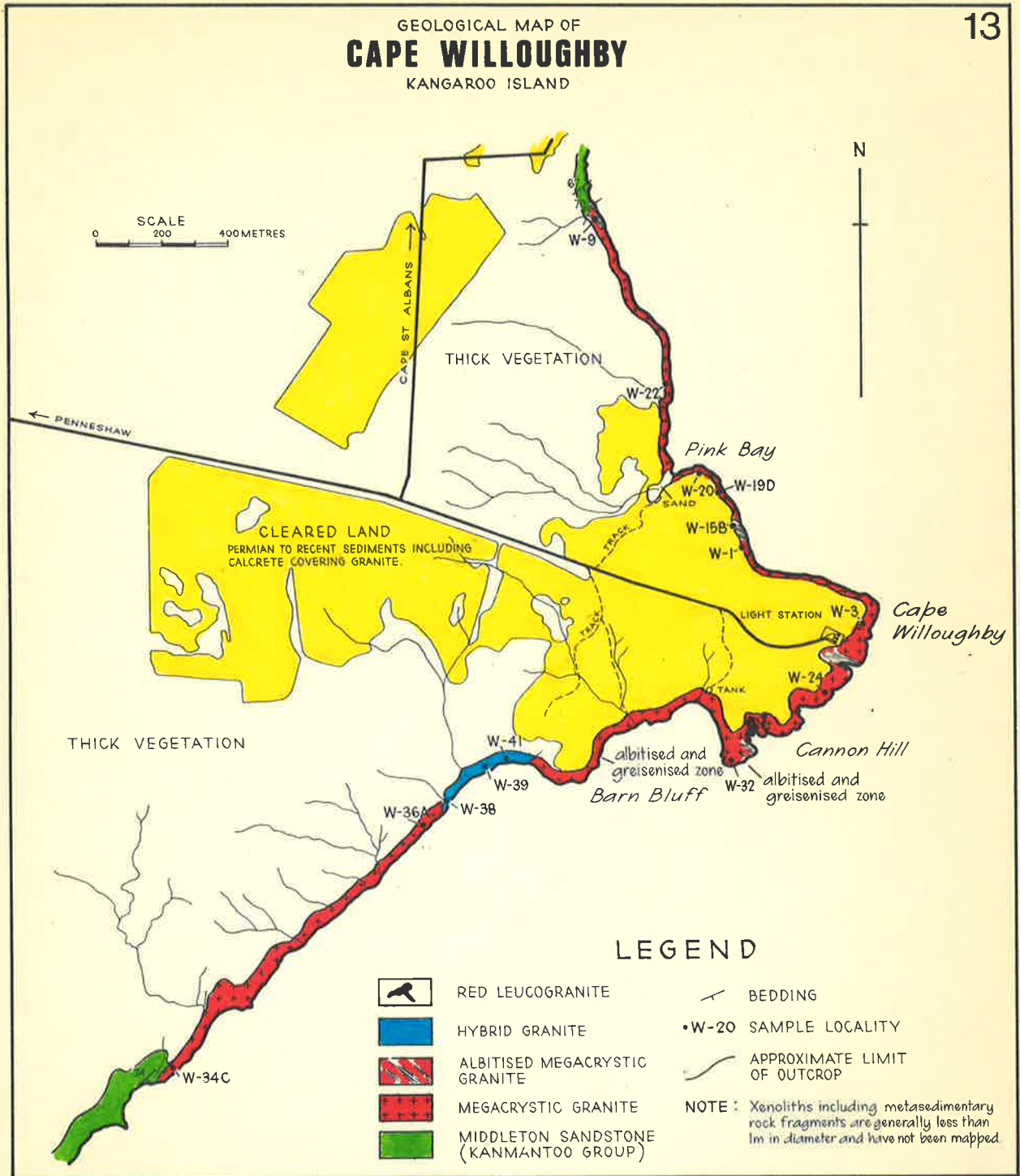
GEOLOGICAL MAP SHOWING THE
FIELD RELATIONS
 OF THE
ENCOUNTER BAY GRANITES AT ROSETTA HEAD



- LEGEND**
- UNDIFFERENTIATED PERMIAN TO RECENT SEDIMENTS.
 - METADOLERITE DYKE.
 - MEGACRYSTIC ALBITE-CHLORITE ROCK.
 - ALBITISED MEGACRYSTIC GRANITE.
 - MEGACRYSTIC GRANITE AND PEGMATITE SHEETS BROADLY CONCORDANT WITH BEDDING IN METASEDIMENTS.
 - BORDER FACIES MEGACRYSTIC GRANITE.
 - PETREL COVE FORMATION METASEDIMENTS.
 - BEDDING
 - F₁ FOLD
 - F₂ FOLD
 - L₁ LINEATION
 - L₂ LINEATION
 - 7-55 SAMPLE LOCALITY

* NOTE : Xenoliths smaller than 1m in diameter have not been mapped.

GEOLOGICAL MAP OF
CAPE WILLOUGHBY
KANGAROO ISLAND



LEGEND

- | | | | |
|--|---------------------------------------|--|------------------------------|
| | RED LEUCOGRANITE | | BEDDING |
| | HYBRID GRANITE | | •W-20 SAMPLE LOCALITY |
| | ALBITISED MEGACRYSTIC GRANITE | | APPROXIMATE LIMIT OF OUTCROP |
| | MEGACRYSTIC GRANITE | | |
| | MIDDLETON SANDSTONE (KANMANTOO GROUP) | | |

NOTE: Xenoliths including metasedimentary rock fragments are generally less than 1m in diameter and have not been mapped.

FIGURE 14

- a. Table showing the relationships of structural elements in Kammantoo Group metasedimentary rocks along the southern coastline of Fleurieu Peninsula, and in the Encounter Bay area.
- b. Equal-area projection of structural elements measured in Kammantoo Group metasedimentary rocks along the southern coastline of Fleurieu Peninsula between Campbell Creek and Tunkalilla Beach.

FOLD PHASE	PLANAR ELEMENT	LINEAR ELEMENT
	S = surface	
	S ₀ = bedding	
First generation structures		
F ₁	S ₁ = schistosity	L ₁ = lination or axis of fold in S ₀ with S ₁ as axial surface
		L ₁ ' = mineral elongation in S ₁
Second generation structures		
F ₂	S ₂ = crenulation cleavage. Axial surface to F ₂ folds.	L ₂ = lination or axis of fold or crenulation in S ₀ or S ₁ with S ₂ as axial surface
β represents estimated direction and plunge of fold axis.		

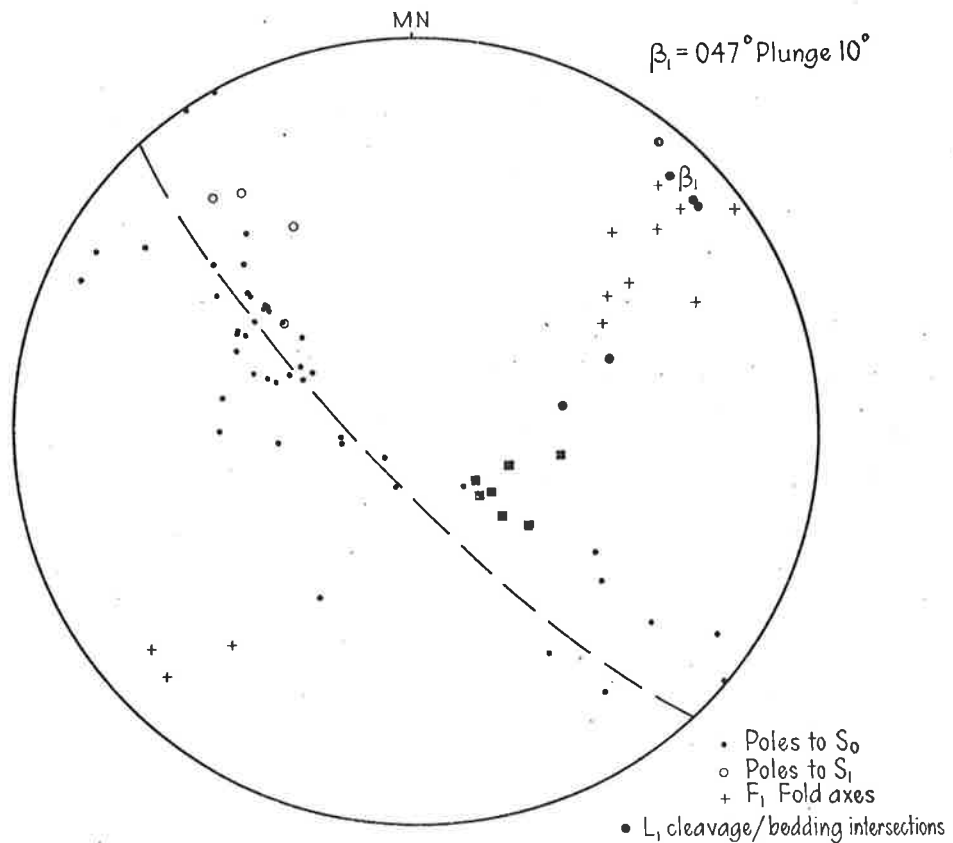


FIGURE 15

Equal-area projections of structural elements in Kanmantoo Group meta-sedimentary rocks along the southern coastline of Fleurieu Peninsula, and in the Encounter Bay area.

- a, b, c and d - the section from Tunkalilla Beach to Rosetta Head.
- e - the Brown Hill area.
- f - the Middleton quarry.

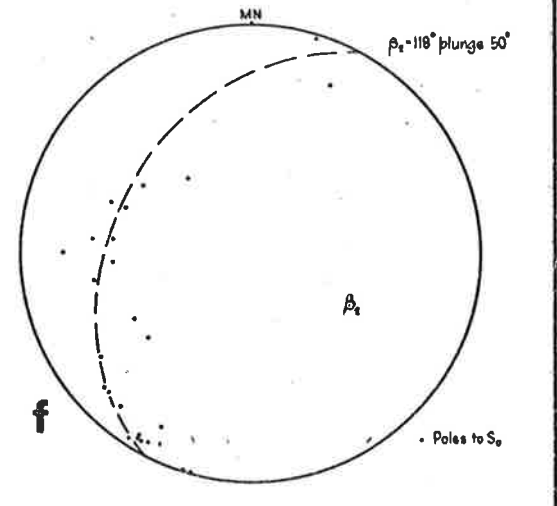
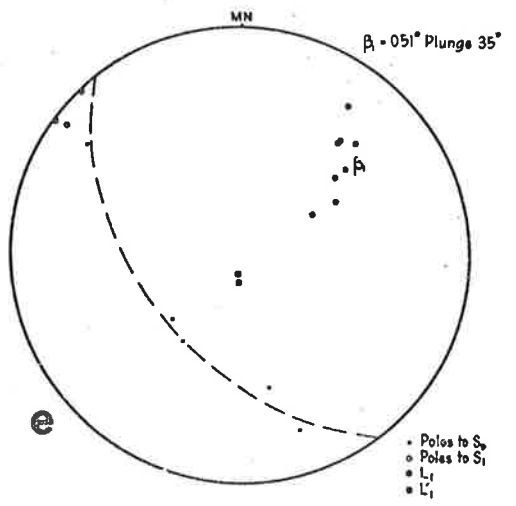
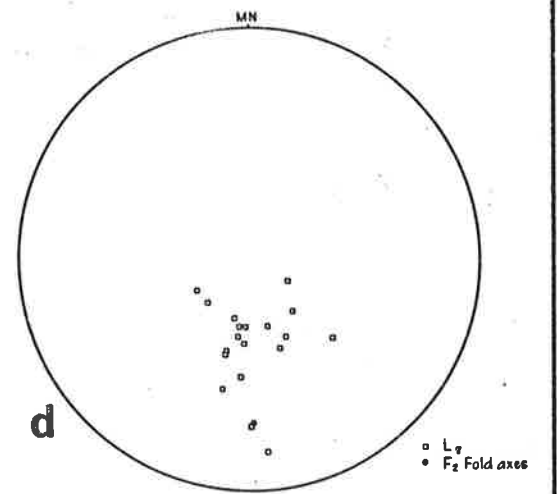
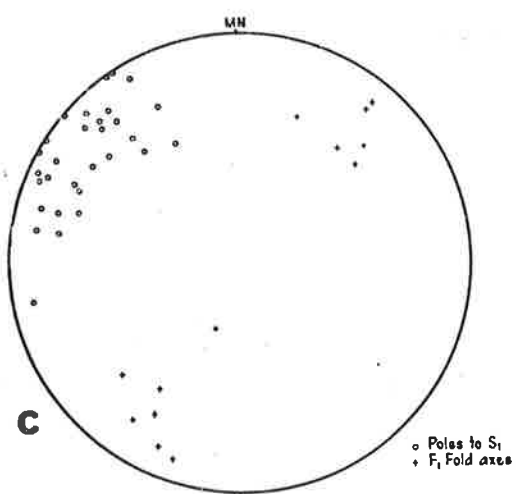
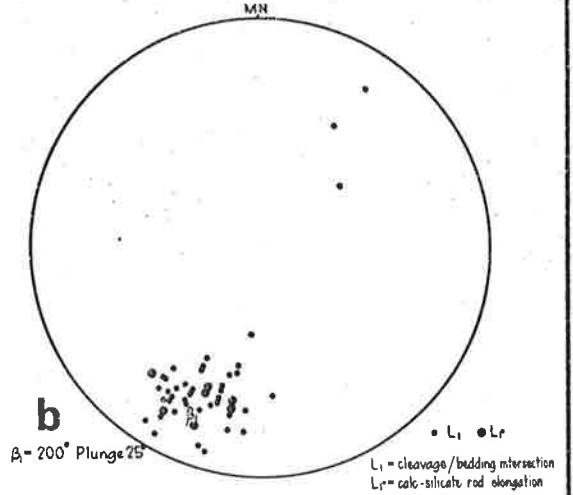
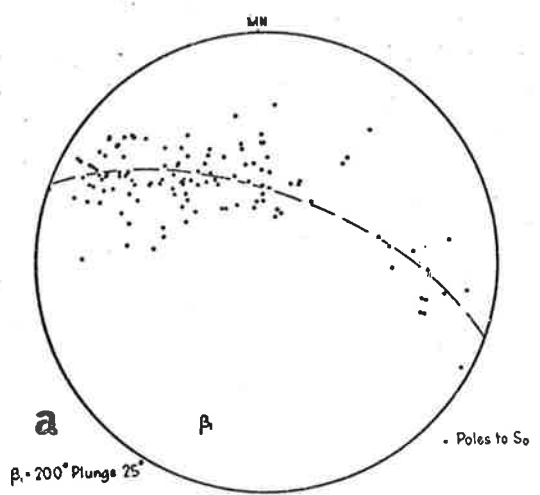


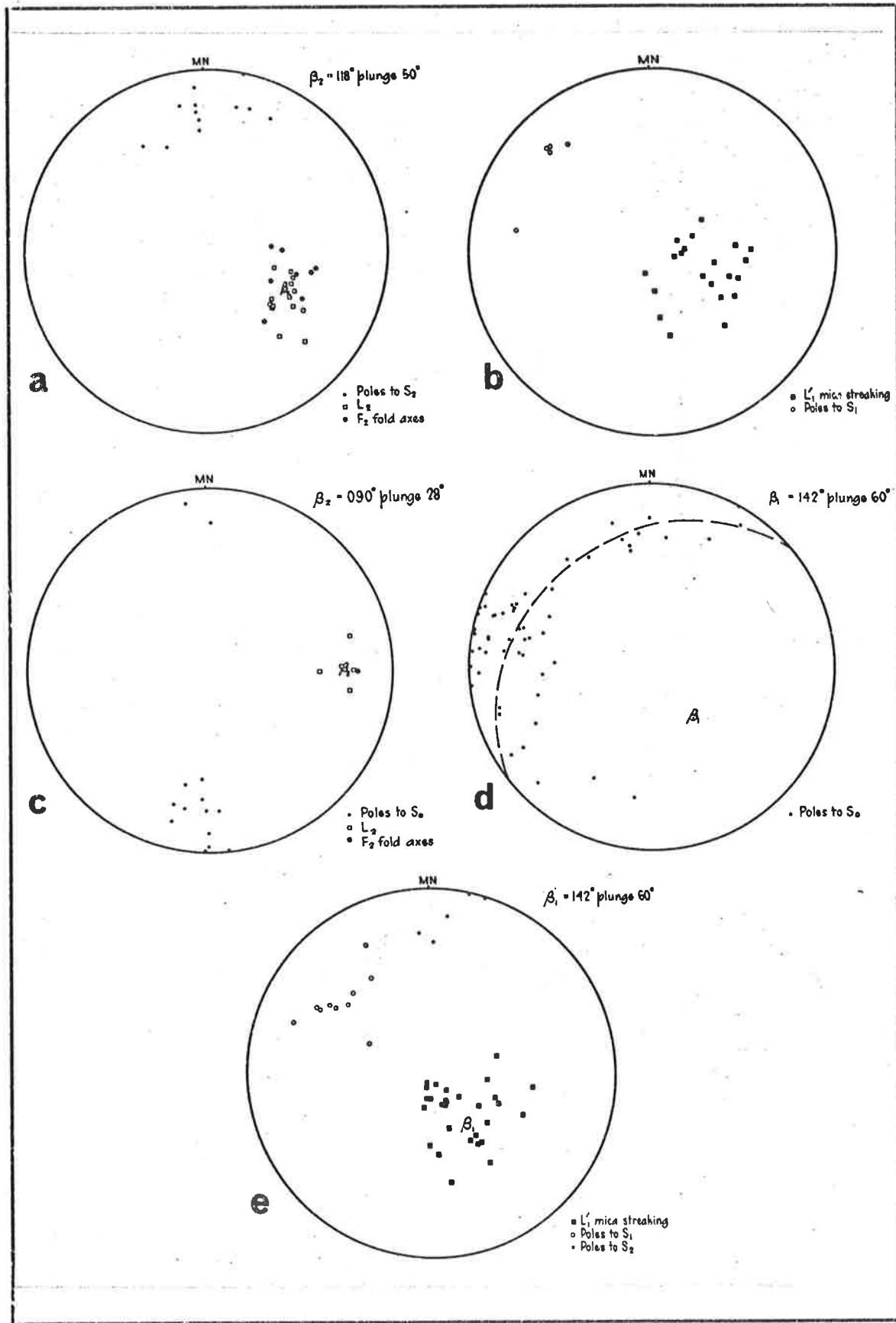
FIGURE 16

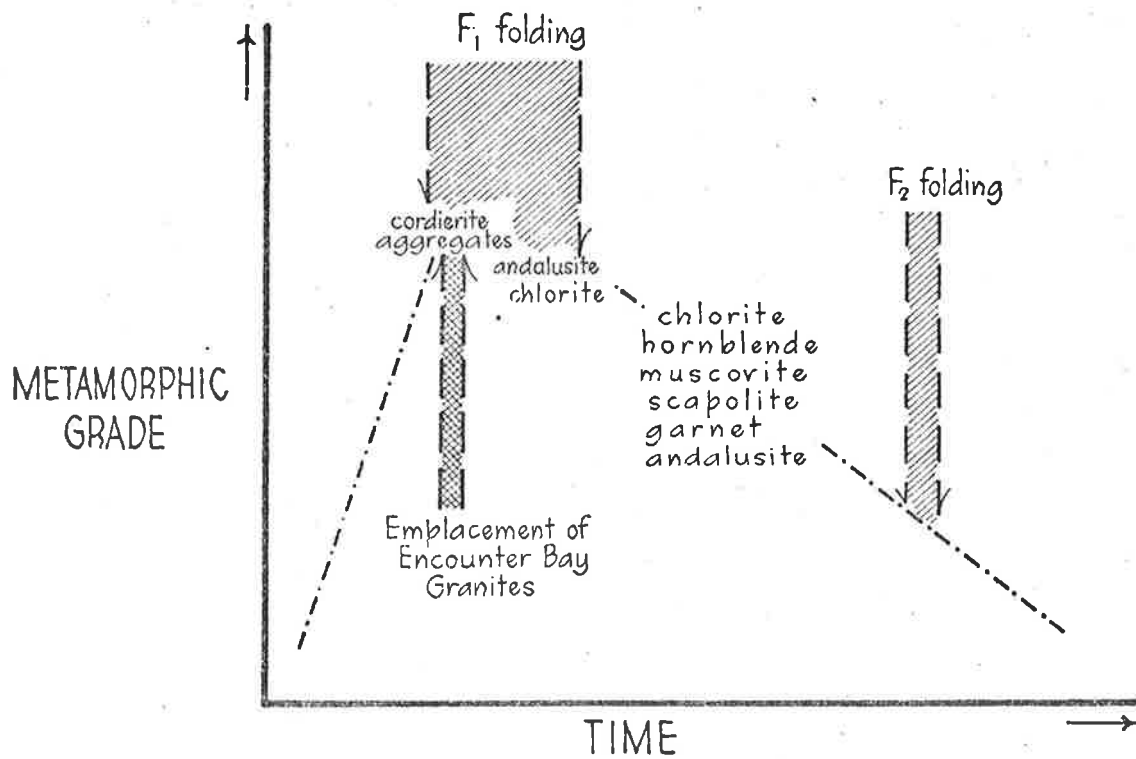
Equal-area projections of structural elements in Kamantoo Group meta-sedimentary rocks along the southern coastline of Fleurieu Peninsula, and in the Encounter Bay area.

a and b - the Middleton quarry.

c - Middleton Beach.

d and e - the Middleton area excluding the Middleton quarry and Middleton Beach.



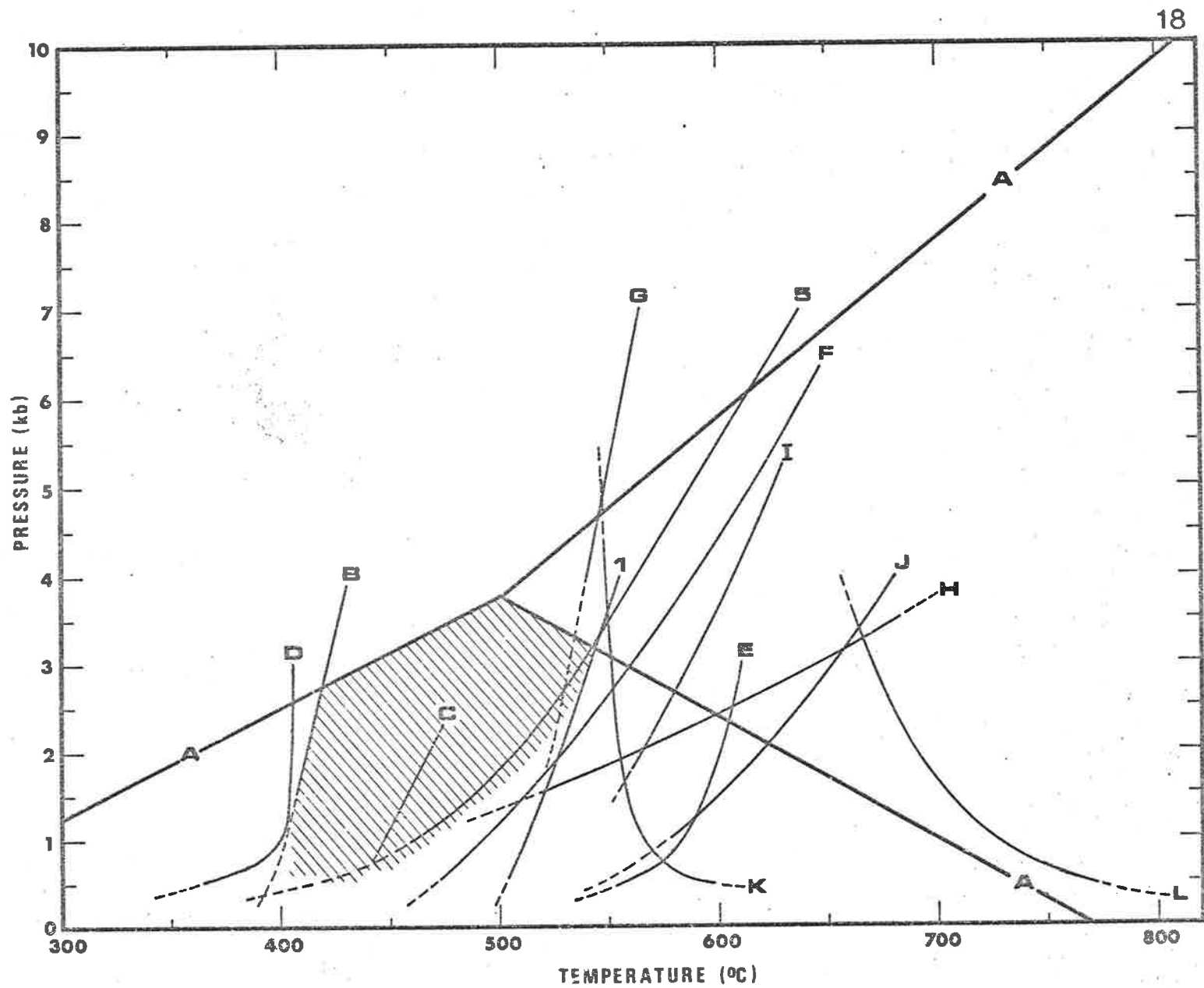


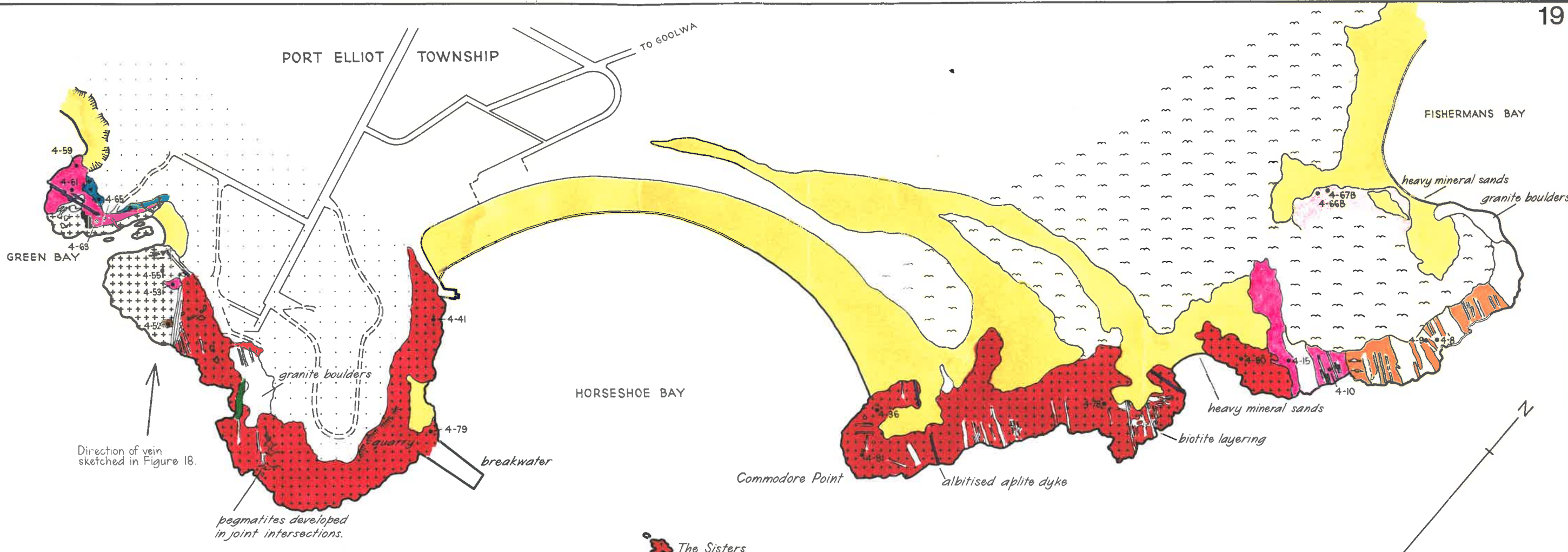
17 Diagrammatic relationships between structural and metamorphic events in Kanmantoo Group metasediments and the emplacement of the Encounter Bay Granites, Encounter Bay area.

FIGURE 18

Pressure ($P_{\text{total}}=P_{\text{H}_2\text{O}}$) versus temperature diagram showing experimental equilibria for a number of mineral-forming reactions under low pressure, intermediate-type metamorphic conditions.

- 1 Chlorite + muscovite + quartz = cordierite + biotite + aluminosilicate + water (Winkler, 1970 - *vide* Hirschberg and Winkler, 1968).
- 5 Chlorite + andalusite + quartz = cordierite + vapour (Siefert and Schreyer, 1970).
- A Aluminosilicate data according to Holdaway (1971).
- B Pyrophyllite = andalusite + quartz + vapour (Kerrick, 1968).
- C Extreme position for the reaction: chlorite + pyrophyllite = cordierite + quartz + vapour (Siefert and Schreyer, 1970).
- D Quartz + Mn-chlorite + fluid = spessartite + fluid (Hsu, 1968).
- E Quartz + Fe-chlorite + fluid = almandine + fluid - QFM buffer (Hsu, 1968).
- F Chlorite + muscovite + quartz = cordierite + phlogopite + water (Siefert, 1970).
- G Chlorite + muscovite = staurolite + biotite + quartz + water (Hoscheck, 1969).
- H Fe-staurolite + quartz = Fe-cordierite + aluminosilicate + water - QFM buffer (Richardson, 1968).
- I Mg-chlorite + quartz = talc + cordierite + vapour (Fawcett and Yoder, 1966).
- J Muscovite + quartz = K-feldspar + aluminosilicate + water (Althaus *et al*, 1970).
- K Beginning of melting of pegmatite (Jahns and Burnham, 1958).
- L Beginning of melting of granite (Tuttle and Bowen, 1958).






Direction of vein
sketched in Figure 18.

pegmatites developed
in joint intersections.

LEGEND

-  RECENT BEACH AND DUNE SANDS, SOIL COVER.
-  PLEISTOCENE BEACH-DUNE SANDSTONE CAPPED BY CALCRETE.
-  GLACIGENE SEDIMENTS.
-  METADOLERITE.
-  APLITE DYKES.
-  ALBITISED JOINT ZONES IN GRANITE VARIETIES.
-  FINE GRAINED MIAROLITIC GRANOPHYRE.
-  RED LEUCOGRANITE.
-  FINE GRAINED GRANITE.
-  MEDIUM EVEN-GRAINED GRANITES.
-  INNER FACIES MEGACRYSTIC GRANITES.
-  BORDER FACIES MEGACRYSTIC GRANITE.

 metasedimentary rock xenoliths

NOTE : Xenoliths smaller than about 1m in diameter have not been mapped.

• 4-61 Sample locality.

GEOLOGICAL MAP SHOWING THE
FIELD RELATIONS
OF THE
ENCOUNTER BAY GRANITES
AT PORT ELLIOT



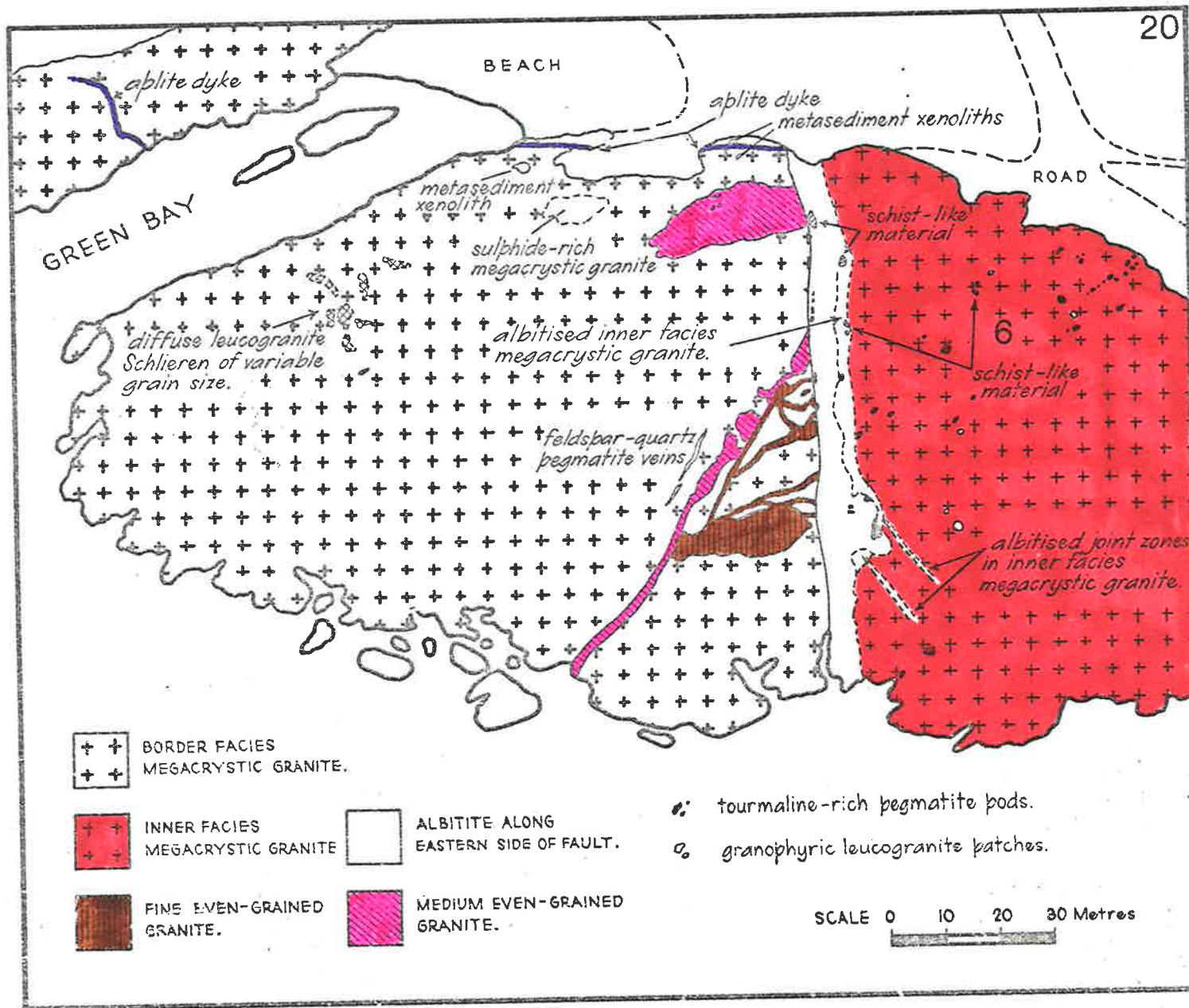
PULLEN ISLAND

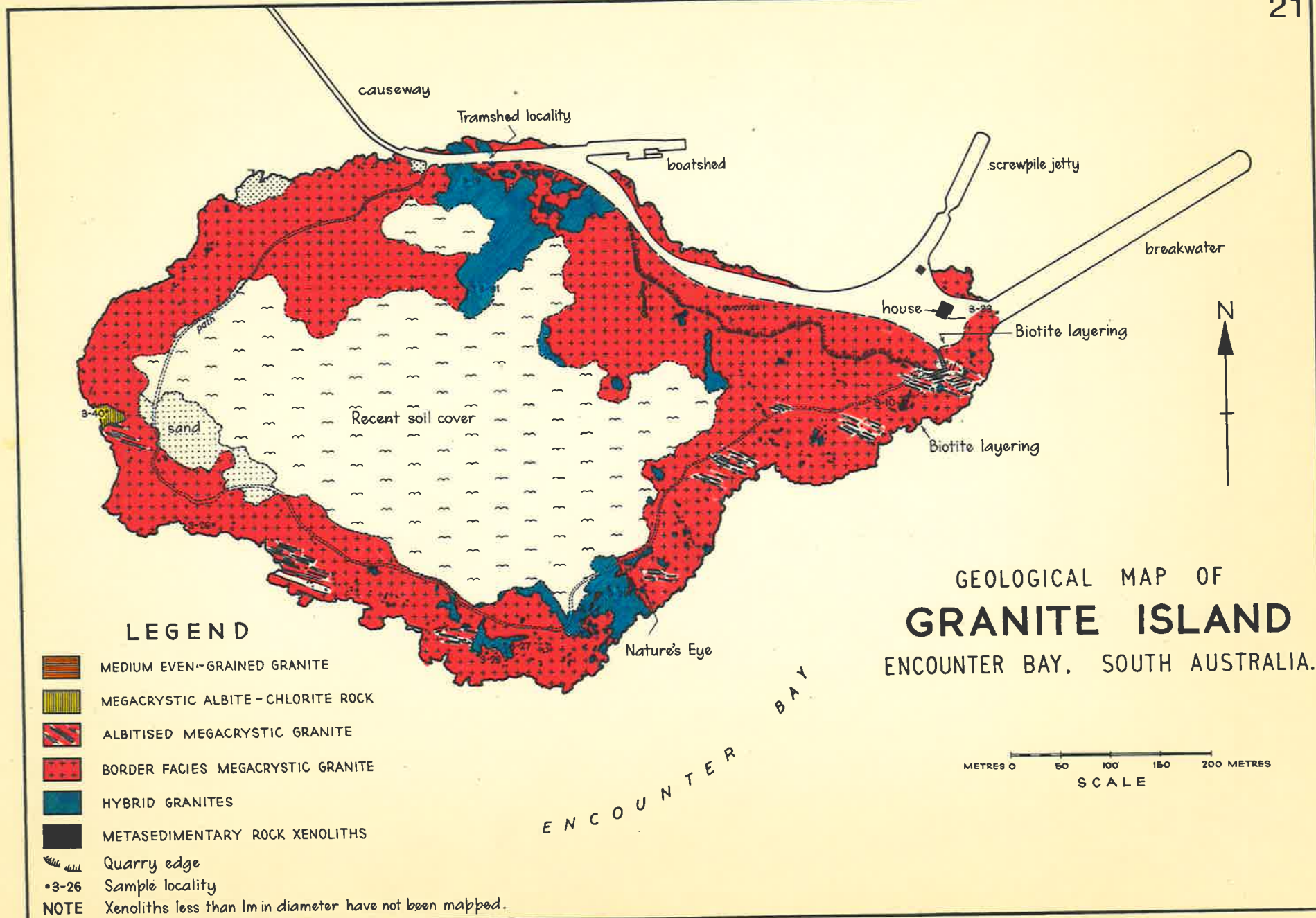
S O U T H E R N

O C E A N

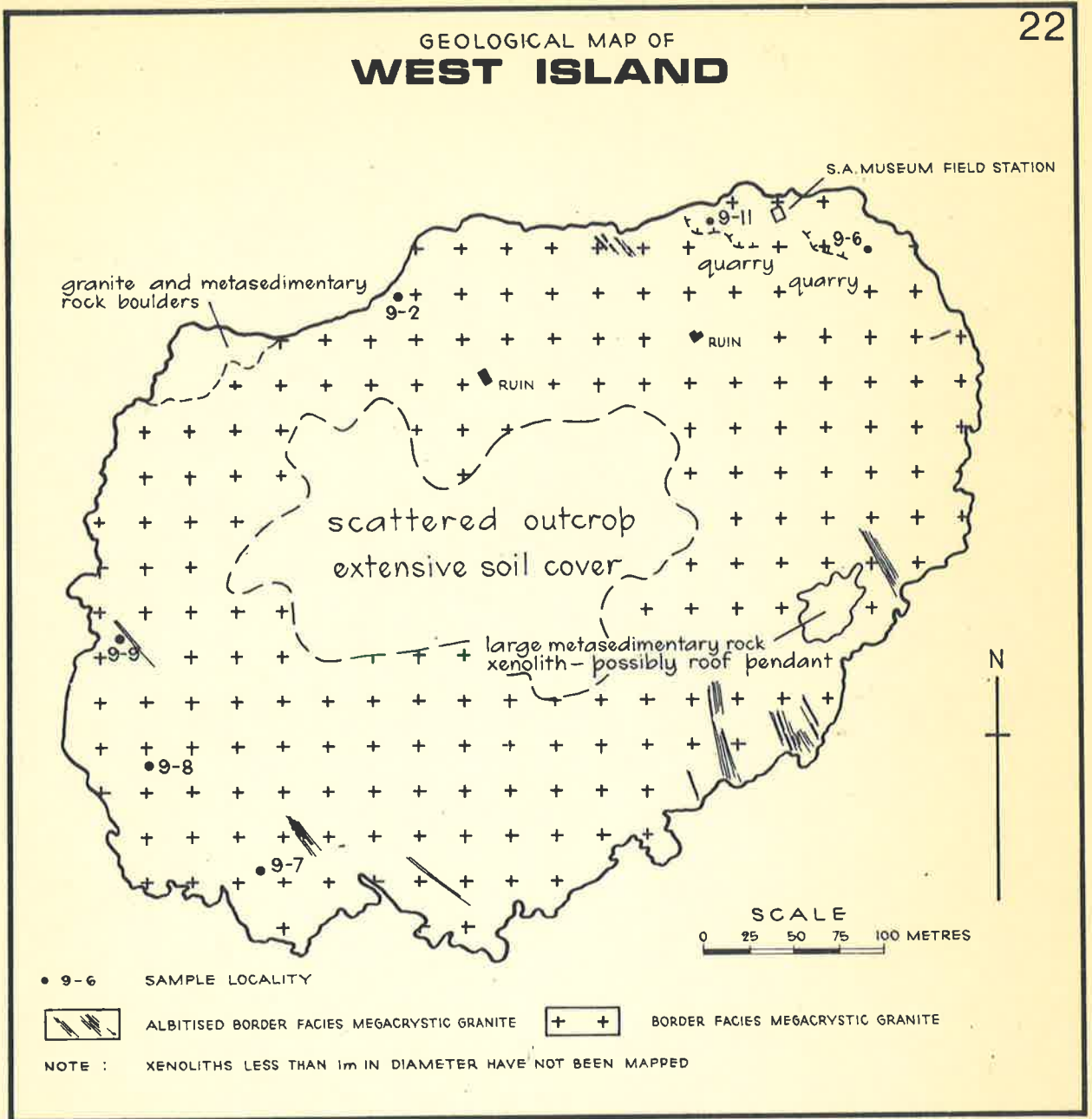
FIGURE 20

Geological sketch map of the area adjacent to the fault separating the types 1 and 2 megacrystic granites at Port Elliot. Drawn from a low-level oblique aerial photograph. View (as indicated in Figure 19) is towards the north-west.





GEOLOGICAL MAP OF WEST ISLAND



• 9-6 SAMPLE LOCALITY



ALBITISED BORDER FACIES MEGACRYSTIC GRANITE



BORDER FACIES MEGACRYSTIC GRANITE

NOTE : XENOLITHS LESS THAN 1m IN DIAMETER HAVE NOT BEEN MAPPED

FIGURE 23

Triangular diagram incorporating the results of macro-modal analyses of the border facies and the inner facies megacrystic granites, and of the medium even-grained granites.

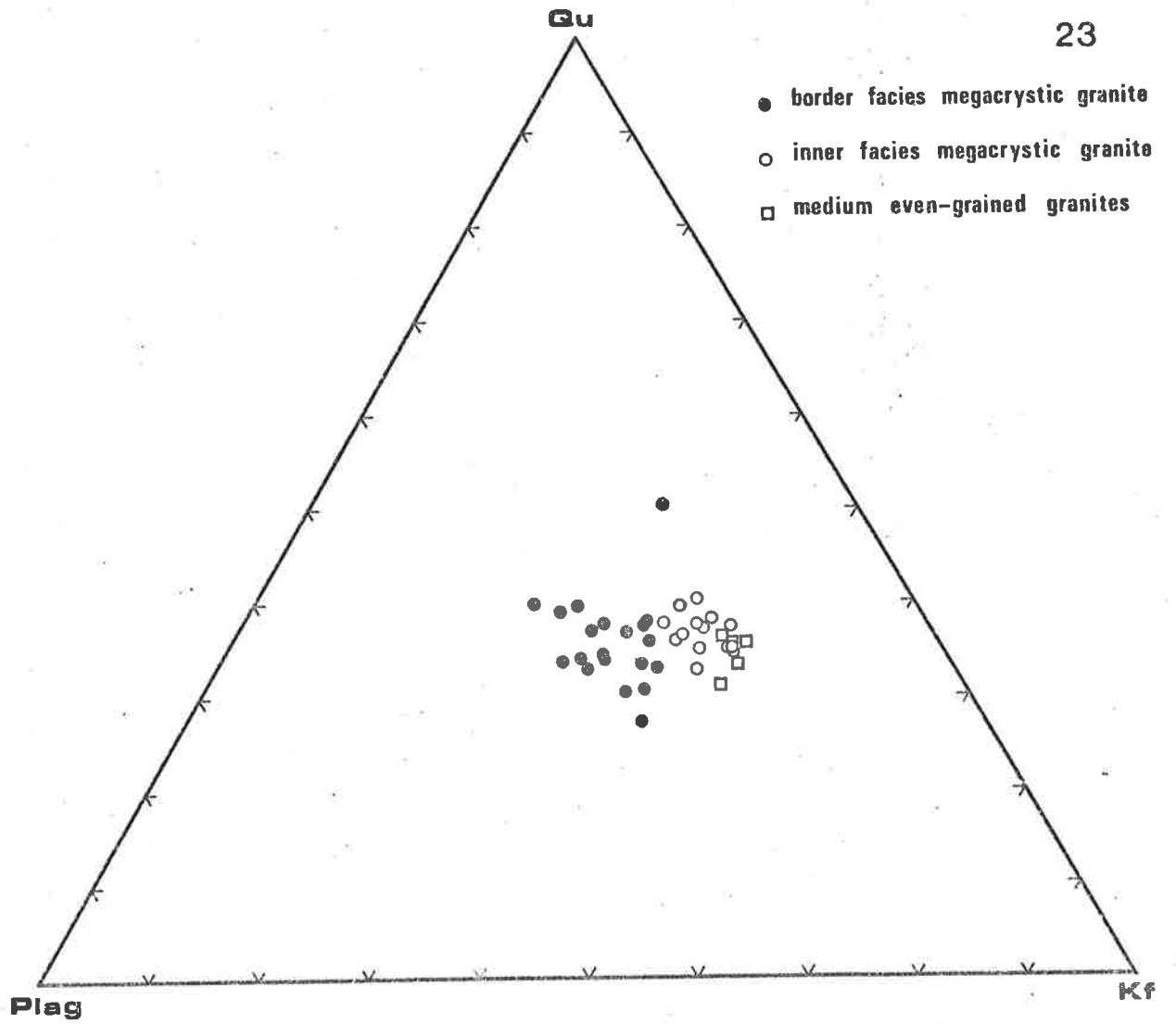


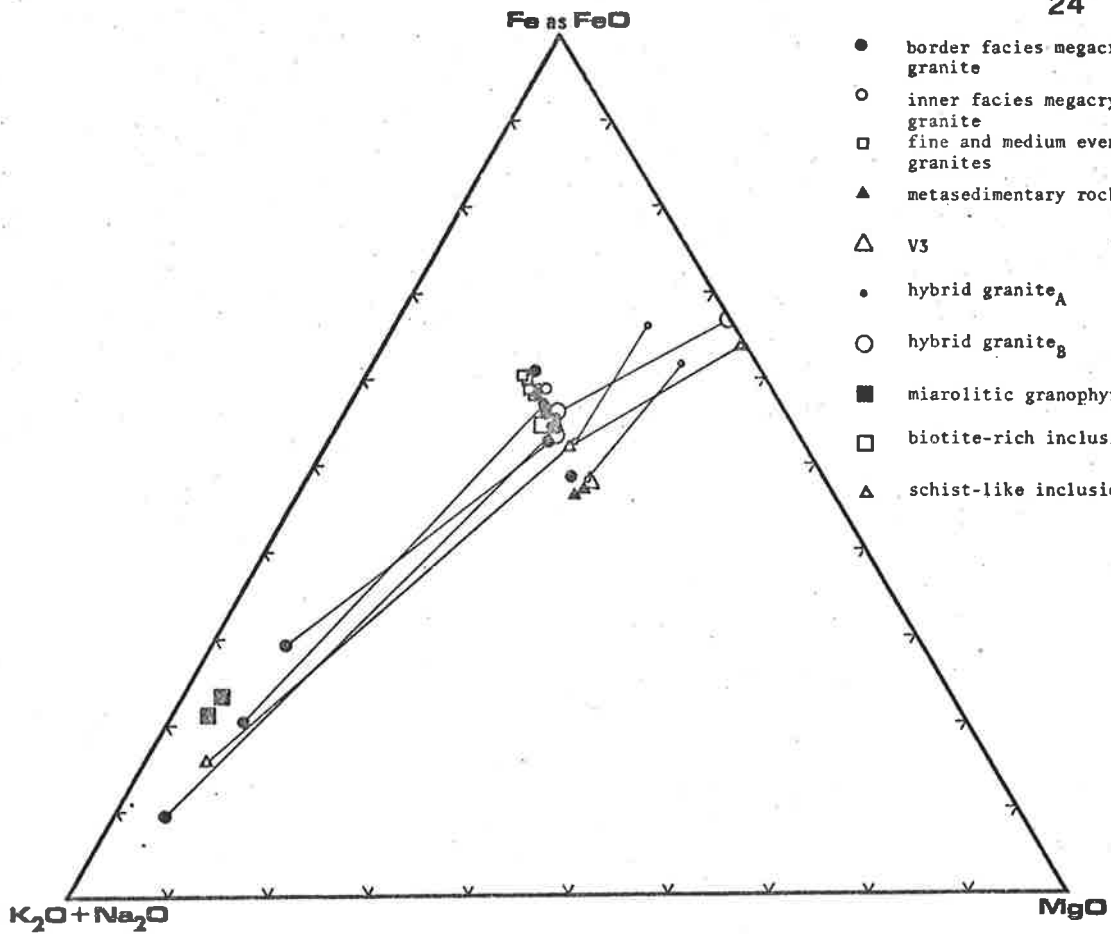
FIGURE 24

Triangular FeO, K_2O+Na_2O , MgO diagram incorporating the results of chemical analysis of micas, chlorites and hornblendes from varieties of the Encounter Bay Granites, and from xenoliths within the Encounter Bay Granites. Tie-lines have been drawn between coexisting minerals.

FIGURE 25

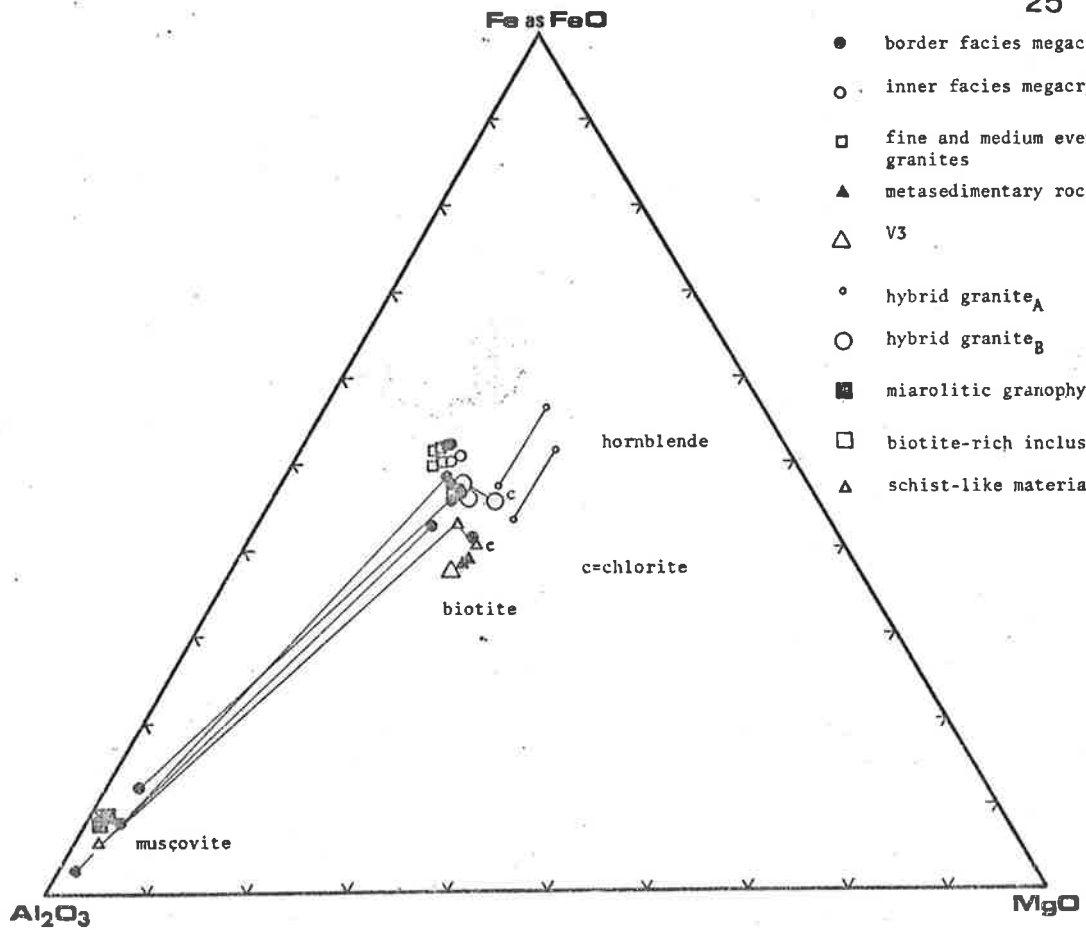
Triangular FeO, Al_2O_3 , MgO diagram incorporating the results of chemical analysis of micas, chlorites and hornblendes from varieties of the Encounter Bay Granites, and from xenoliths within the Encounter Bay Granites. Tie-lines have been drawn between coexisting minerals.

24



- border facies megacrystic granite
- inner facies megacrystic granite
- fine and medium even-grained granites
- ▲ metasedimentary rock xenoliths
- △ V3
- hybrid granite_A
- hybrid granite_B
- miarolitic granophyre
- biotite-rich inclusion
- △ schist-like inclusion

25



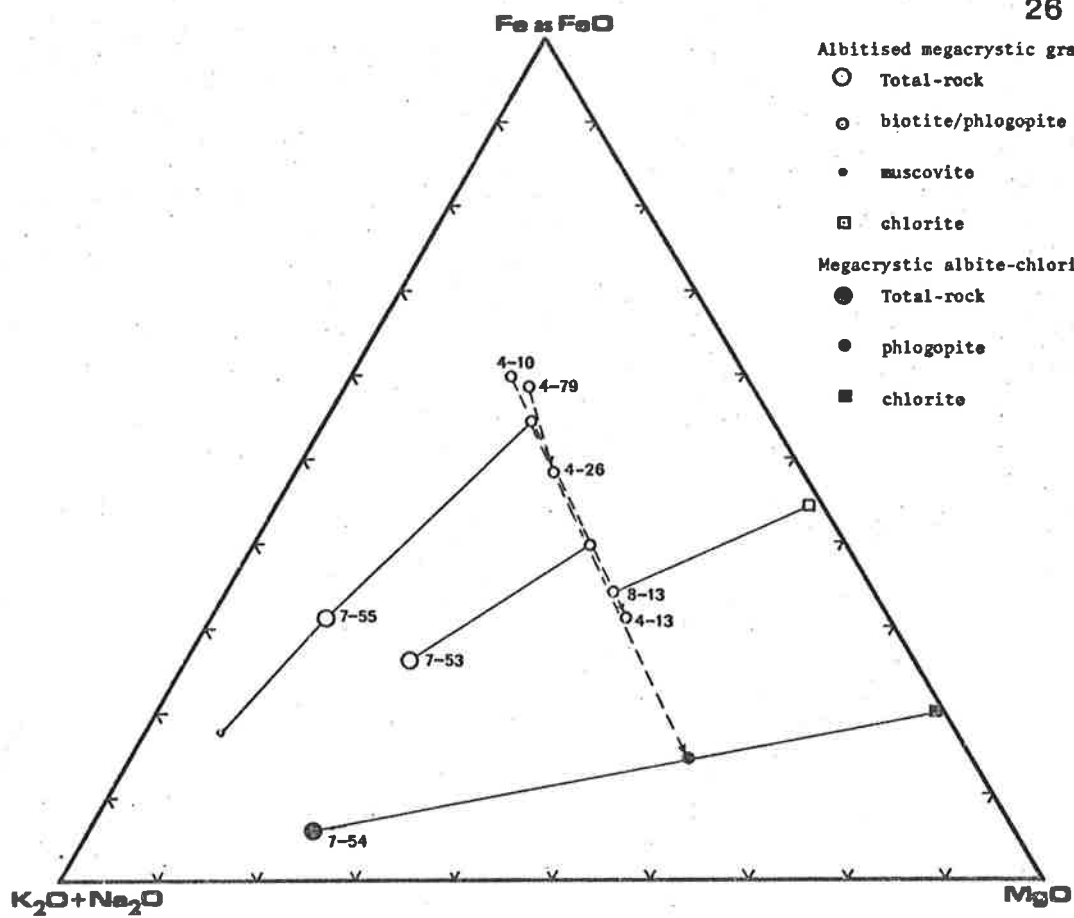
- border facies megacrystic granite
- inner facies megacrystic granite
- fine and medium even-grained granites
- ▲ metasedimentary rock xenoliths
- △ V3
- hybrid granite_A
- hybrid granite_B
- miarolitic granophyre
- biotite-rich inclusion
- △ schist-like material

FIGURE 26

Triangular FeO, K₂O+Na₂O, MgO diagram incorporating the results of chemical analysis of coexisting micas and chlorites from specimens of the albitised megacrystic granite and the megacrystic albite-chlorite rock. The respective total-rock compositions have also been plotted on the diagram, and are joined by lines to their constituent micas and chlorites. Dashed lines join the compositions of biotites in unaltered granites to the compositions of biotites/phlogopites in nearby albitised granites, and so indicate the trend of compositional changes in biotite during albitisation.

FIGURE 27

Triangular FeO, Al₂O₃, MgO diagram incorporating the results of chemical analysis of coexisting micas and chlorites from specimens of the albitised megacrystic granite and the megacrystic albite-chlorite rock. The compositions of the micas and chlorites are practically coincident. The respective total-rock compositions have also been plotted, and are joined by lines to their constituent micas and chlorites. Dashed lines join the compositions of biotites in unaltered granites to the compositions of biotites/phlogopites in nearby albitised granites, and so indicate the trend of compositional changes in biotite during albitisation.

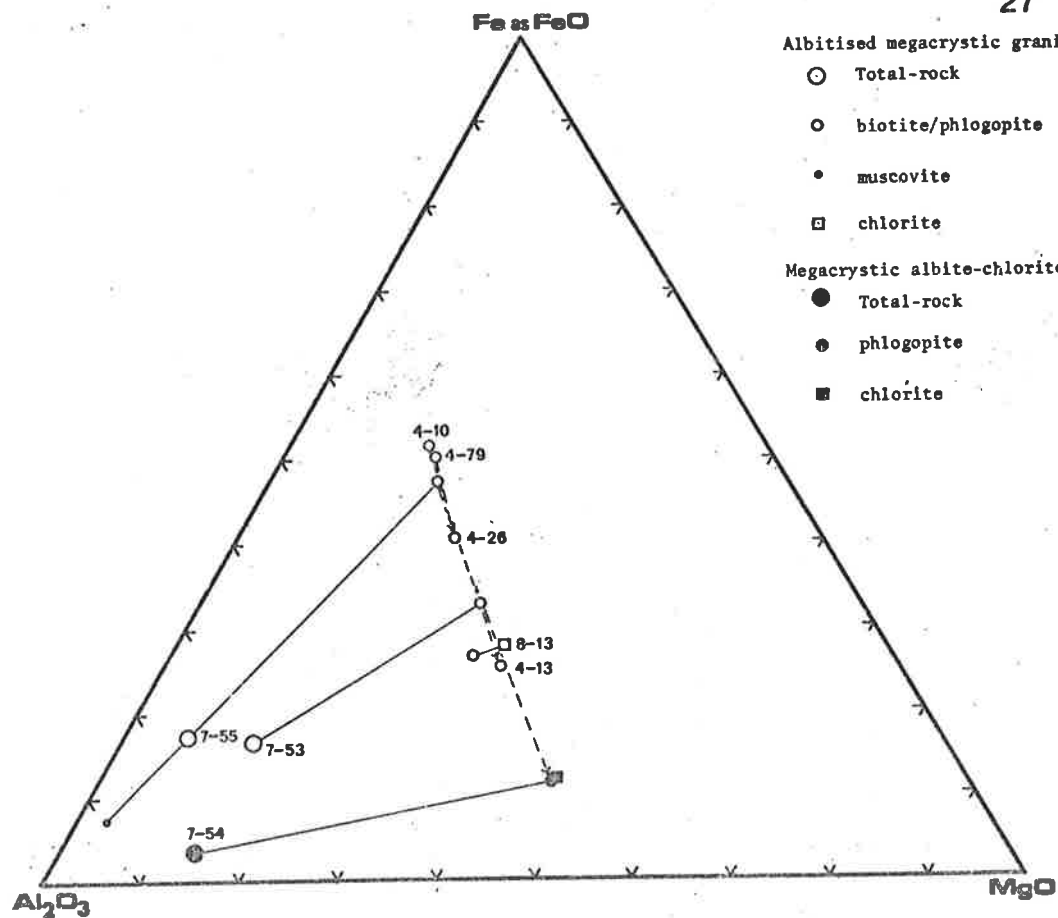


Albitised megacrystic granite

- Total-rock
- biotite/phlogopite
- muscovite
- chlorite

Megacrystic albite-chlorite rock

- Total-rock
- phlogopite
- chlorite



Albitised megacrystic granite

- Total-rock
- biotite/phlogopite
- muscovite
- chlorite

Megacrystic albite-chlorite rock

- Total-rock
- phlogopite
- chlorite

FIGURE 28

Graph of $2\theta_{204/060}$ versus degree of Al,Si order for "standard" alkali feldspars (see Appendix I). The graph illustrates three distinct distributions corresponding to albites, normal potash feldspars, and anomalous potash feldspars of Pellotsalo type.

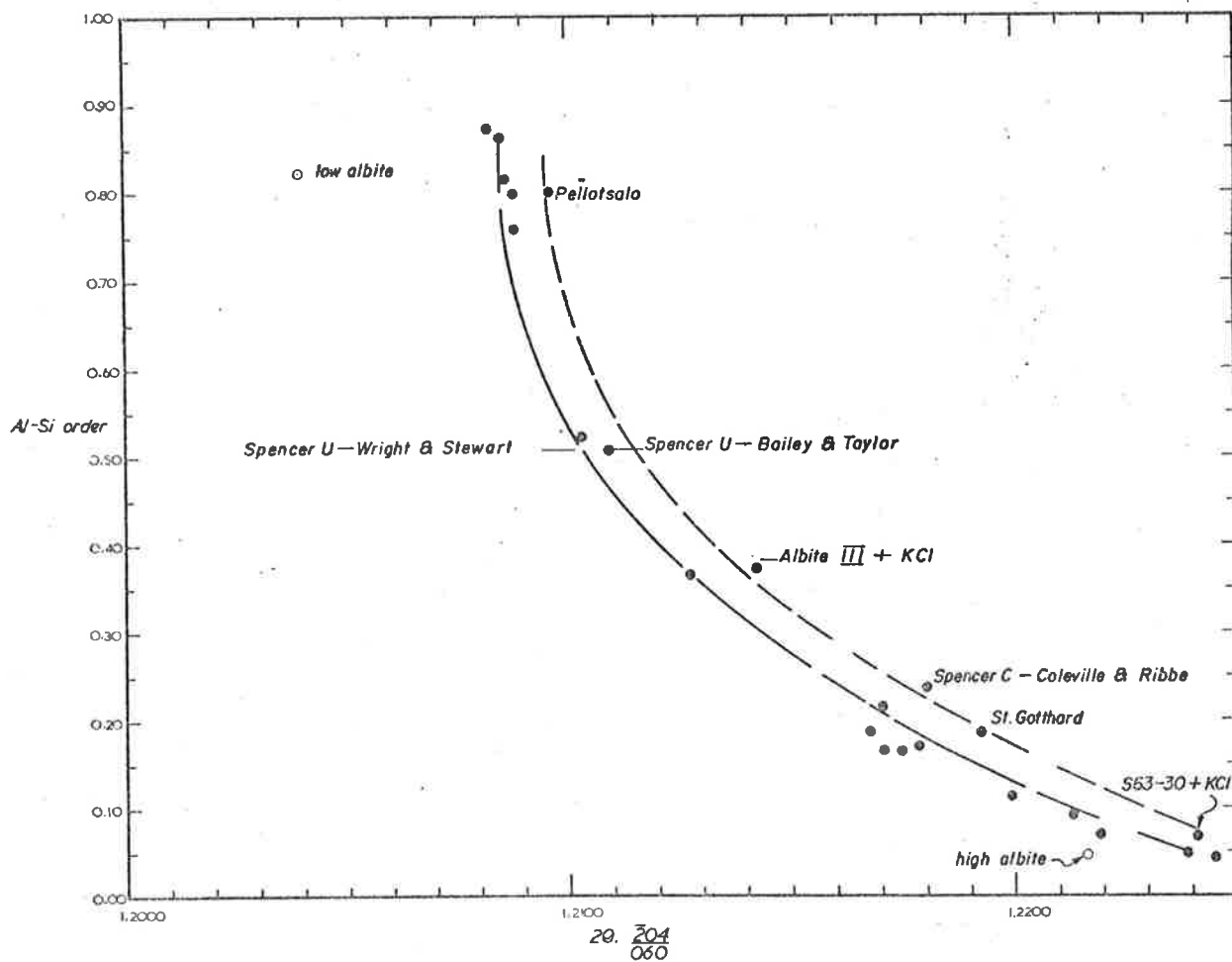


FIGURE 29

Potash feldspar specimens from potash feldspar megacrysts in samples of the border facies and inner facies megacrystic granites, and the type B hybrid granite, plotted on part of the 20.204 - 060 graph of Wright (1968).

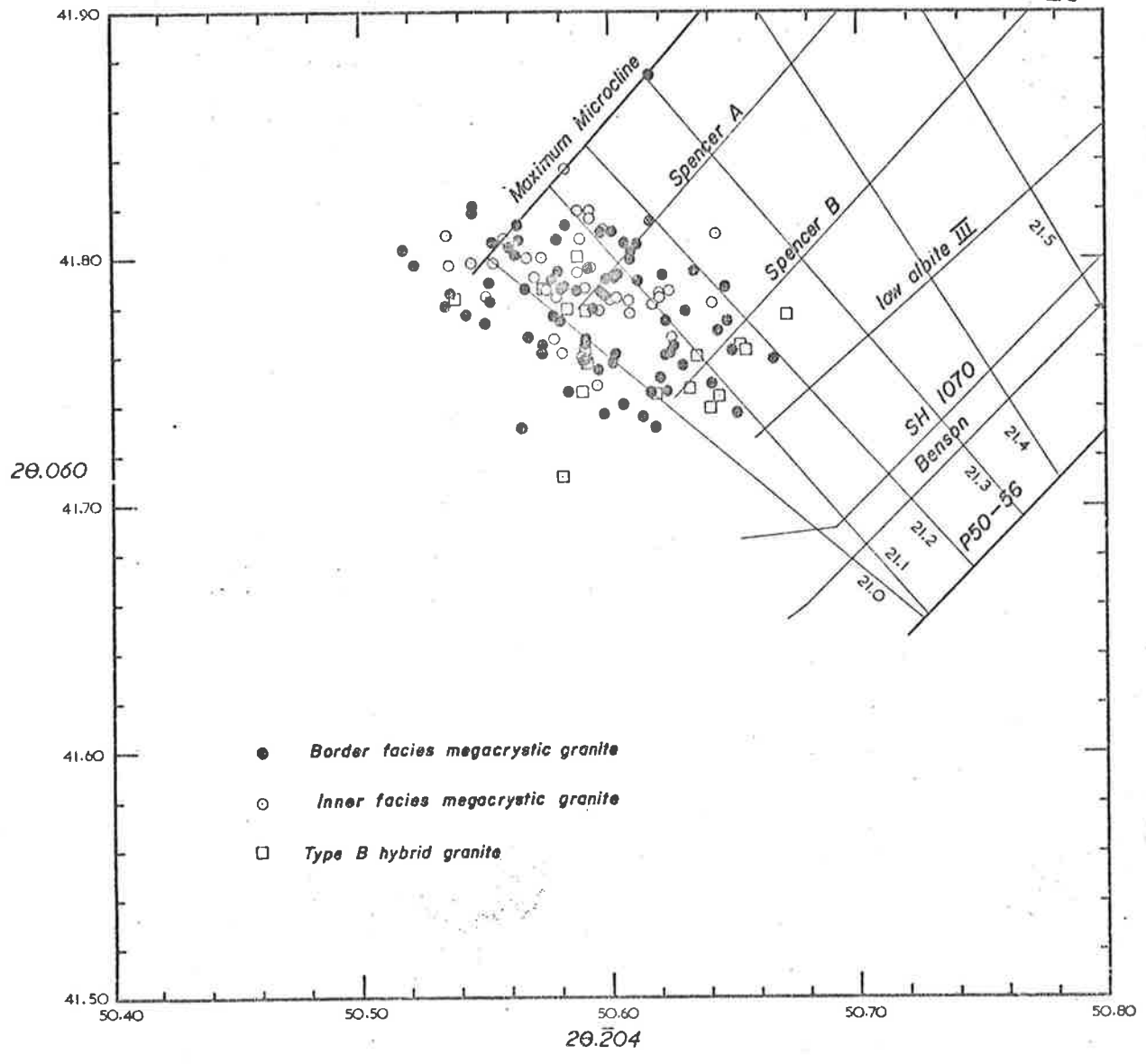


FIGURE 30

Graphs showing the degree of Al,Si order (estimated from $2\theta.204/060$ with reference to FIGURE 28), and the angular difference between the 131 and $1\bar{3}1$ diffraction lines plotted against position of specimens in potash feldspar megacrysts from samples of the border facies and inner facies megacrystic granites, and from the type B hybrid granite. Data from Tables I5-I7.

- 4-61A, 4-61B, 9-11, 4-55 - border facies megacrystic granite.
- 4-79, 4-81 - inner facies megacrystic granite.
- 3-27 - type B hybrid granite.

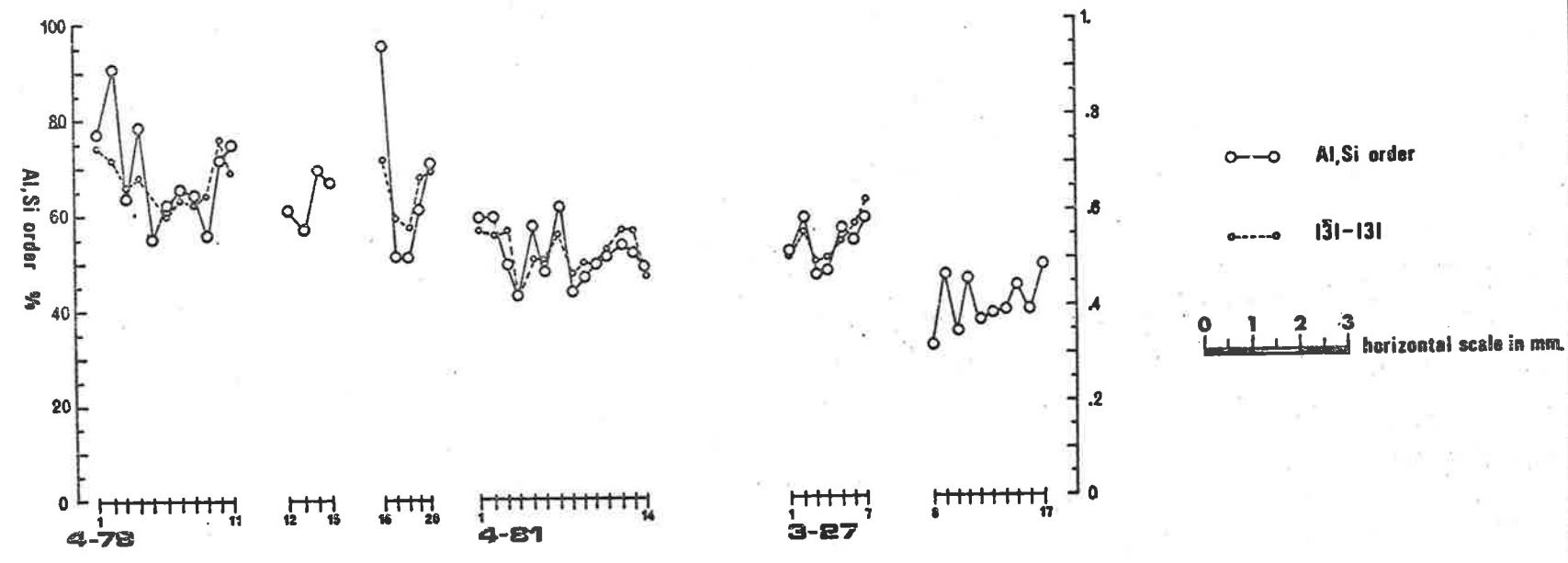
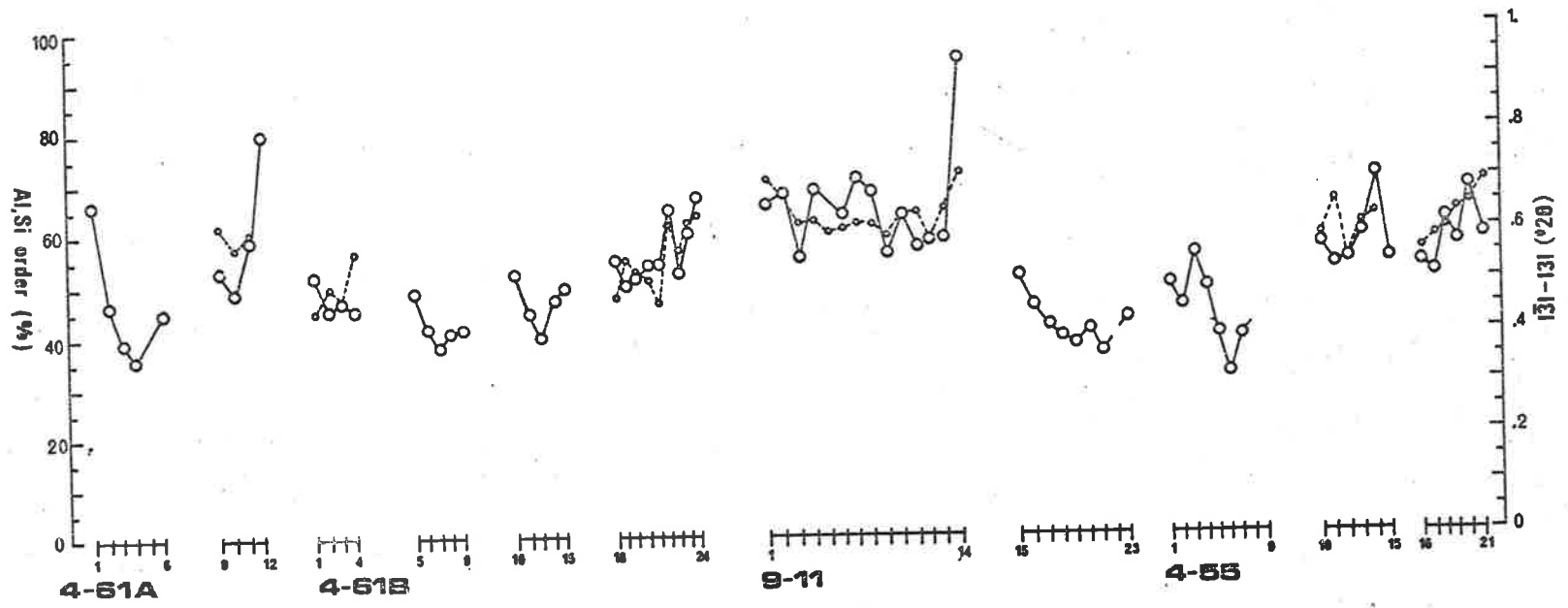
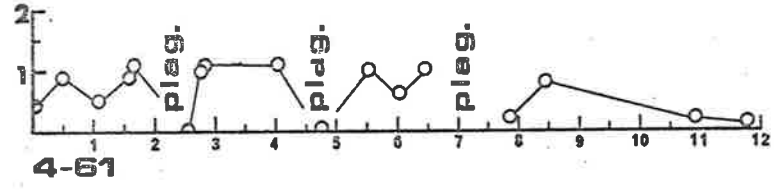
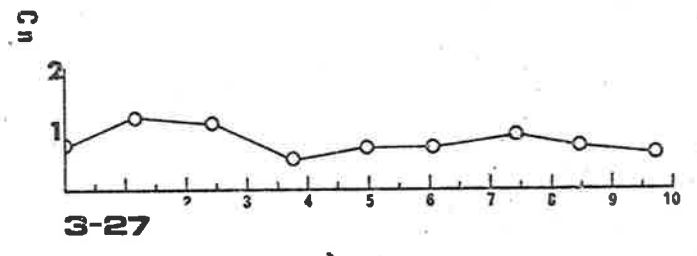
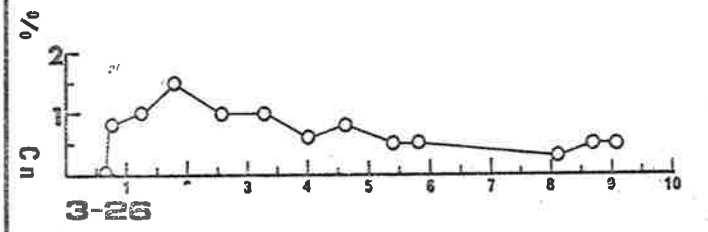
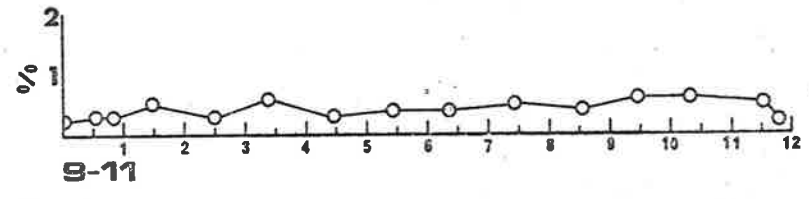
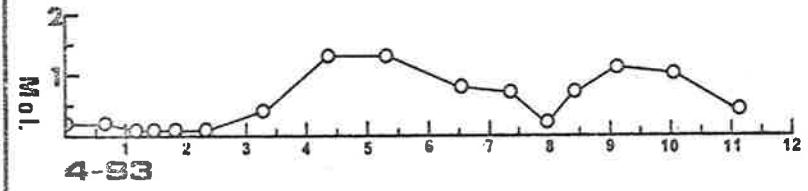
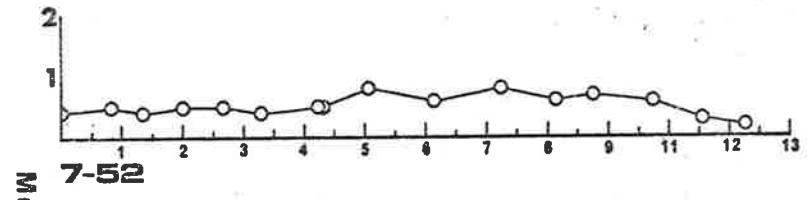
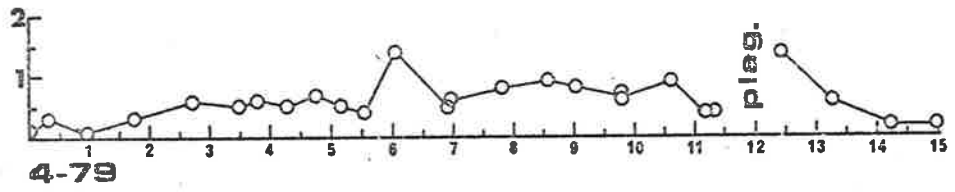


FIGURE 31

Graphs showing the variation in molecular percentage of celsian (as determined from electron microprobe analyses of Ba) across potash feldspar megacrysts in specimens of the border facies and inner facies megacrystic granites, and the type B hybrid granite. The horizontal scales (in mm.) indicate the actual positions of the microprobe analyses in the potash feldspar megacrysts. Data from Tables J1-J8 (excluding Table J7).

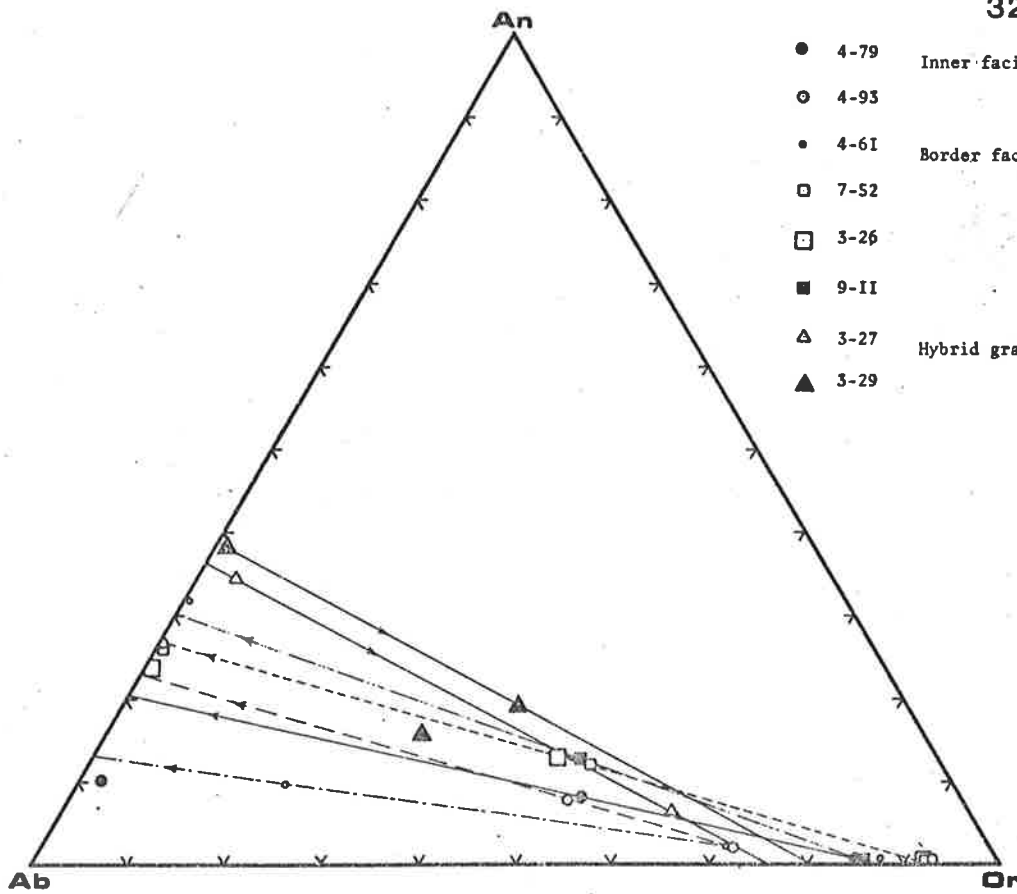
- 4-79, 4-93 - inner facies megacrystic granite
- 3-26, 4-61, 7-52, 9-11 - border facies megacrystic granite
- 3-27 - type B hybrid granite



Horizontal scale is in mm.

FIGURE 32

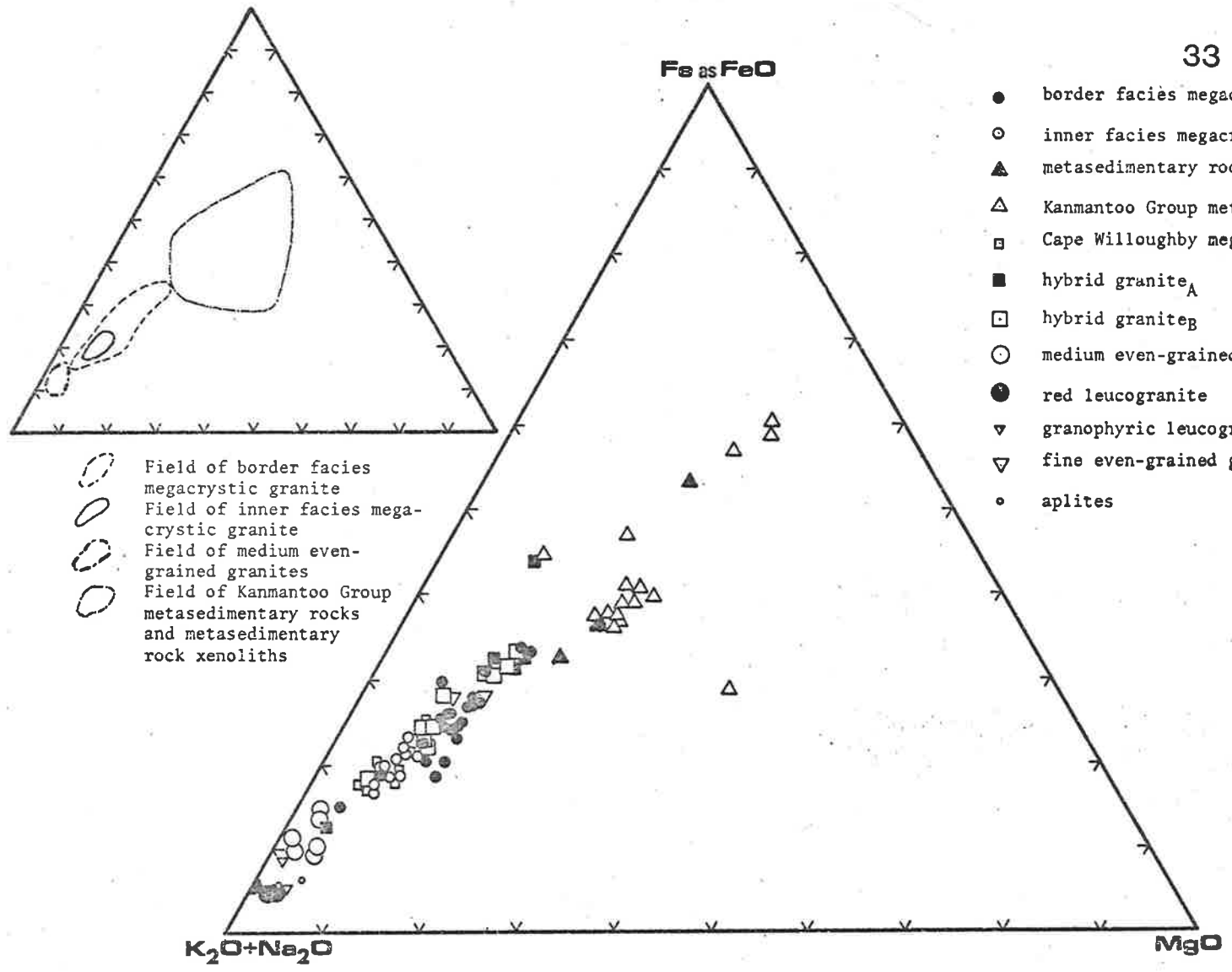
Triangular An-Ab-Or diagram incorporating the calculated average compositions of coexisting potash feldspar and plagioclase in specimens of the border facies and inner facies megacrystic granites, and the hybrid granites. The average compositions were calculated from electron probe microanalyses (see Table J9). Compositions of the respective total-rocks have also been plotted on the diagram, in terms of CIPW normative An, Ab and Or. Tie-lines have been drawn from the calculated average potash feldspar or plagioclase composition through the total-rock composition and projected onto the An-Ab on Ab-Or sides of the triangular diagram. The arrows indicate the direction of projection of the tie-lines.



- 4-79 Inner facies megacrystic granite
- 4-93
- 4-61 Border facies megacrystic granite
- 7-52
- ◻ 3-26
- 9-II
- △ 3-27 Hybrid granite
- ▲ 3-29

FIGURE 33

Triangular total Fe (FeO), total alkalis (K₂O+Na₂O), MgO diagram incorporating the results of chemical analysis of varieties of the Encounter Bay Granites (including xenoliths) and the contiguous Kanmantoo Group metasedimentary rocks. The inset shows outlines of the compositional fields occupied by the main rock types.



○ Field of border facies megacrystic granite
 ○ Field of inner facies megacrystic granite
 ○ Field of medium even-grained granites
 ○ Field of Kanmantoo Group metasedimentary rocks and metasedimentary rock xenoliths

- border facies megacrystic granite
- inner facies megacrystic granite
- ▲ metasedimentary rock xenoliths
- △ Kanmantoo Group metasedimentary rocks
- Cape Willoughby megacrystic granite
- hybrid granite_A
- hybrid granite_B
- medium even-grained granites
- red leucogranite
- ▼ granophyric leucogranite inclusions
- ▽ fine even-grained granites
- aplites

FIGURE 34

Triangular total Fe (FeO), total alkalis (K_2O+Na_2O), MgO diagram incorporating the total-rock compositions of several varieties of the Encounter Bay Granites and the compositions of their constituent biotites. Tie-lines join the rocks to their constituent biotites.

FIGURE 35

Graph of K(%) versus Rb(ppm) in varieties of the Encounter Bay Granites and some contiguous Kanmantoo Group metasedimentary rocks.

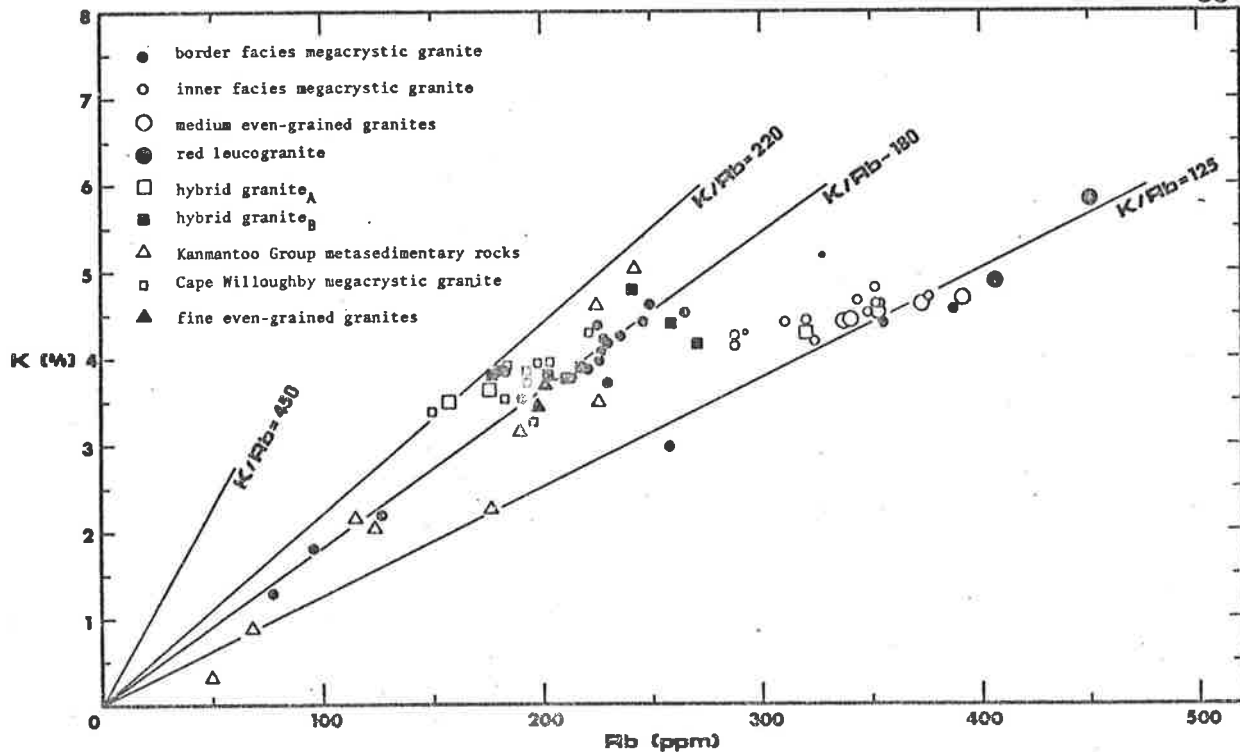
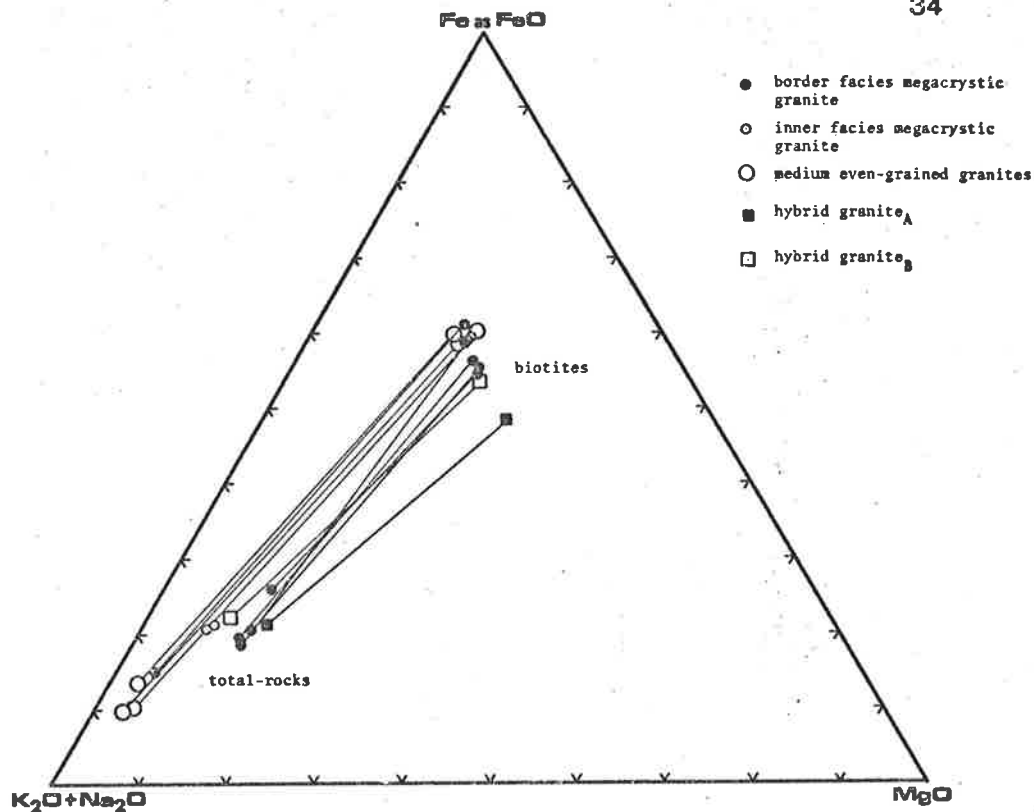
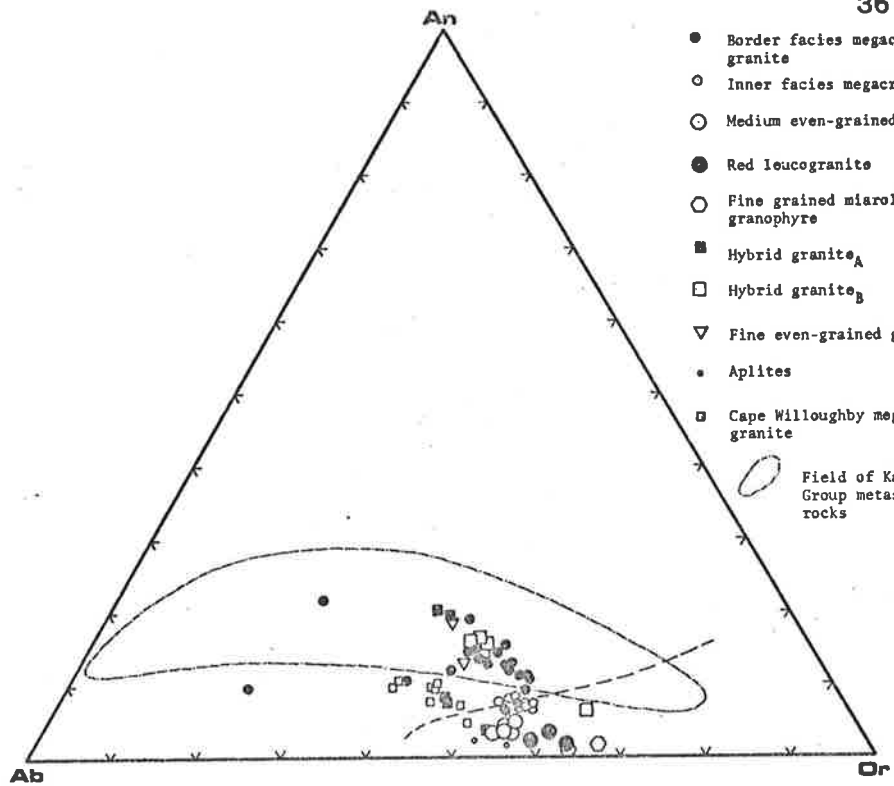


FIGURE 36

Triangular An-Ab-Or diagram incorporating the CIPW normative compositions of total-rock specimens of varieties of the Encounter Bay Granites. The dashed line is the projection of the quartz-saturated two-feldspar cotectic line at 1kb P_{H_2O} (James and Hamilton, 1969).

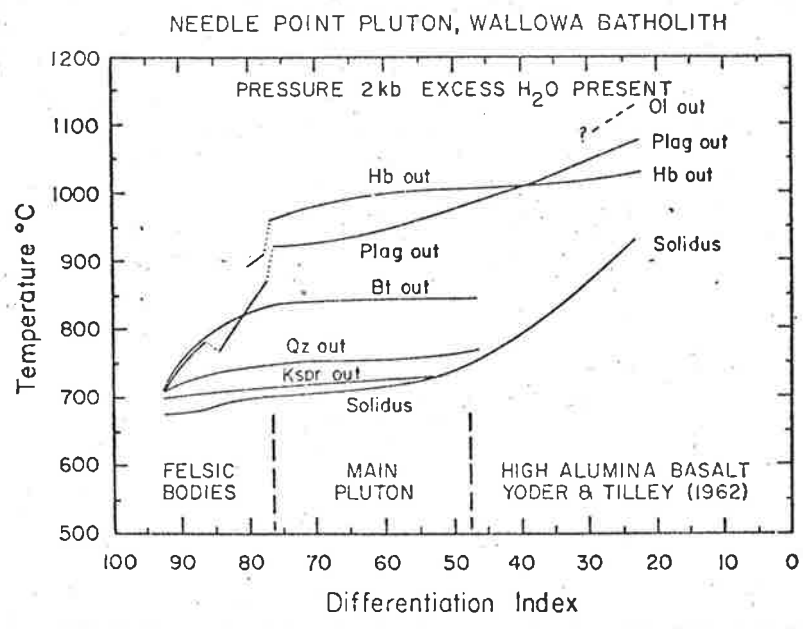


- Border facies megacrystic granite
- Inner facies megacrystic granite
- Medium even-grained granites
- Red leucogranite
- Fine grained microlitic granophyre
- Hybrid granite_A
- Hybrid granite_B
- ▽ Fine even-grained granites
- Aplites
- ◇ Cape Willoughby megacrystic granite

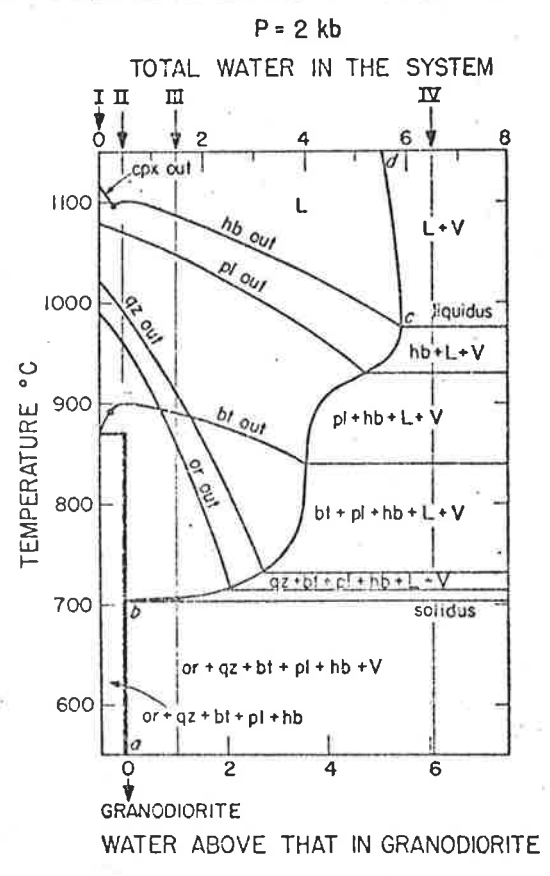
○ Field of Kanmantoo Group metasedimentary rocks

FIGURE 37

- a. Temperature - differentiation index diagram showing the mineral stability boundaries for granitic rocks of the Needle Point Pluton, Wallowa Batholith, at 2kb P_{H_2O} (after Piwinskii and Wyllie, 1970), and for a high alumina basalt. Diagram from Wyllie (1971).
- b. Schematic isobaric T-X section for a granodiorite. The inferred upper stability limits for individual minerals in the vapour-absent region were obtained by interpolation between the results for dry Type 1 mineral assemblages and for water-excess Type IV mineral assemblages (Robertson and Wyllie, 1971). The vapour-present phase boundaries were experimentally determined. Diagram from Wyllie (1971). According to Wyllie, there is little variation possible in the positions of the boundaries for the anhydrous minerals, but there is more uncertainty for amphibole and biotite. The stability temperatures of these minerals increase with decreasing H_2O content in the vapour-absent region. In addition, the temperatures of the biotite and the amphibole boundaries are sensitive to mineral composition and to the oxygen fugacity.



a



b

FIGURE 38

Triangular Q-Ab-Or diagram incorporating the CIPW normative compositions of total-rock specimens of the Encounter Bay Granites. The compositions have been plotted with respect to the trend indicated by the positions of the ternary minima and eutectics at pressures between 0.5kb and 10kb (Luth, Jahns and Tuttle, 1964), and the piercing points for particular compositions of An in the quaternary Q-Ab-Or-An system (James and Hamilton, 1969).

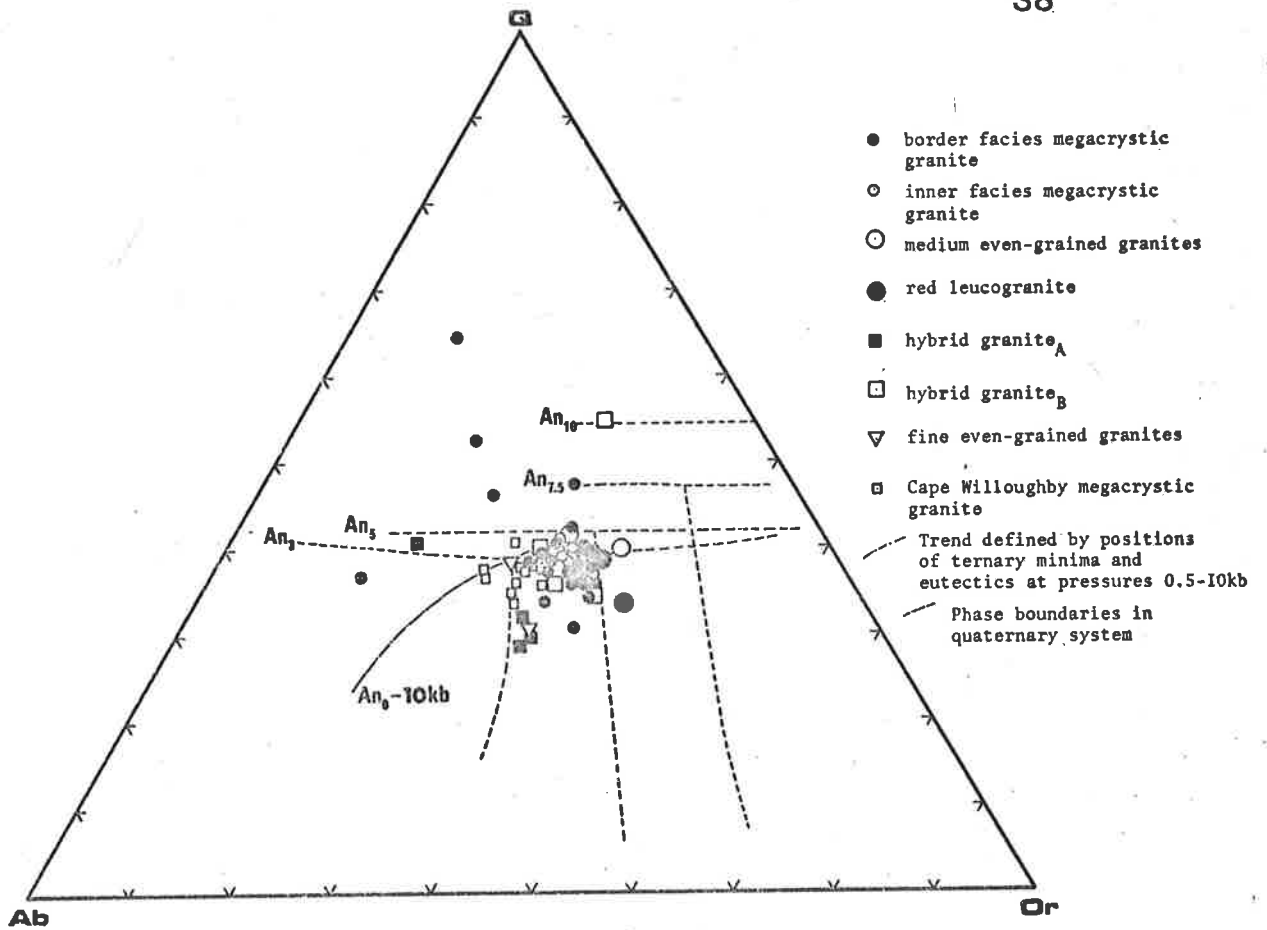


FIGURE 39

Rb-Sr isochron diagram incorporating the results of isotope dilution analyses of the contaminated border facies megacrystic granite, metasedimentary rock xenoliths and Kanmantoo Group metasedimentary rocks, hybrid granites, and albitised border facies megacrystic granites, and some constituent minerals of these rocks.

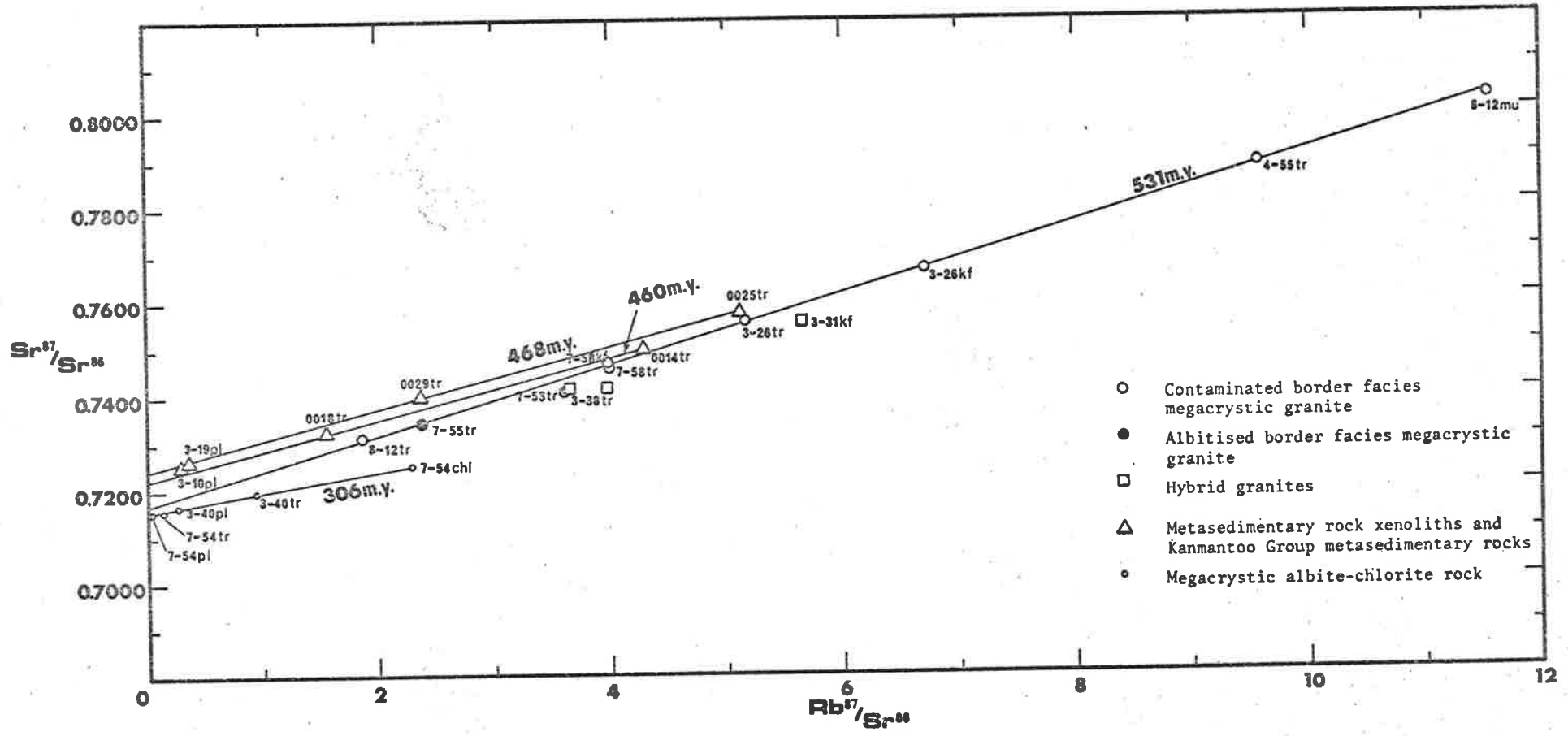


FIGURE 40

Rb-Sr isochron diagram incorporating the results of isotope dilution analyses of micas from varieties of the Encounter Bay Granites and Kangaroo Island granitic rocks. The isochrons shown on the diagram are mica - total-rock isochrons.

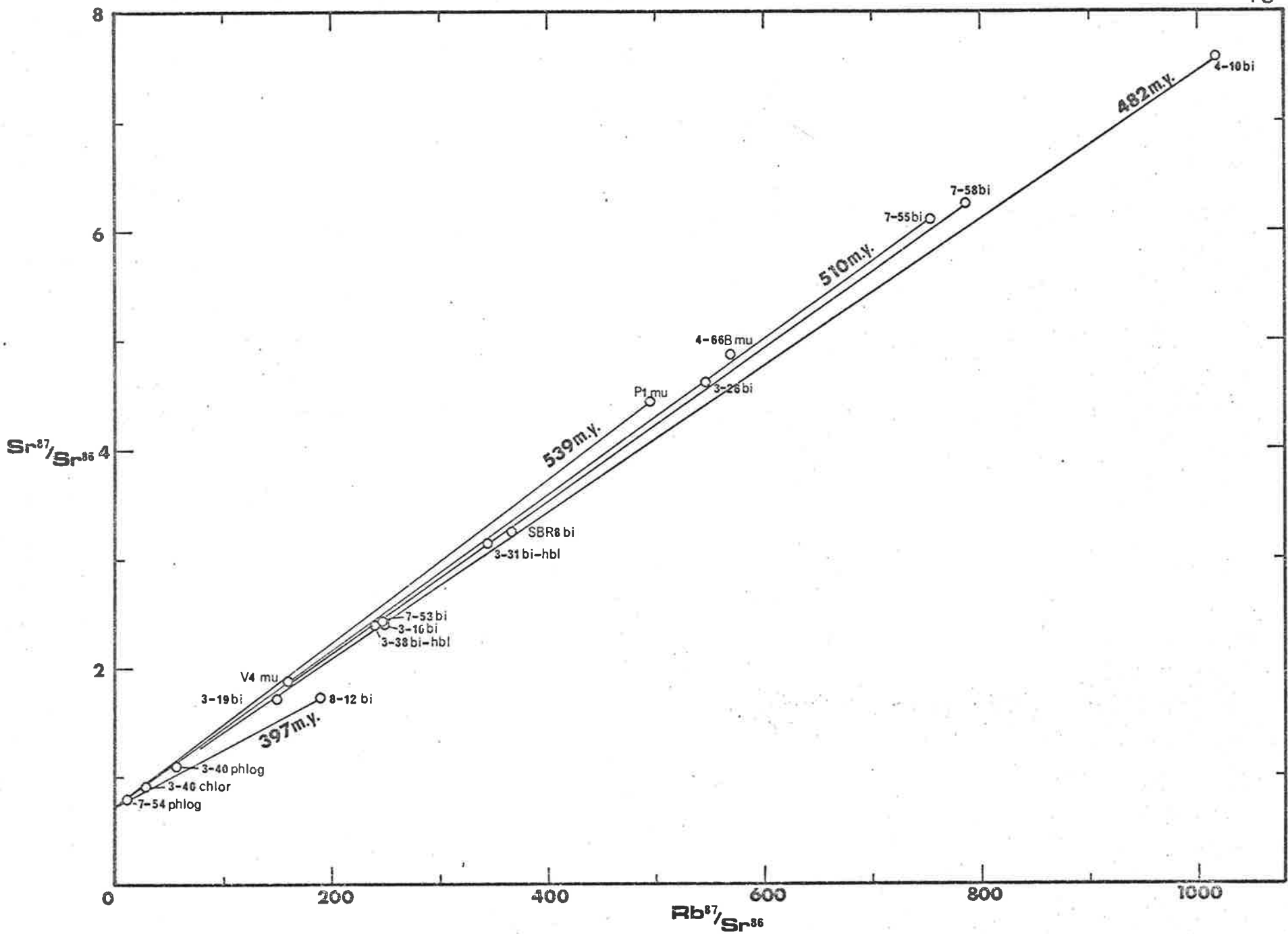


FIGURE 41

Rb-Sr isochron diagram incorporating the results of isotope dilution analyses of the contaminated border facies megacrystic granite and uncontaminated granite varieties.

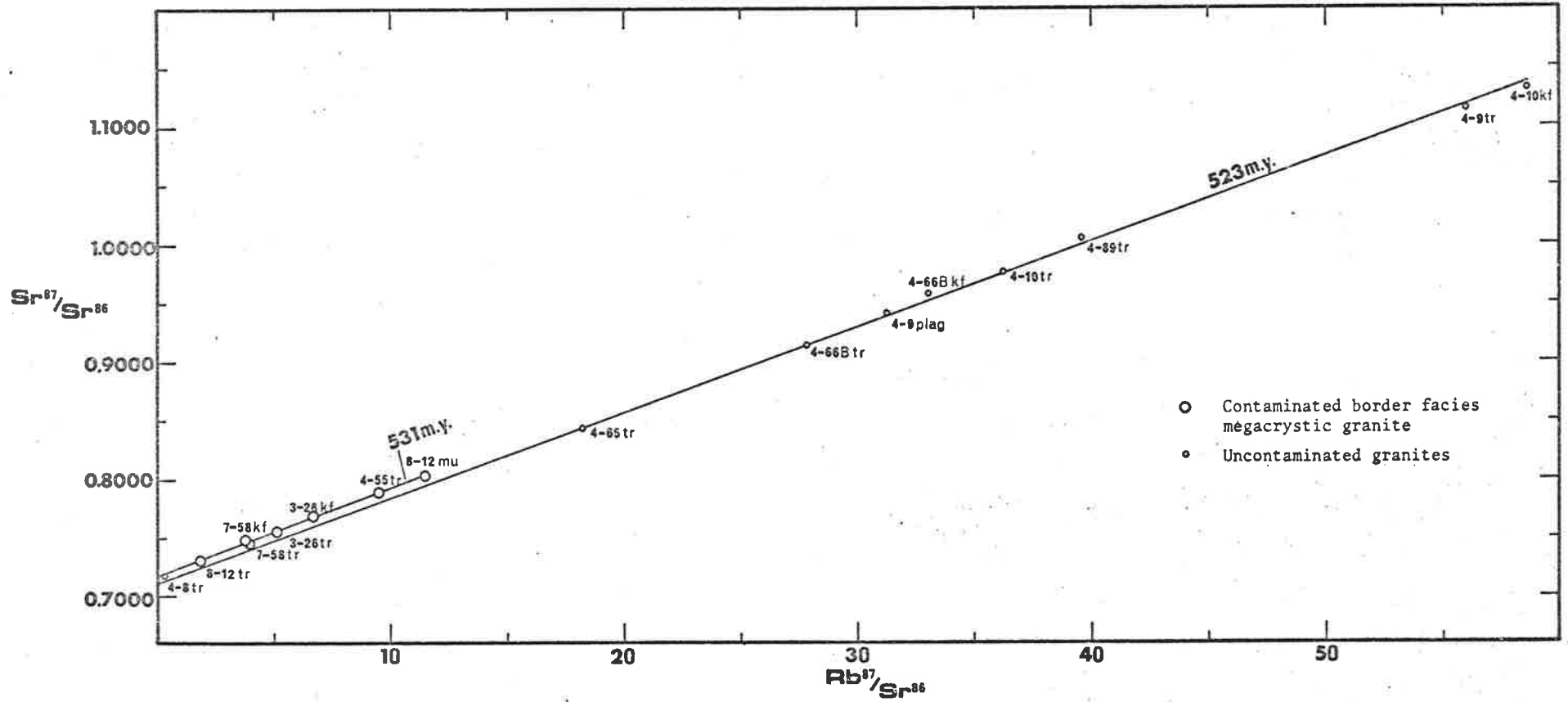


PLATE 1

Aerial view of the coastline in the Encounter Bay area (see Figures 2 and 7) looking north-eastwards along the line of outcrops of Encounter Bay Granites. Victor Harbour is visible on left hand side of photograph. The contact between the granites and the Kanmantoo Group metasedimentary rocks is exposed only at Rosetta Head and on Wright Island, as indicated by the arrows. The Kanmantoo Group metasedimentary rocks are well exposed in the cliffs to the left of Rosetta Head (the highest point of which is about 100m above sea level), and form the low hills in the left background.

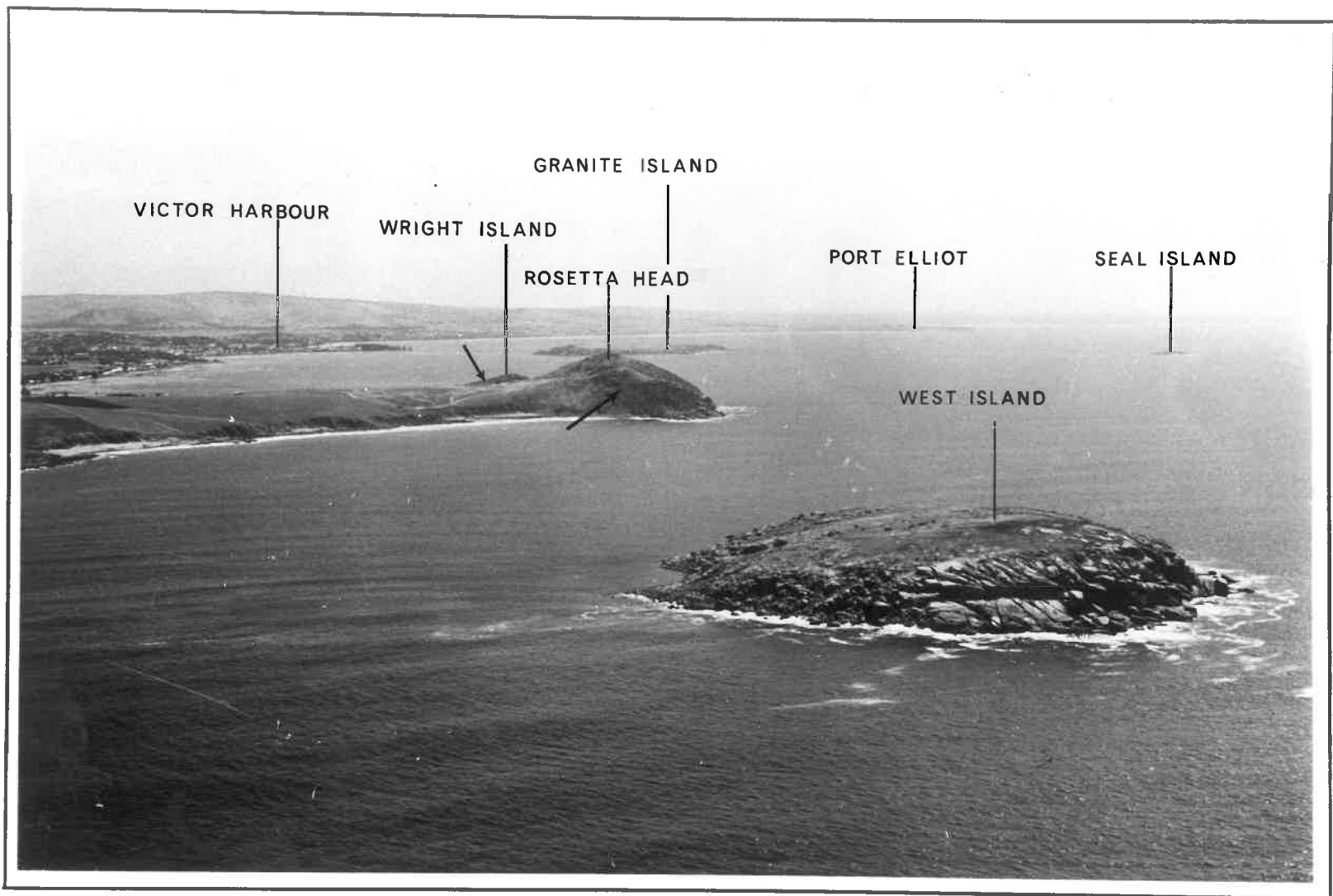
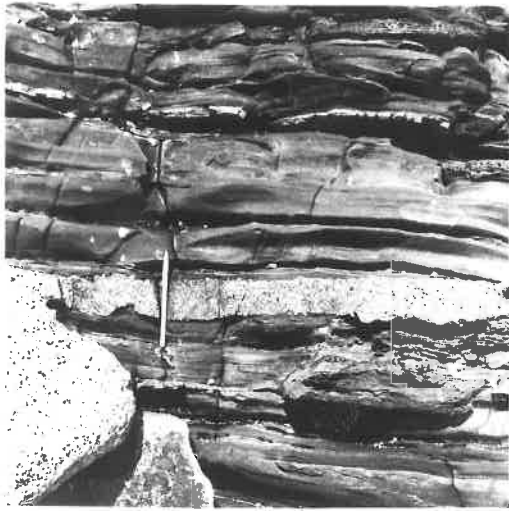


PLATE 2

1, 2 and 3. Photographs of concordant granite sheets in Petrel Cove Formation metasiltsstones adjacent to the contact with the Encounter Bay Granites on Wright Island. Thin sheets, as shown in 1, are generally composed of fine to medium grained megacrystic granite. Thicker sheets, as shown in 3, are always composed of medium to coarse grained megacrystic granite. The large crystals in the megacrystic granite in 3 are potash feldspar. Two small metasedimentary rock xenoliths can be seen in this megacrystic granite sheet. (Pen in each of the photographs is 15cm long).



1



2



3

PLATE 3

1. Wedging concordant (lower) and discordant (upper) megacrystic granite veins in Petrel Cove Formation metasiltsstones adjacent to the contact with the Encounter Bay Granites on Wright Island. (Pen is 15cm long).
2. Partly concordant megacrystic granite vein with discordant termination in laminated Petrel Cove Formation metasandstones adjacent to the contact with the Encounter Bay Granites at Rosetta Head. Note fine grain size of the granite in the thinnest portions of the vein, and dislocation of laminations along vertical discordant veinlet (arrowed). (Coin is 1.9cm in diameter).
3. Concordant and discordant granite veinlets in laminated Petrel Cove Formation metasiltsstones adjacent to megacrystic granite sheet shown in Plate 2: 3. Note small-scale folds in granite veinlets and sedimentary laminations (arrowed). (Pen is 11cm long).
4. Concordant and sharp but serrated contact between megacrystic granite sheet and laminated Petrel Cove Formation metasandstone on Wright Island. The serrations are due to the projection of feldspar and quartz crystals from the granite into the metasiltsstone. (Pen is 14cm long).



1



2



3



4

PLATE 4

1. Discordant xenoliths of laminated metasilstone stoped from the Petrel Cove Formation at its contact with the marginal megacrystic granite facies of the Encounter Bay Granites on Wright Island. (Pen is 15cm long).
- 2 and 3. Laminated metasandstones of the Middleton Sandstone as xenoliths in the marginal megacrystic granite facies of the Encounter Bay Granites along the coastline north of the light station at Cape Willoughby, Kangaroo Island. The Encounter Bay Granites here are in contact with the Middleton Sandstone. (Hammer head is 13cm long).



2



3



PLATE 5

1. Mesoscopic F_1 folds in Campana Creek Member of Carrickalinga Head Formation, about 1.6km east of Madigan Inlet in type section of Kanmantoo Group. View is towards the south. These folds mimic the style of the regional overturned anticline that occurs at Madigan Inlet. Note dislocation of overturned limbs along small-scale thrust planes that approximately parallel the axial plane schistosity S_1 . (Pen is 14cm long).
2. Mesoscopic F_1 fold in fine grained metasandstones and andalusite schists of the Petrel Cove Formation in wave-cut platform just west of Petrel Cove. Fold has a broad, open, upright style compared with folds of the same generation in the western part of the type section (as shown in 1). Note S_1 schistosity axial plane to the fold, striped layering (S_S), and crenulation cleavage (S_2). Andalusite poikiloblasts are concentrated along the margins of some stripes and are depleted adjacent to others (arrows). (Pen is 14cm long).
3. Mesoscopic F_1 fold in laminated Petrel Cove Formation metasiltstones in the wave-cut platform just west of King Point. Note dislocation of bedding laminations along fractures that are approximately parallel to the axial plane schistosity. Alteration has occurred along these fractures. (11cm of pen appears in the photograph).
4. Tight mesoscopic F_1 folds in laminated Petrel Cove Formation metasiltstones along wave-cut platform between King Point and Petrel Cove. The right-hand limbs of the folds appear to have been dislocated along planes (arrowed) that are approximately parallel to the axial plane schistosity of the folds. (Coin is 2.1cm in diameter).

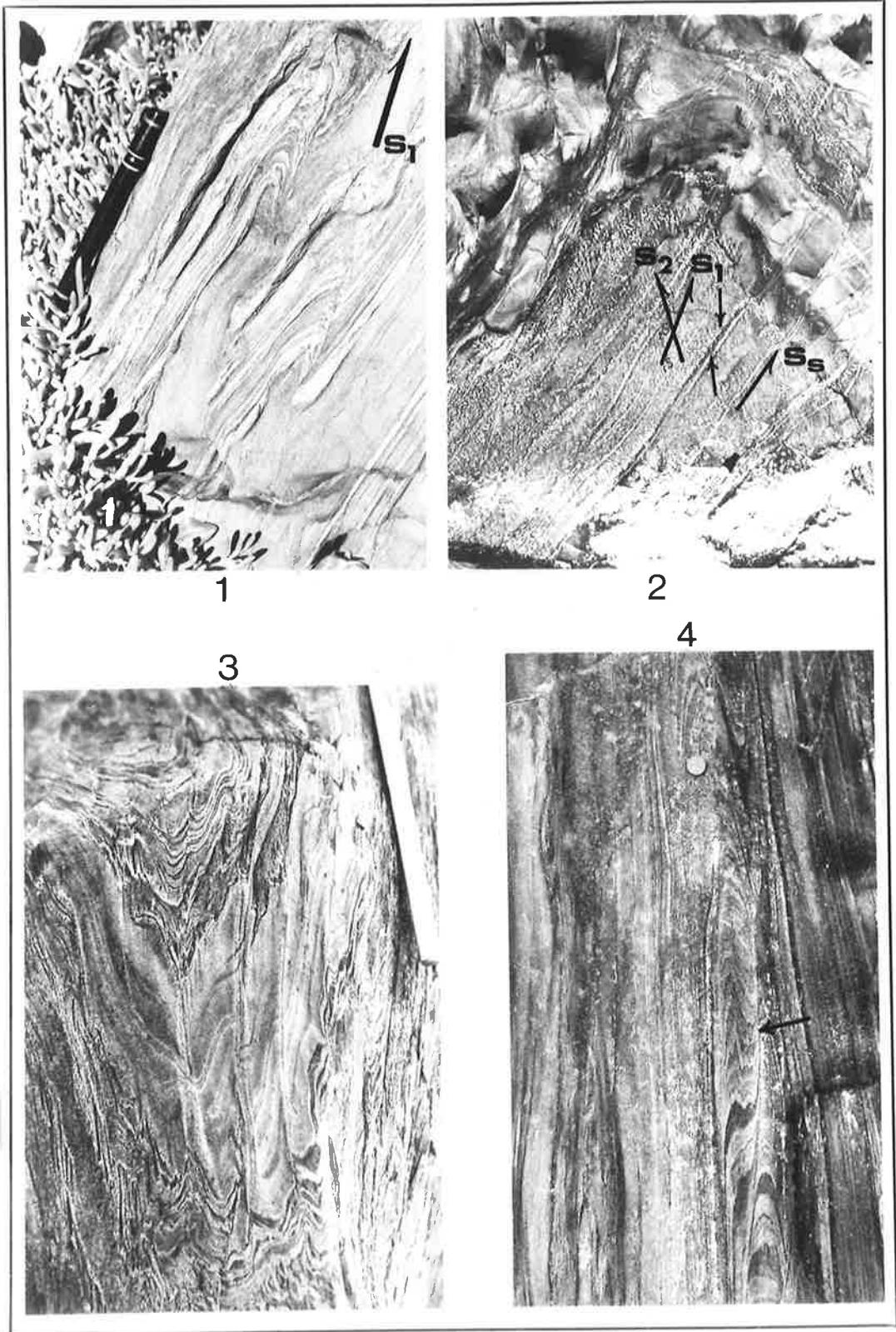


PLATE 6

1. Sedimentary structures including load-casts and associated climbing ripple-trains that have been deformed by the S_1 schistosity. Petrel Cove Formation metasandstones in wave-cut platform between King Beach and Petrel Cove. (Pen is 14cm long).
2. Similar view to that shown in 1. Elongation of sedimentary structures on bedding plane defines L_1 lineation (arrow) which is parallel to the axes of F_1 folds. (Pen is 14cm long).
3. Quartz-rich augen aligned parallel to the S_1 schistosity. Petrel Cove Formation metasilstone (bedding laminations shown as S_0) in wave-cut platform west of King Point. (10cm of pen appears in photograph).
4. Andalusite and chlorite augen aligned parallel to the S_1 schistosity in Petrel Cove Formation andalusite schist. Bedding laminations are well displayed in thin metasilstone band. Wave-cut platform west of King Point. (Pen is 14cm long).

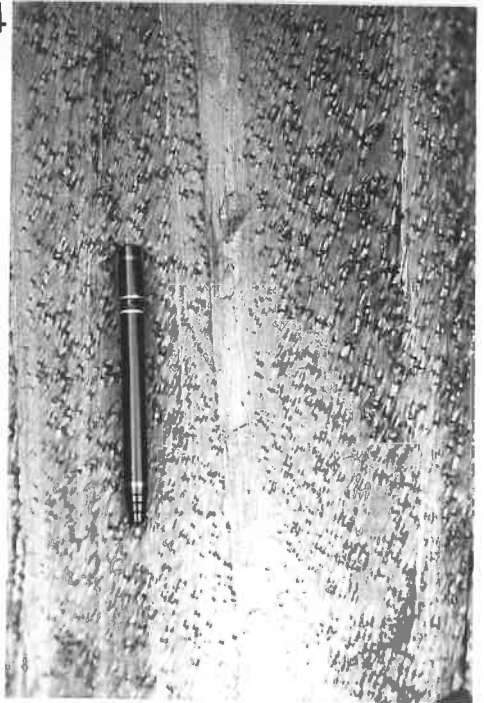


1



2

4



3

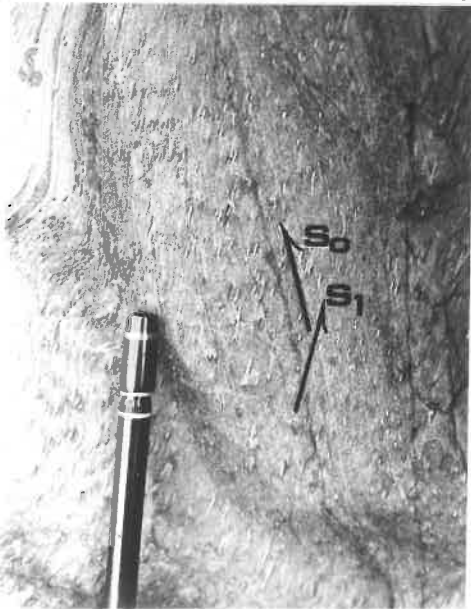
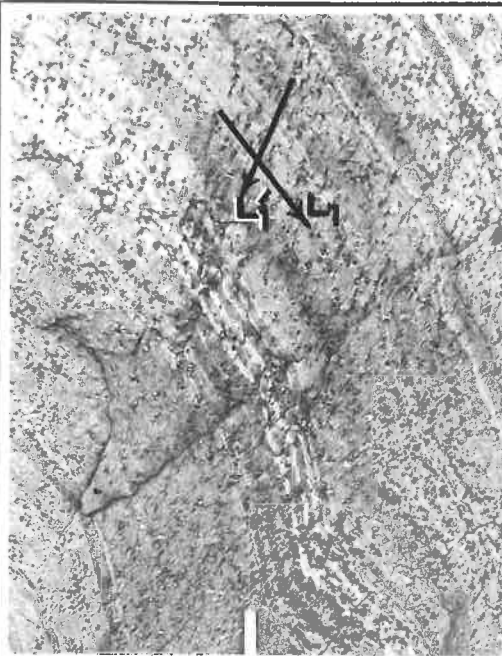


PLATE 7

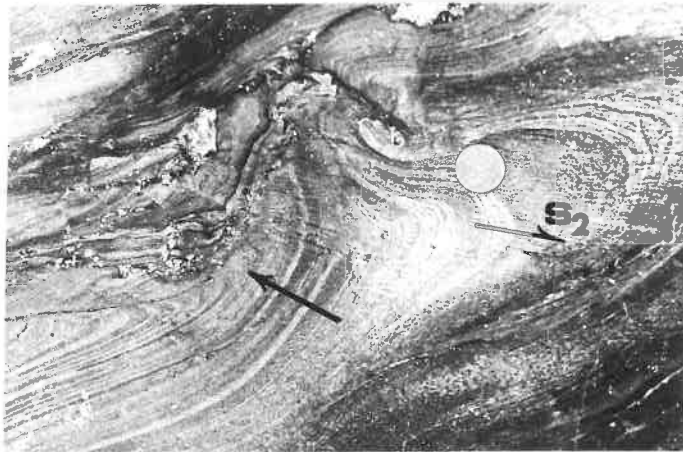
1. S_1 schistosity surface in Petrel Cove Formation andalusite schist just west of King Point. Intersection between bedding and the S_1 surface defines an L_1 lineation that is parallel to the axes of F_1 folds. The elongation of andalusite augen in S_1 defines a second lineation (L_1') which is oriented at a high angle to L_1 . (2cm of pen appears in photograph).
- 2, 3 and 4. Mesoscopic F_2 folds in Petrel Cove Formation laminated metasiltsstones in wave-cut platform between Petrel Cove and King Beach. Note refolded F_1 folds in 2 and 3 (arrowed). S_2 crenulation cleavage axial plane to F_2 folds is well displayed in 3 and 4. (Coin in 2 and 3 is 2.1cm in diameter; coin in 4 is 1.9cm in diameter).



1



2



3



4

PLATE 8

1. Mesoscopic F_2 fold in Petrel Cove Formation phyllite in wave-cut platform between King Beach and Petrel Cove. Note well developed crenulation cleavage (S_2) axial plane to the fold. (Hammer is 28cm long).
2. Striped layering oriented at a moderate angle to S_1 in Petrel Cove Formation metasandstone in wave-cut platform just west of Petrel Cove. Note biotite-rich border zones and biotite-filled central fractures. (Coin is 2.3cm in diameter).
3. Refraction of striped layering across boundaries between interbedded phyllites and metasandstones on coastline just west of Petrel Cove. Note well developed sedimentary structures at base of metasandstone beds, especially near top of photograph. Crenulation cleavage (S_2) visible in vicinity of andalusite porphyroblasts in phyllite near bottom of photograph. (Hammer is 28cm long).
4. Flaring of striped layering in Petrel Cove Formation metasandstones along coastline just west of Petrel Cove. (Hammer is 28cm long).



1



2

3

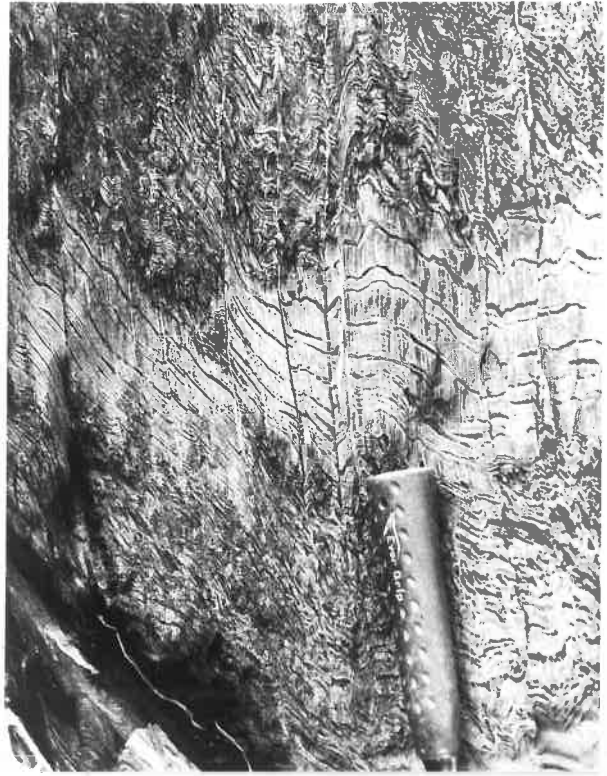


4

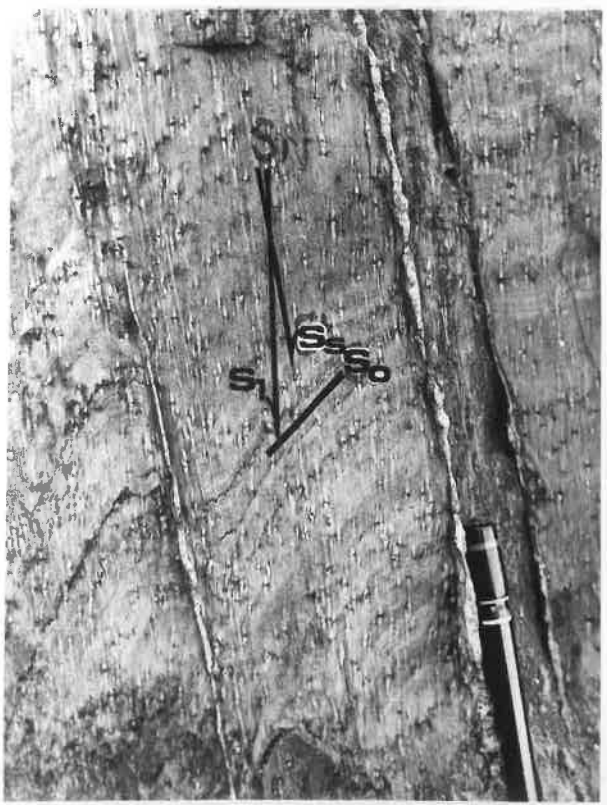


PLATE 9

1. Fractures and thin pegmatites defining dislocation planes parallel to the striped layering in hinge zone of mesoscopic F_1 fold in Petrel Cove Formation laminated metasiltstone. Striped layering is approximately parallel to S_1 schistosity. Wave-cut platform just west of King Point. (Hammer grip is 15cm long).
2. Thin quartzo-feldspathic pegmatites defining dislocation planes parallel to striped layering (S_s) in Petrel Cove Formation andalusite schist on coastline west of King Point. Striped layering is at a low angle to S_1 , which is marked by the elongation of andalusite augen. Bedding is designated S_0 . (10cm of pen appears in photograph).



1



2

PLATE 10

1. Fractured and brecciated zone along limb of mesoscopic F_1 fold in Petrel Cove Formation metasiltsstones in wave-cut platform just west of King Point. Bedding can still be traced through the fractured and brecciated zone. (Coin is 1.7cm in diameter).
2. Fractured and brecciated zone in fine grained metasandstones in Petrel Cove Formation along coastline just east of King Beach. Note light coloured zones of alteration along fractures. (Hammer is 28cm long).
3. Refraction of striped layering across boundaries between andalusite schists and metasiltsstones in Petrel Cove Formation on western side of Petrel Cove. Striped layers are folded by S_2 crenulation in andalusite schist bands. (Pen is 14cm long).
4. Small scale F_1 fold (arrowed) is thinly bedded fine grained metasandstones on northern limb of large scale F_2 fold in Middleton Sandstone, north wall of Middleton quarry near entrance. (Scale on right hand side of photograph is in millimetres).
5. Refolded small scale F_1 fold in metasandstones with epidote-rich bands in hinge of mesoscopic F_2 fold in Middleton Sandstone. North side of Middleton quarry. (Coin is 2.1cm in diameter).

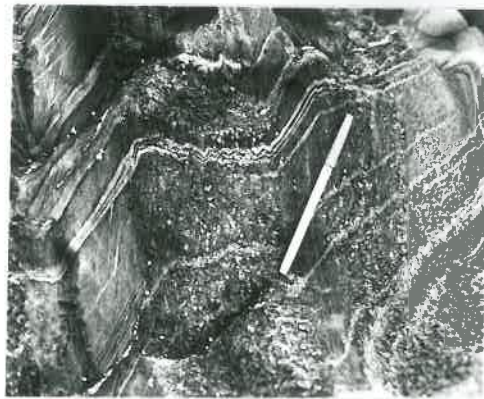


PLATE 11

1. Large scale south-easterly plunging F_2 fold in metasandstones of Middleton Sandstone, south side of Middleton quarry. Light coloured layers in metasandstones are epidote-rich. Note prominent fracture set (interpreted as S_2 fracture cleavage) parallel to inferred axial plane of fold. (Height of fold hinge above quarry floor approximately 11m).
2. Prominent ridge-and-furrow lineation (L_2) defined by the intersection of bedding with the S_2 fracture cleavage in metasandstones of the Middleton Sandstone. Steeply pitching mica streaking lineation (L_1) also occurs on bedding surfaces. Light coloured layers in metasandstones are enriched in epidote and plagioclase. South side of Middleton quarry near entrance. (Compass is 5cm wide).
3. S_2 fracture cleavage in hinge and limb of mesoscopic F_2 fold in metasandstones in Middleton Sandstone, north side of Middleton quarry. (Hammer is 28cm long).
4. Thin pegmatites in S_2 fracture cleavage cutting across epidote-rich bands (light coloured) in metasandstones near hinge of fold shown in 3. (Bar represents 5cm).



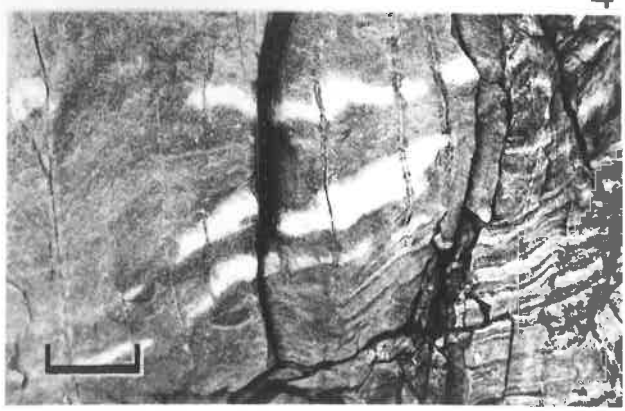
1



2



3



4

PLATE 12

1. Mesoscopic fold in thinly bedded metasediments in Middleton Sandstone, north-western wall of Middleton quarry. Note distinct lineation (L) defined by fold hinges, and contrast with mica-streaking lineation (ms) present on axial plane schistosity surface (S). (Bar scale represents 5cm).
2. Large thin section cut from face of fold in 1. Note pronounced axial plane mica schistosity (S) which folds pre-existing mica schistosity (S_p) in some beds. Note also that some folds do not persist from one bed to the next. (Scale is in millimetres).
3. Mesoscopic F_2 fold in thinly bedded metasediments in Middleton Sandstone, northern end of Middleton quarry. L_2 lineation defined by intersection of bedding with S_2 fracture cleavage. Mica-streaking lineation (ms) occurs in S_1 schistosity, which is approximately parallel to bedding in this specimen. (Bar scale represents 5cm).
4. L_2 ridge-and-furrow lineation and mica-streaking lineation (ms) on metasediment bedding surface in Middleton Sandstone, southern wall of Middleton quarry near entrance. (Pen is 14cm long).

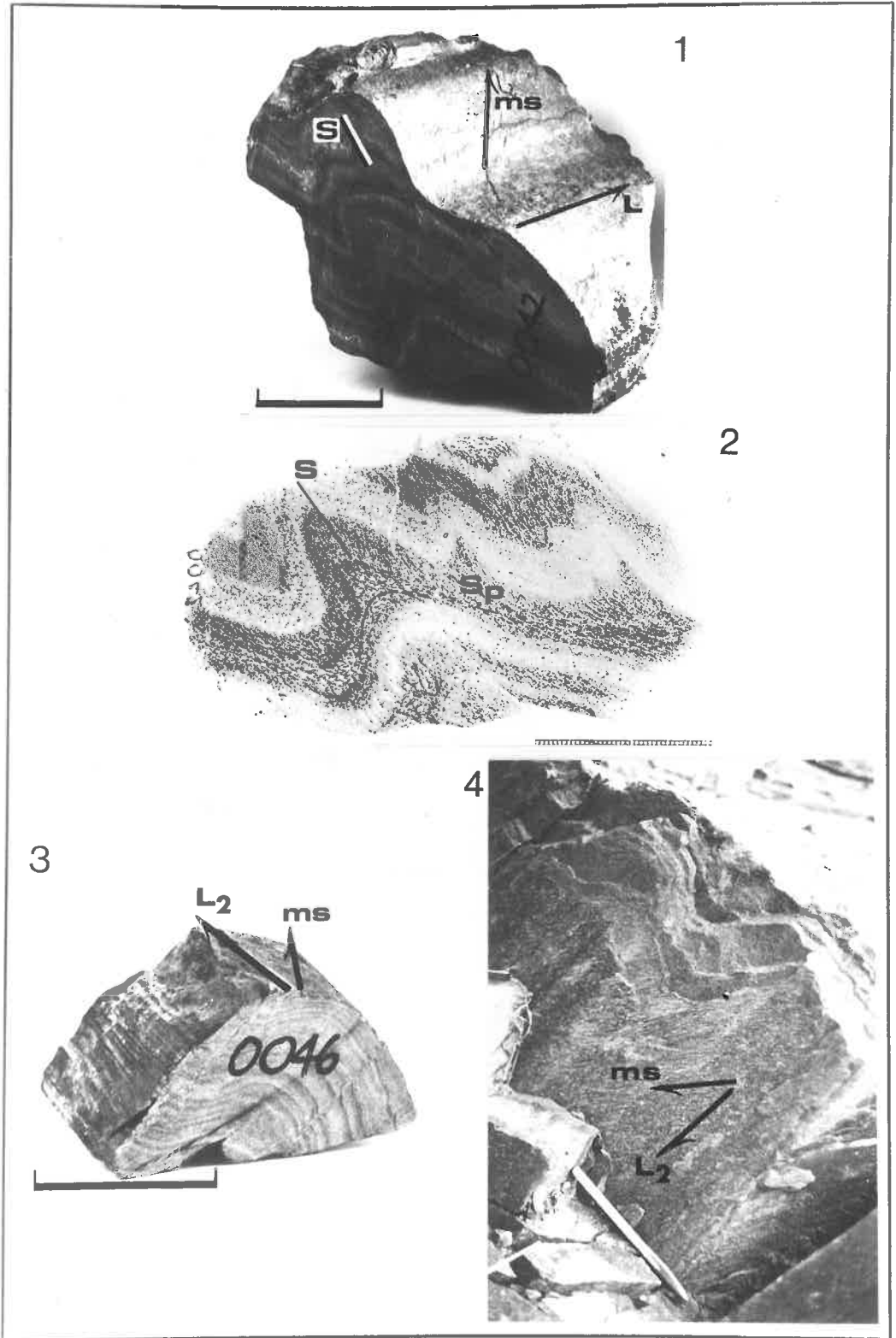


PLATE 13

1. Contact between thick megacrystic granite sheet and Petrel Cove Formation metasandstone on south-western side of Wright Island. Note S_1 schistosity (parallel to pen) in parts of border of granite sheet and in the adjacent metasandstone. Note also small-scale F_1 folds (F) in thin granite veins. (Pen top is 4.6cm long).
2. Well developed S_1 schistosity in borders and constricted portion of boudinaged megacrystic granite sheet in Petrel Cove Formation meta-sediments on south-western side of Wright Island. Many of the large feldspar megacrysts have been deformed into augen. (Hammer is 28cm long).
3. Prominent S_1 schistosity (parallel to hammer handle) in marginal 1m or so of the main mass of megacrystic granite at its contact (outlined in ink) with Petrel Cove Formation metasiltstones on the north-western side of Wright Island. Dark coloured metasiltstones within the granite have been deformed in the plane of the schistosity. (Hammer is 28cm long).
4. Partly polished slab of schistose megacrystic granite from marginal part of the main granite mass on Wright Island. Collected from the vicinity of photograph 3. Note well developed layered schistosity which enwraps potash feldspar (K) and plagioclase (P) augen. (Scale is in millimetres).

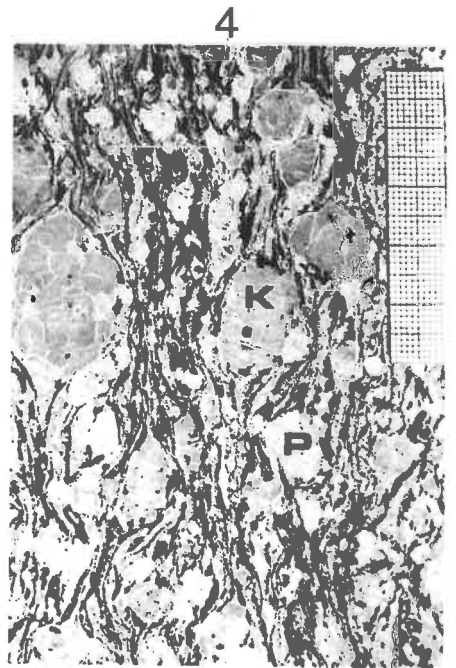


PLATE 14

- 1 and 2. Microfolds in layered schistosity in marginal parts of the main granite mass on Wright Island. The folded layers are alternately quartz-rich and biotite-rich. Note that the axial plane schistosity of the folds is defined by a preferred orientation of biotite crystals which also defines the layered schistosity on a broader scale. (Bar scale represents 0.50mm).
3. S₂ crenulations in biotite-rich border zone of thin granite sheet (G) within Petrel Cove Formation metasediments on Wright Island. (Bar scale represents 0.50mm).
4. Broad scale kink fold in thin concordant megacrystic granite sheet and Petrel Cove Formation metasediments on north-western side of Wright Island. Fractures parallel to pen are possibly axial plane to the fold. (Pen is 14cm long).

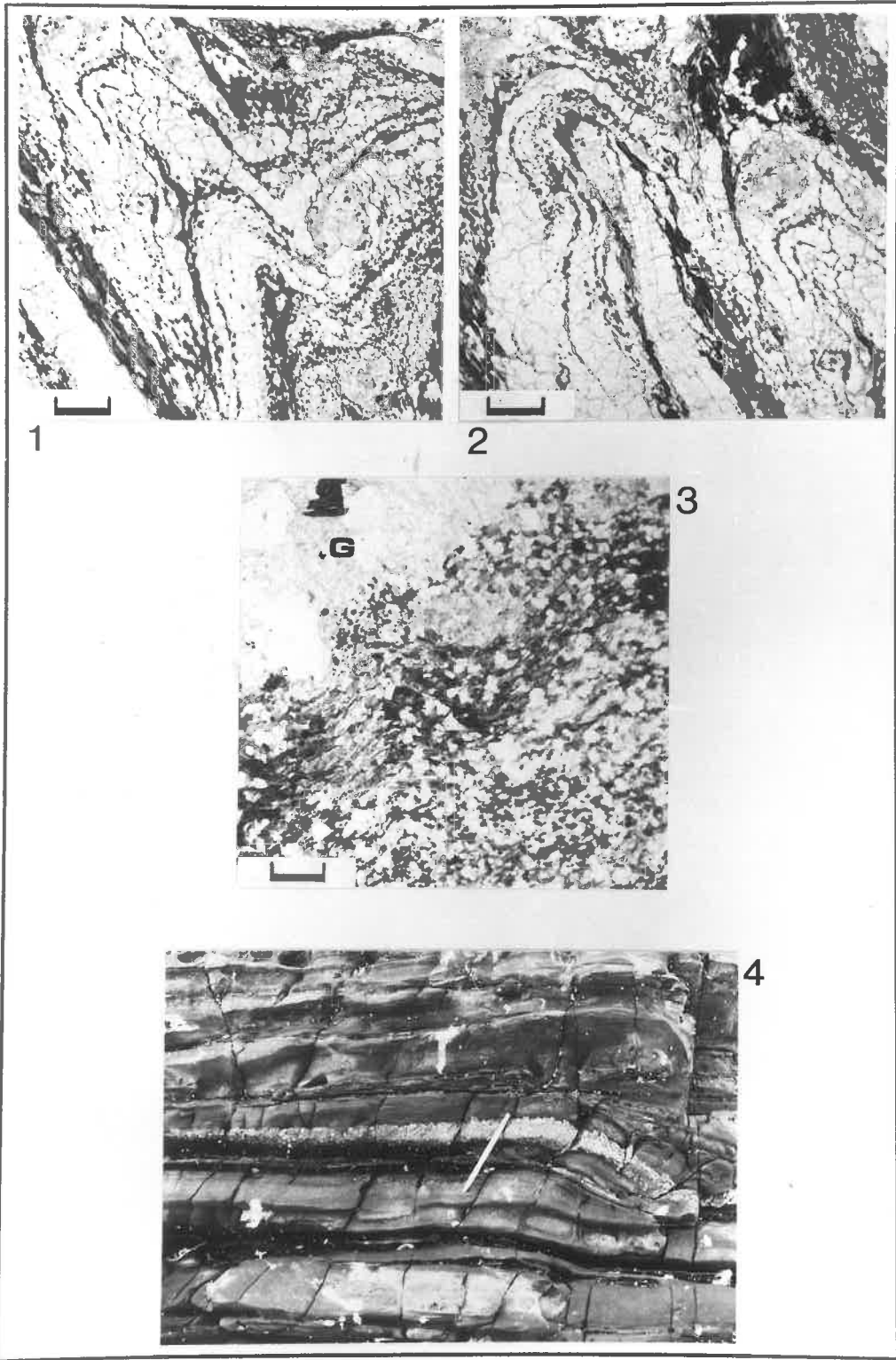


PLATE 15

1. View of contact zone between Encounter Bay Granites and Petrel Cove Formation metasediments (dark material in foreground) on south-western side of Wright Island, showing prominent joint planes (dipping steeply towards right) along which albitisation and subsequent cataclasis occurred. Figure (arrowed) is about 1.8m tall.
2. Well developed fluxion structure in cataclastic albitite from jointed zone shown in 1. Note fractured albite megacrysts (A). (Scale is in millimetres).
3. Part of albitised contact zone between the marginal megacrystic granite facies of the Encounter Bay Granites and the Petrel Cove Formation metasediments near south-western tip of Rosetta Head. The megacrystic granite has been altered to megacrystic albite-chlorite rock (the conspicuous large crystals were originally potash feldspar but are now composed of albite) and contains albitised xenoliths of Petrel Cove Formation metasediments. (Hammer is 28cm long).
4. Mesoscopic folds in Petrel Cove Formation metasandstones near contact with the Encounter Bay Granites, south-western tip of Rosetta Head. Note the complex style of the structures at the points arrowed. (Coin is 1.9cm in diameter).

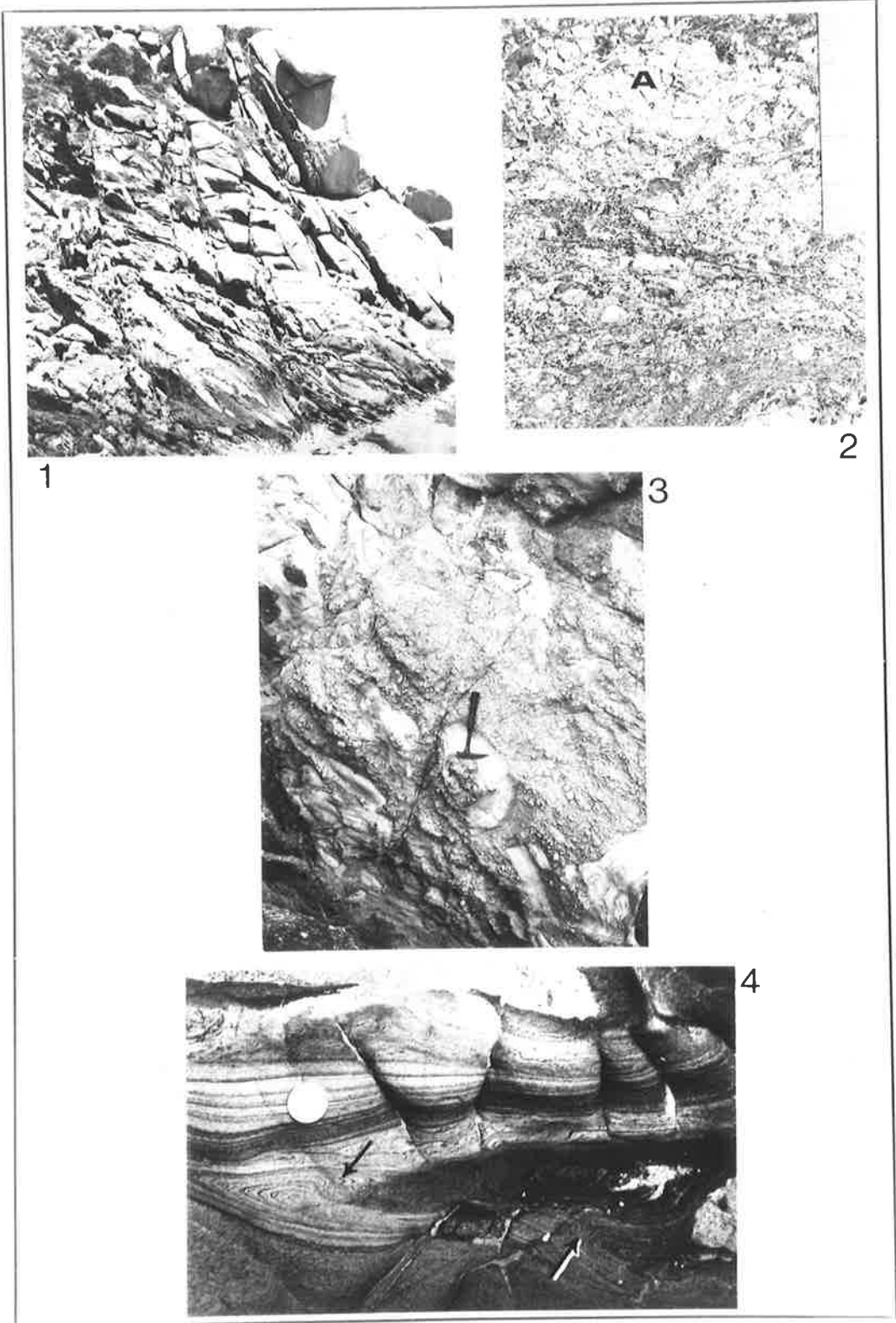


PLATE 16

1. Mesoscopic folds of presumed sedimentary origin in Petrel Cove Formation metasandstones near contact with Encounter Bay Granites, south-western tip of Rosetta Head. Note completely closed structures (arrowed). (Coin is 1.9cm in diameter).
2. Dislocated fold structure in Petrel Cove Formation metasandstones near contact with Encounter Bay Granites, south-western tip of Rosetta Head. Structure is probably of sedimentary origin. Dark layer above structure is a continuous thin bed. (Coin is 1.9cm in diameter).
- 3 and 4. Mesoscopic folds along small-scale dislocation zones in Petrel Cove Formation metasandstones near contact with Encounter Bay Granites, south-western tip of Rosetta Head. (Coin is 1.9cm in diameter).

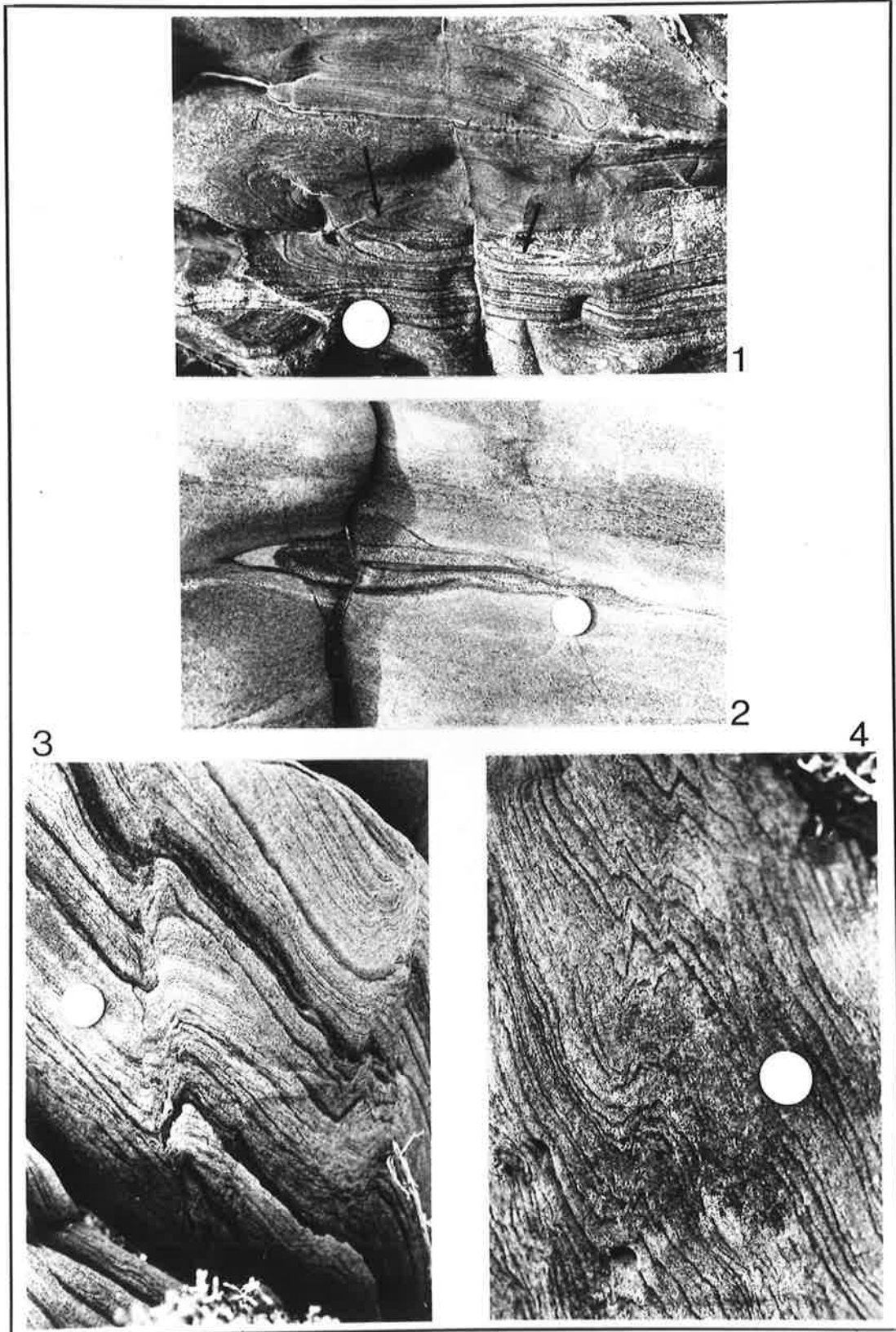
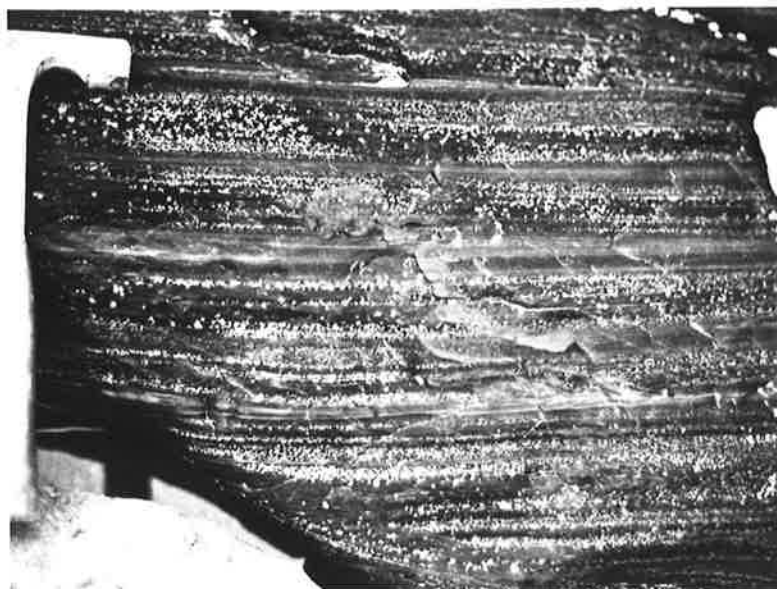


PLATE 17

1. Small post-F₁ andalusite porphyroblasts confined to thin beds in Petrel Cove Formation metasilstone in wave-cut platform on eastern side of Petrel Cove. (Hammer is 28cm long).
2. Small post-F₁ andalusite porphyroblasts concentrated along thin post-F₁ granitic veinlet in Petrel Cove Formation metasilstone. Locality as in 1. Note very small andalusite spots throughout the rock. (Hammer is 28cm long).



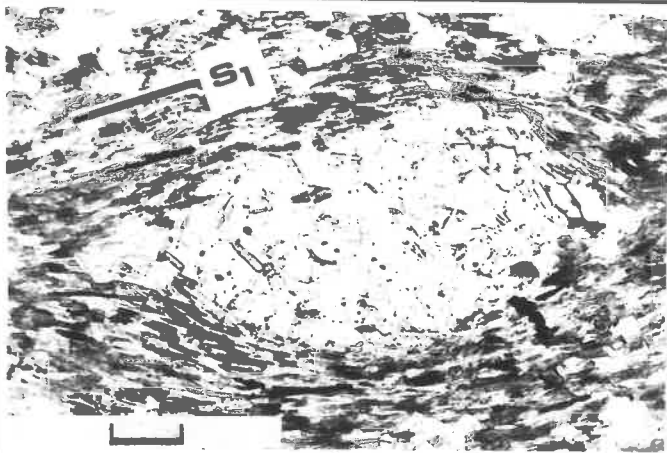
1



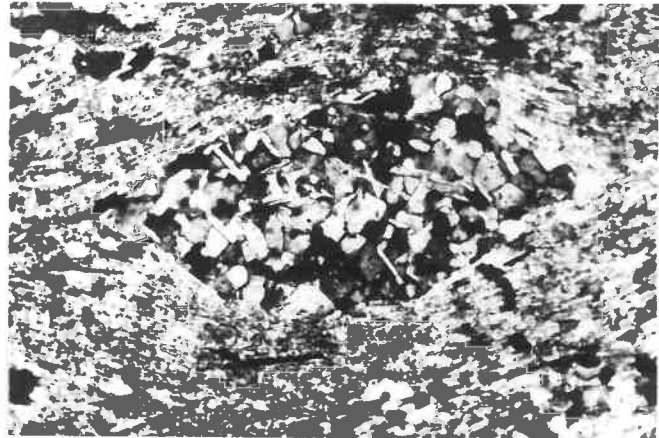
2

PLATE 18

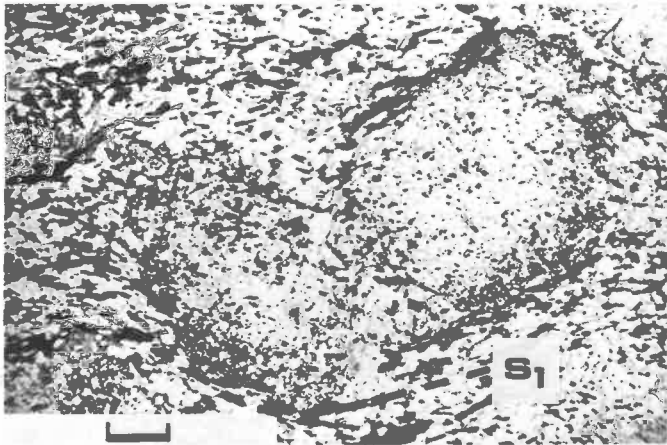
1. Pre-F₁ quartz-rich aggregate containing randomly to poorly oriented micas. The aggregate is enwrapped by well developed external S₁ mica schistosity. Thin section of Balquhadder Formation spotted schist SC97. Transmitted plane polarised light. (Bar scale represents 0.10mm).
2. Field in 1 - crossed nicols.
3. Pre-F₁ cordierite poikiloblasts which are enwrapped by external S₁ mica schistosity and have been rotated by it. Note lack of internal fabric in poikiloblasts. Thin section of Petrel Cove Formation cordierite schist 7-68. Transmitted plane polarised light. (Bar scale represents 0.50mm).
4. Field in 3 - crossed nicols.



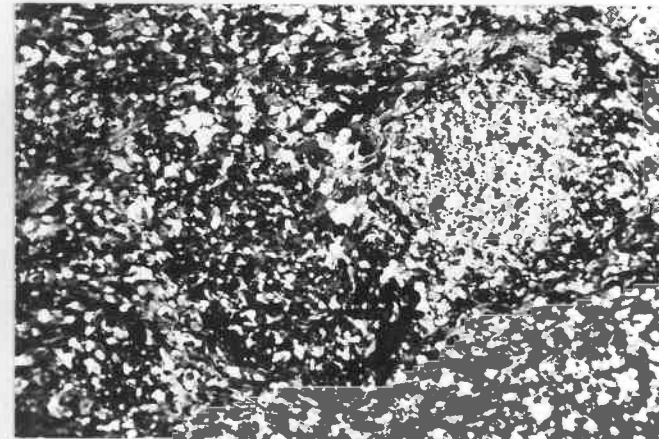
1



2



3



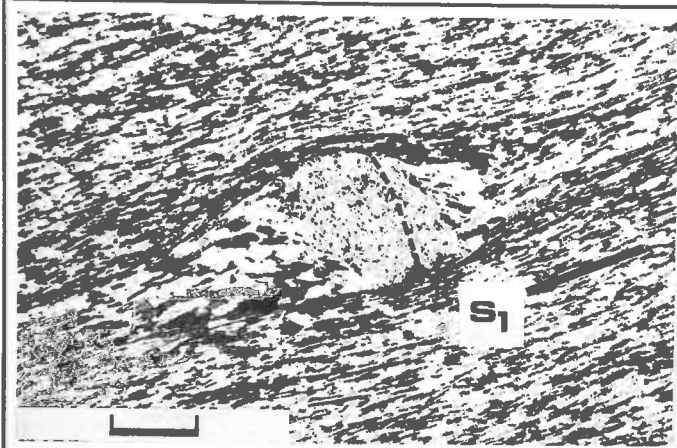
4

PLATE 19

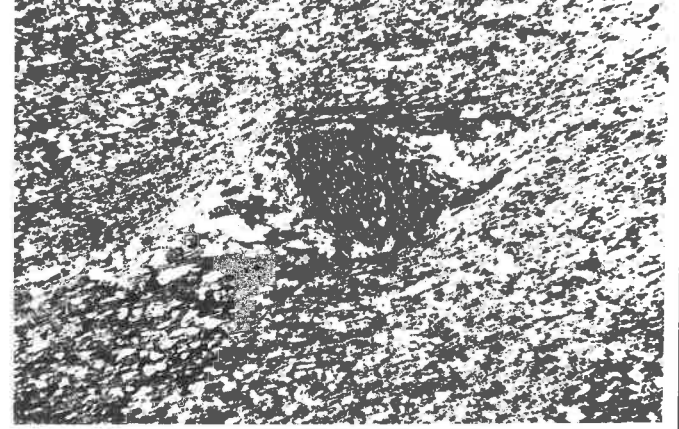
1 and 2. Early syn-F₁ altered cordierite poikiloblast containing a planar internal fabric outlined by inclusions that are significantly finer grained than the same minerals in the groundmass of the rock. The poikiloblast is enwrapped by a well developed external S₁ mica schistosity. Although difficult to see, the poikiloblast internal fabric is continuous with the external fabric. Thin section of Petrel Cove Formation porphyroblastic schist T130A*. Transmitted plane polarised light in 1; crossed nicols in 2. (Bar scale represents 0.50mm).

3 and 4. Early syn-F₁ altered cordierite poikiloblast containing a sigmoidal internal fabric outlined by inclusions that are finer grained than the same minerals in the groundmass of the rock. The internal poikiloblast fabric is continuous with the external S₁ schistosity. Thin section of Petrel Cove Formation cordierite schist SC106a. Transmitted plane polarised light in 3; crossed nicols in 4. (Bar scale represents 0.50mm).

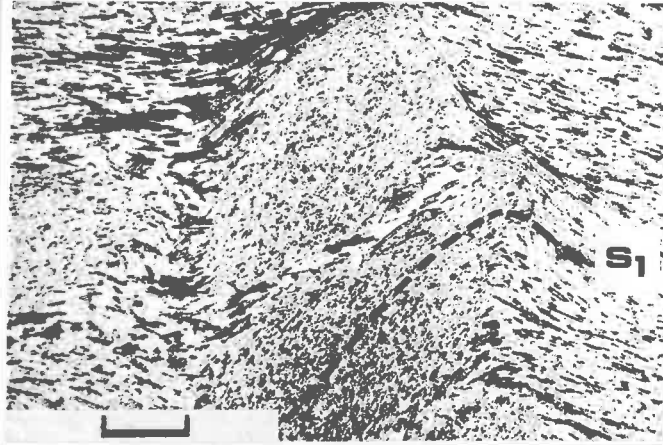
*Specimens numbered with prefix T were kindly loaned by Professor J.L. Talbot (Department of Geology, University of Montana, Missoula)



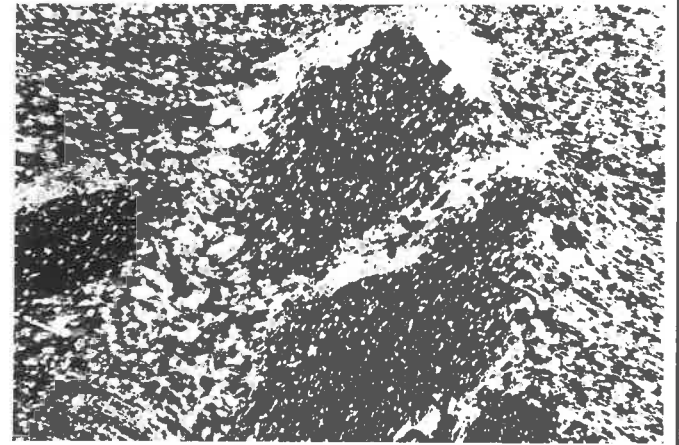
1



2



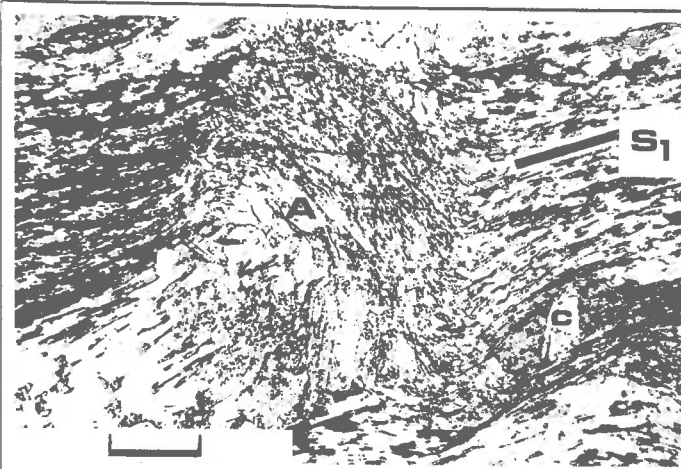
3



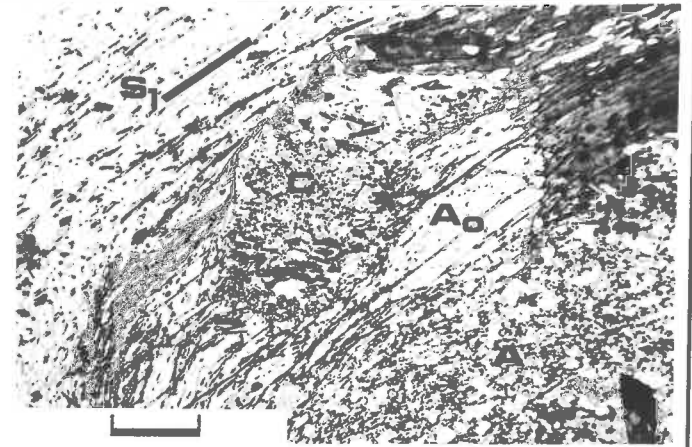
4

PLATE 20

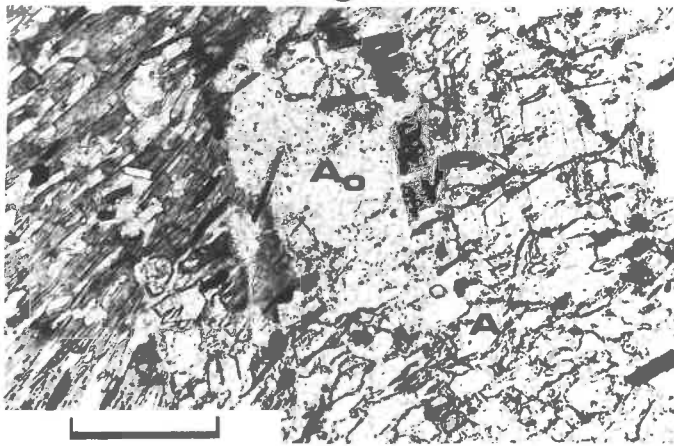
1. Syn-F₁ S-shaped andalusite poikiloblast (A) with S-shaped internal fabric. The internal fabric is continuous with the external S₁ schistosity. Note post-S₁ overgrowth on bottom right of poikiloblast just left of post-F₁ chlorite lath (c). Thin section of Petrel Cove Formation andalusite-cordierite schist T108. Transmitted plane polarised light. (Bar scale represents 0.50mm).
2. Post-F₁ overgrowth (A₀) on syn-F₁ andalusite poikiloblast (A). The overgrowth cuts across the groundmass S₁ mica schistosity and has engulfed a small cordierite poikiloblast (C). Thin section of Petrel Cove Formation andalusite-cordierite schist T135A. Transmitted plane polarised light. (Bar scale represents 0.50mm).
3. Post-F₁ overgrowth (A₀) on syn-F₁ andalusite poikiloblast (A). S₁ schistosity in the groundmass of the rock is defined by the preferred orientation of biotite and opaque mineral laths. Note similar orientation of opaque mineral laths within the andalusite. Note also the sharp contacts between the post-F₁ andalusite fingers and the groundmass biotite. Thin section of Petrel Cove Formation andalusite schist SC102. Transmitted plane polarised light. (Bar scale represents 0.20mm).
4. Syn-F₁ porphyroblastic clot with quartz core (Q) and chlorite margins (c) in thin section of Petrel Cove Formation porphyroblastic schist SC101. The clot has been rotated relative to the groundmass S₁ schistosity during the crystallisation of the chlorite. Transmitted plane polarised light. (Bar scale represents 0.20mm).



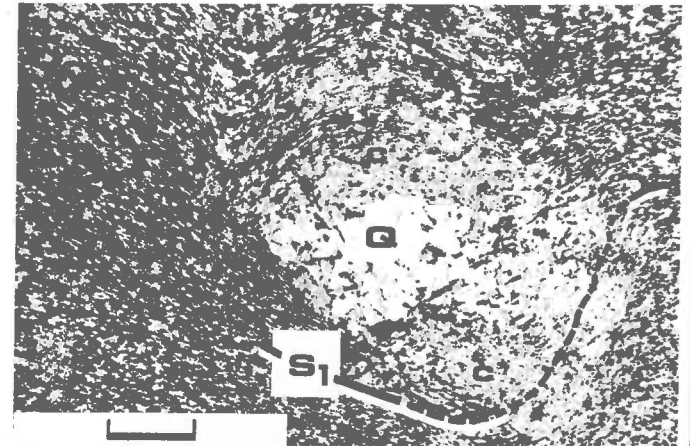
1



2



3



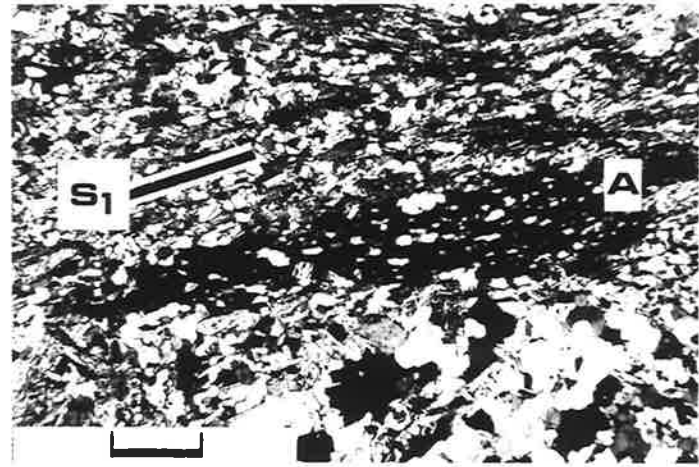
4

PLATE 21

1. Field shown in Plate 20: 4. Crossed nicols. Chlorite is in extinction and appears black. Note relict S_1 schistosity preserved as elongate inclusions within chlorite, especially in crystal nearest top of photograph. Note also post- F_1 overgrowth on left side of this crystal.
2. Post- F_1 andalusite poikiloblast (A) elongate parallel to the groundmass S_1 schistosity, and containing a planar internal fabric (also parallel to external S_1 schistosity) defined by elongate quartz grains. Thin section of Petrel Cove Formation andalusite schist 0081. Transmitted light, crossed nicols. (Bar scale represents 0.50mm).
3. Post- F_1 chlorite poikiloblasts (c) that have inherited relicts of the groundmass S_1 schistosity in the form of oriented opaque mineral laths and quartz grains. Thin section of Petrel Cove Formation andalusite schist SC102. Transmitted plane polarised light. (Bar scale represents 0.50mm).
4. Post- F_1 chlorite poikiloblasts (c) that have inherited relicts of the groundmass S_1 schistosity in the form of oriented quartz grains and opaque mineral laths. Thin section of Tapanappa Formation porphyroblastic phyllite SC50. Transmitted plane polarised light. (Bar scale represents 0.20mm).



1

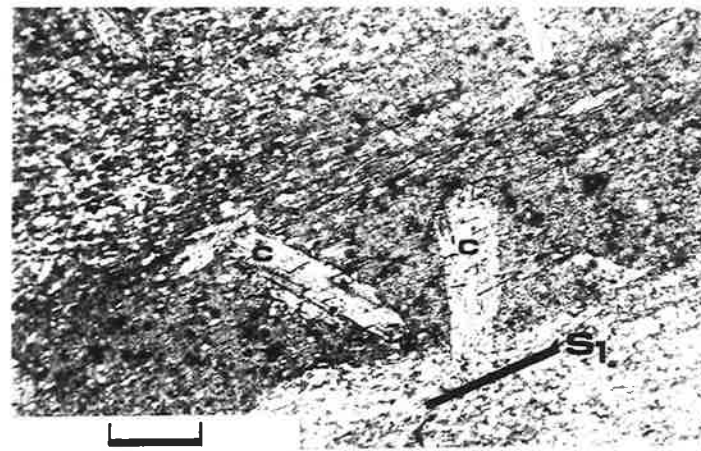


S₁

A

2

3

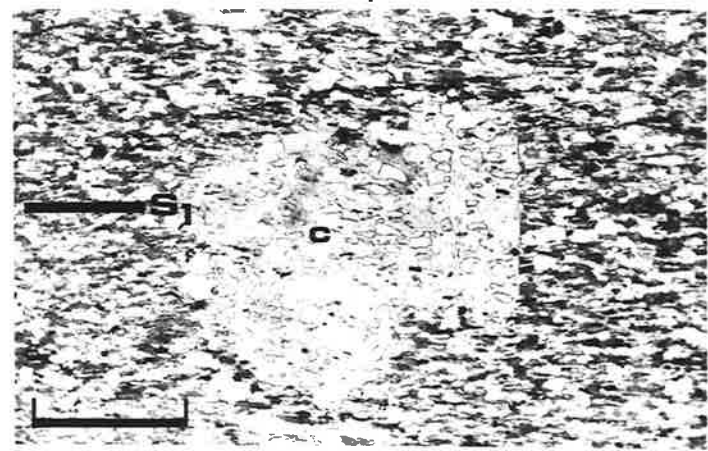


c

c

S₁

4

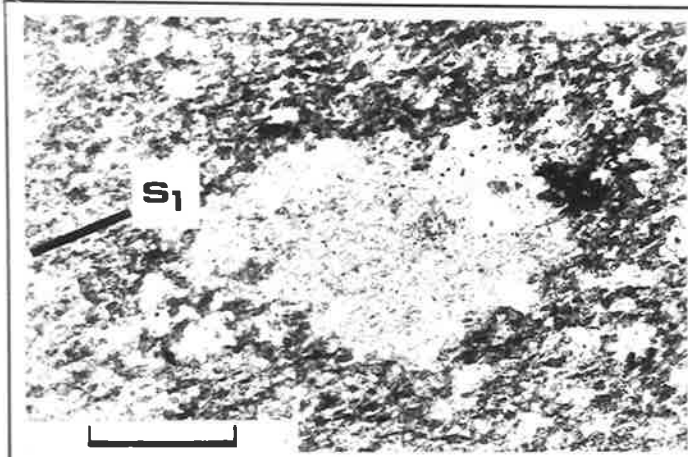


S₁

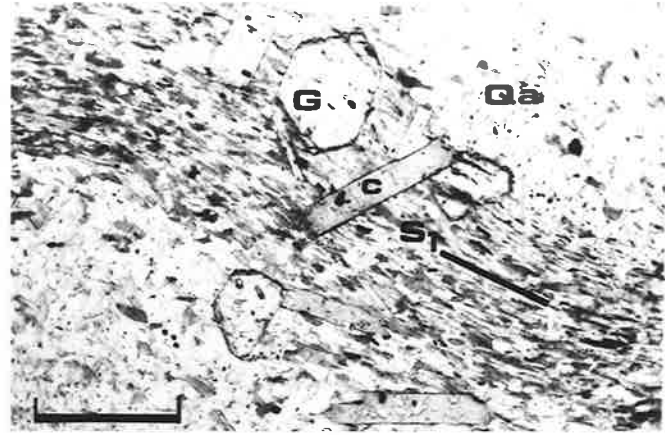
c

PLATE 22

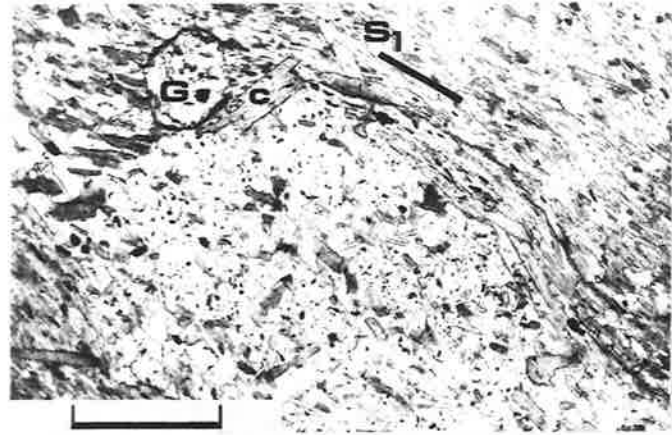
1. Post-F₁ scapolite clot in thin section of Balquhider Formation scapolite-bearing metasilstone SC87c. Transmitted plane polarised light. (Bar scale represents 0.20mm).
2. Post-F₁ garnet (G) and chlorite (c) poikiloblasts with pre-F₁ quartz-rich augen (Qa) in thin section of Tunkalilla Formation porphyroblastic metasilstone SC58a. Transmitted plane polarised light. (Bar scale represents 0.20mm).
3. Post-F₁ garnet (G) and chlorite (c) poikiloblasts at edge of pre-F₁ quartz-rich augen in thin section of Tunkalilla Formation porphyroblastic metasilstone SC58a. Transmitted plane polarised light. (Bar scale represents 0.20mm).
4. Post-F₁ subhedral garnet porphyroblast (G) in thin section of Tapanappa Formation metasandstone SC53. Groundmass S₁ mica schistosity is defined by the preferred orientation of micas, and is approximately horizontal in the photograph. Transmitted plane polarised light (Bar scale represents 0.20mm).



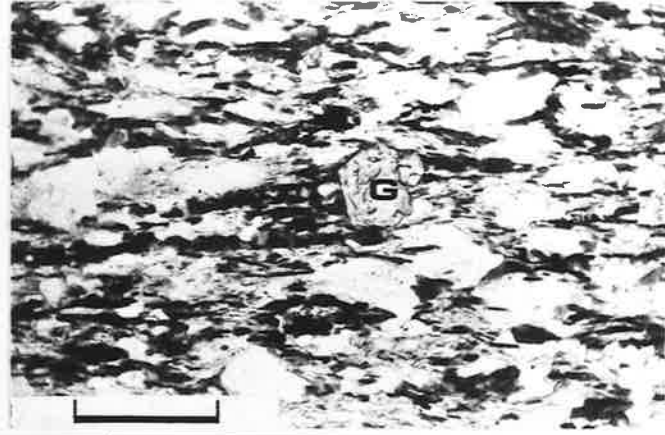
1



2



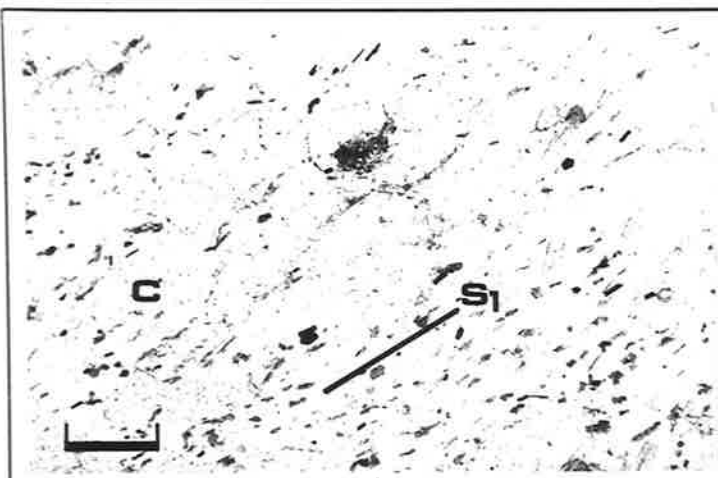
3



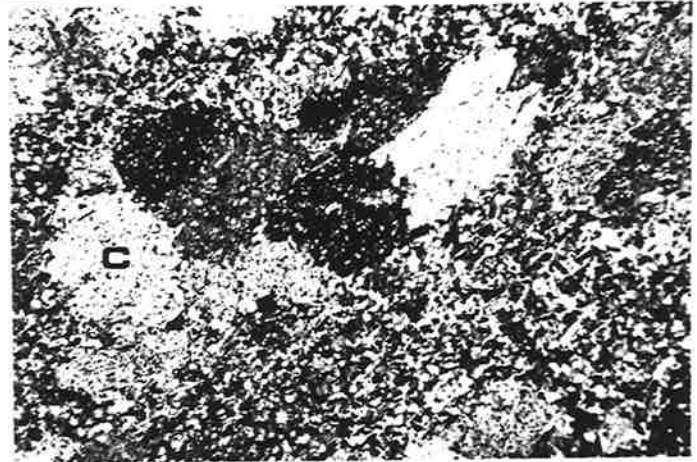
4

PLATE 23

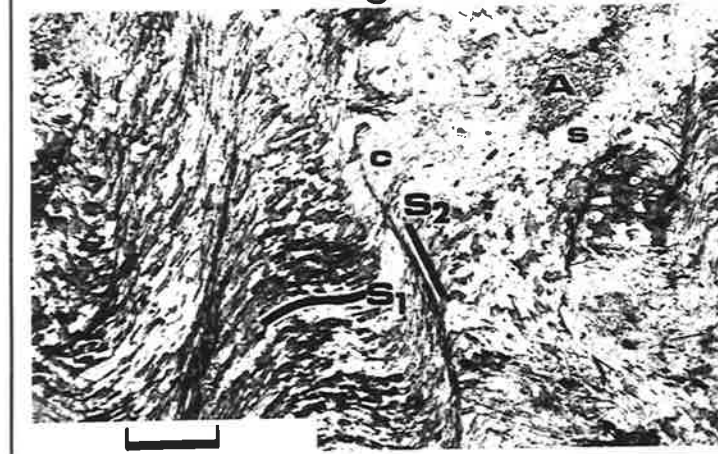
- 1 and 2. Post-F₁ cordierite poikiloblasts (C) in thin section of Petrel Cove Formation metasiltstone (SC104a) adjacent to post-F₁ meta-dolerite dyke. Note relict S₁ schistosity in 1 outlined by micas and opaque mineral laths. Transmitted plane polarised light in 1; crossed nicols in 2. (Bar scale represents 0.50mm).
3. Development of strain-slip cleavage (S₂) along limbs of S₂ crenulations in S₁ mica schistosity in thin section of Petrel Cove Formation andalusite schist SC103. Strain-slip zones are outlined by opaque mineral laths. Note the incipient slip zone crossing crenulated post-F₁ chlorite poikiloblast (c). Syn-F₁ andalusite poikiloblast (A) surrounded by alteration zone composed of sericite (s). Transmitted plane polarised light. (Bar scale represents 0.50mm).
4. Strain-slip cleavage (S₂) crossing crenulated syn-F₁ andalusite poikiloblast (A) marginally altered to sericite (s), and post-F₁ chlorite poikiloblast (c). The strain-slip zones have developed along the limbs of S₂ crenulations in S₁ mica schistosity and are outlined by opaque mineral laths. Thin section of Petrel Cove Formation andalusite schist SC103. Transmitted plane polarised light. (Bar scale represents 0.50mm).



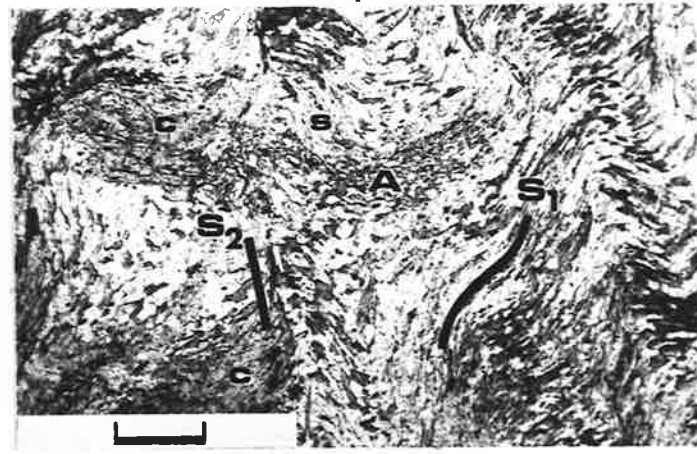
1



2



3



4

PLATE 24

- 1 and 2. Photographs of natural surfaces of the megacrystic granite facies of the Encounter Bay Granites near Knights Beach (Port Elliot) showing texture. Note large subhedral to round-shaped potash feldspar megacrysts (Kf), which are commonly mantled by light coloured plagioclase as in typical wiborgite rapakivi. Some potash feldspar megacrysts contain internal zones of plagioclase and/or biotite inclusions. Plagioclase megacrysts are light coloured and are smaller than potash feldspar megacrysts. Biotite appears black; quartz appears dark grey. Black patch in top right corner of 2 is lichen covering granite surface. (Lens cap is 4.5cm in diameter).
3. Natural surface of megacrystic granite in locality in 1 and 2 showing subhedral potash feldspar megacryst with zonally arranged biotite (black) and other inclusions (plagioclase and quartz). (Coin is 1.7cm in diameter).
4. Natural surface of megacrystic granite in locality in 1 and 2 showing subhedral potash feldspar megacryst mantled by light coloured plagioclase. Note also biotite inclusions. (Coin is 1.7cm in diameter).

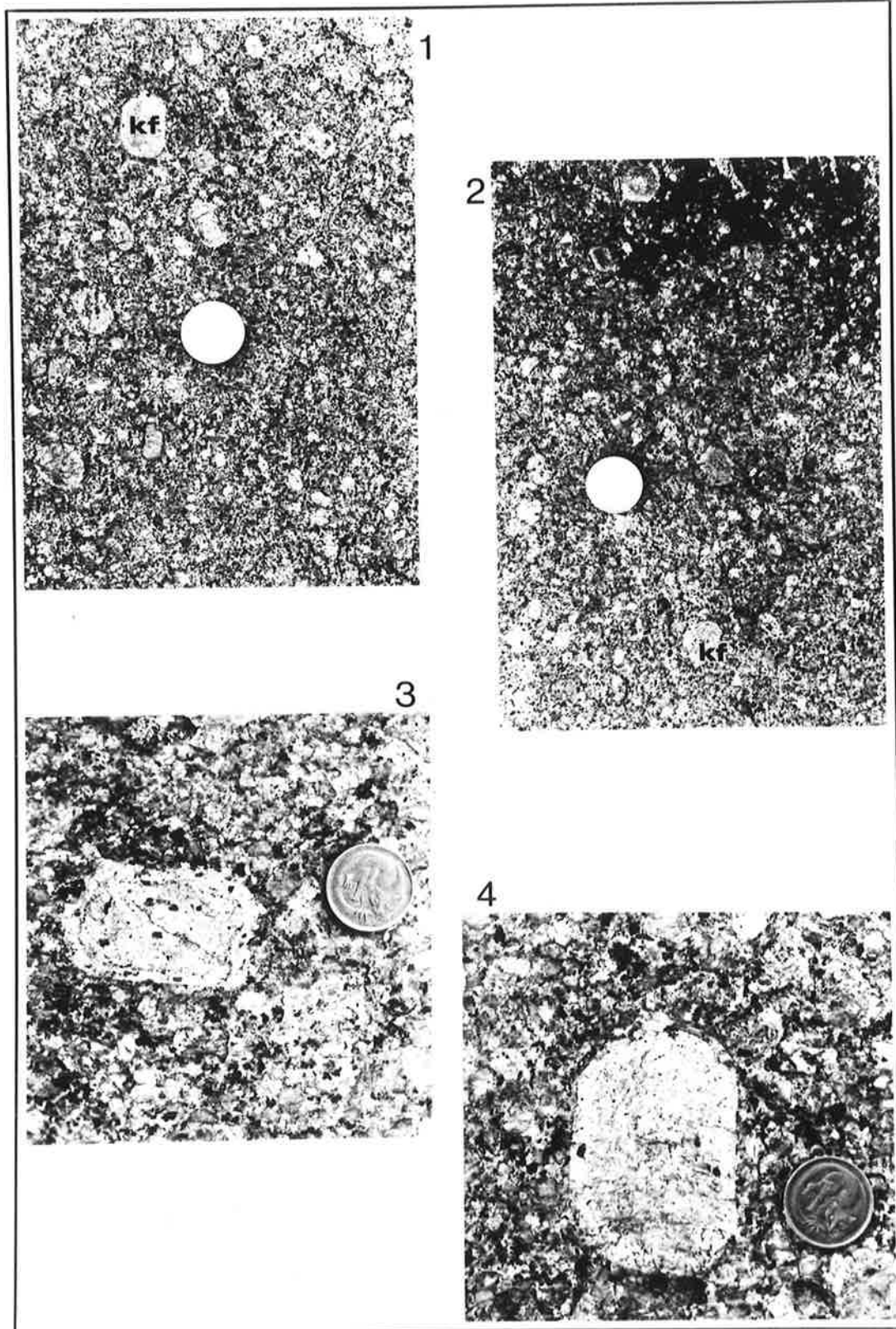


PLATE 25

1. Slab of type 1 megacrystic granite stained with sodium cobaltinitrite after etching with hydrofluoric acid. Granite is composed of potash feldspar (kf), plagioclase (pl) and quartz (q) megacrysts in a fine grained granophyric textured groundmass of these minerals in addition to biotite. Note that potash feldspar megacrysts may be mantled by plagioclase. Specimen 4-61. (Scale is in centimetres).
- 2 and 3. Two views of type 1 megacrystic granite in vicinity of Green Bay (Port Elliot) showing diffuse schlieren (arrowed) of light coloured granite of variable grain size.
4. Slab of type 2 megacrystic granite stained with sodium cobaltinitrite after etching with hydrofluoric acid. Granite is composed of potash feldspar (kf), plagioclase (pl) and quartz (q) megacrysts in a fine to medium grained groundmass of these minerals in addition to biotite. Its texture contrasts with that of the type 1 megacrystic granite shown in 1. (Scale is in centimetres).

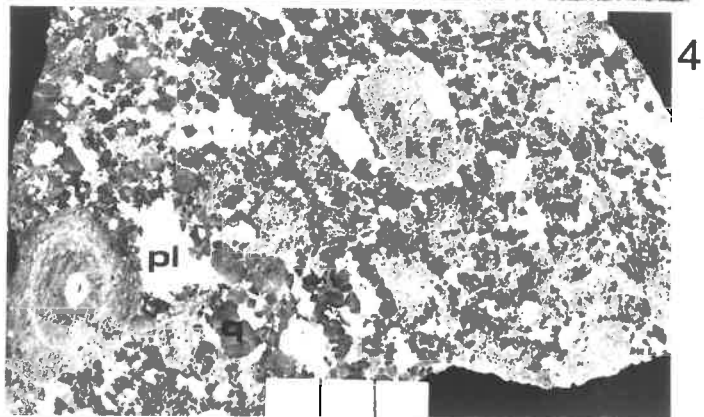
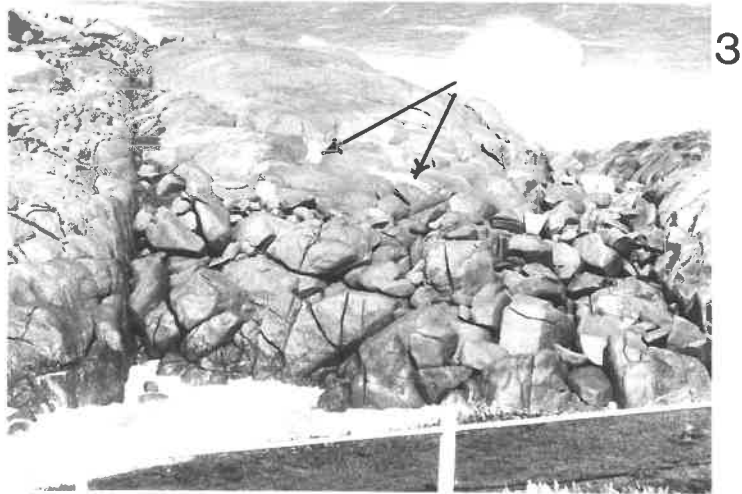
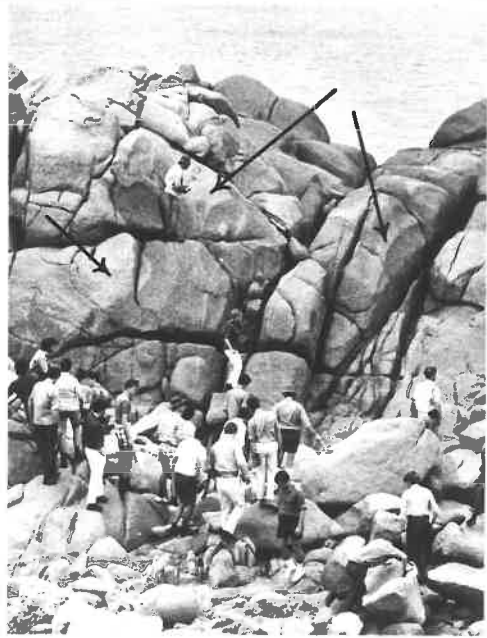
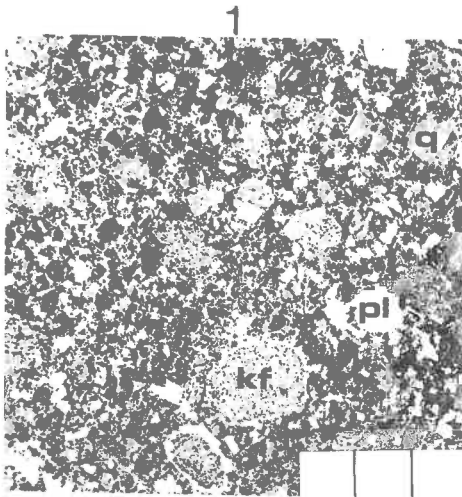
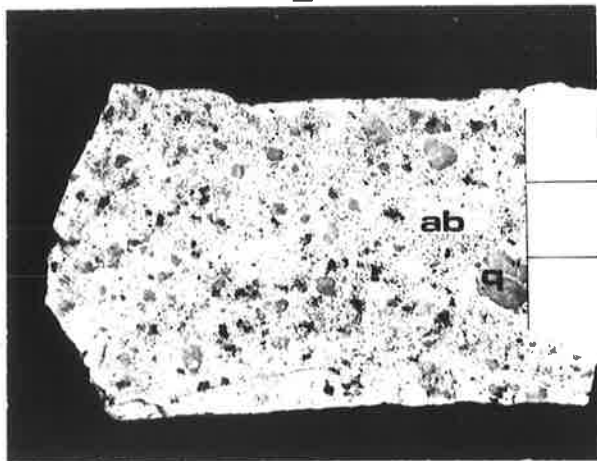


PLATE 26

1. View of healed fault contact (F) between type 1 megacrystic granite (on left) and type 2 megacrystic granite (top right). Note that fine grained granite dykes (arrowed) within type 1 megacrystic granite are truncated by the fault. Light coloured rock type on right hand side of fault is megacrystic albitite shown in 2. (Hammer is 40cm long).
2. Slab of megacrystic albitite collected from eastern side of fault shown in 1. Albitite consists of quartz (q) and albite (ab) megacrysts in a fine grained groundmass containing biotite clots (which appear black) with quartz and albite crystals. (Scale is in centimetres).



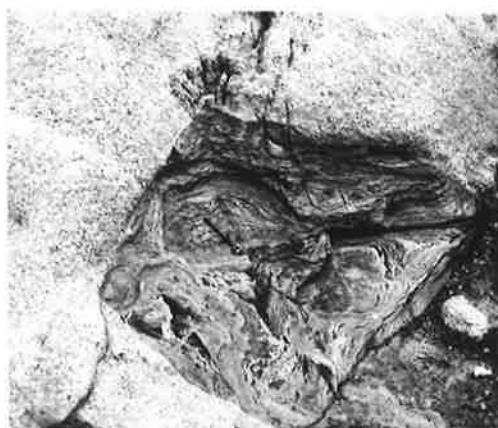
1



2

PLATE 27

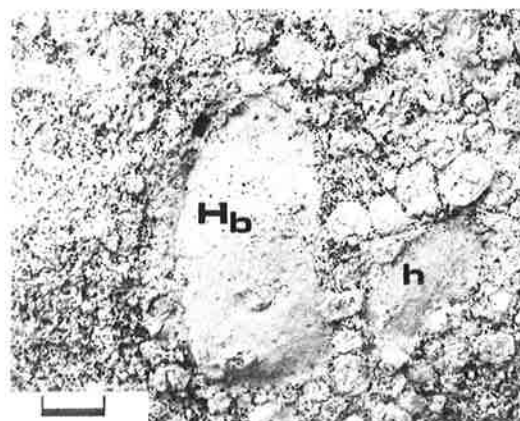
1. Laminated metasilstone xenolith in border facies megacrystic granite just east of Green Bay, Port Elliot. Note sharp contacts between xenolith and granite. Lens cap (arrowed) is 5.5cm in diameter.
2. Laminated metasilstone xenoliths in border facies megacrystic granite at tramshed locality, Granite Island. Note sharp contacts between xenolith and granite. Sunglasses (arrowed) are 14cm long.
3. Hornfels inclusion (h) with type B hybrid granite inclusion (H_b) in border facies megacrystic granite at rock-pile locality, Granite Island. The xenoliths are associated with an accumulation of large potash feldspar megacrysts. (Bar scale represents 5cm).
4. Type A hybrid granite xenolith (H_a) associated with type B hybrid granite xenolith (H_b) and several small laminated metasediment xenoliths in border facies megacrystic granite at rock-pile locality, Granite Island. (Pen is 14cm long).
5. Type B hybrid granite xenolith within border facies megacrystic granite along roadway on northern side of Granite Island. Note large potash feldspar (and smaller plagioclase and quartz) megacrysts, and dark coloured laminated metasedimentary rock inclusions (arrowed) in hybrid granite xenolith. (Lens cap is 5.5cm in diameter).



1



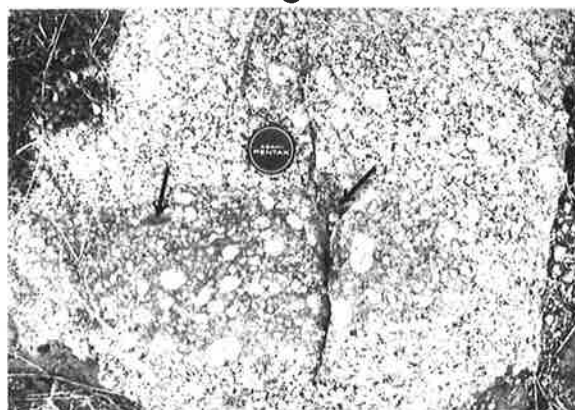
2



3



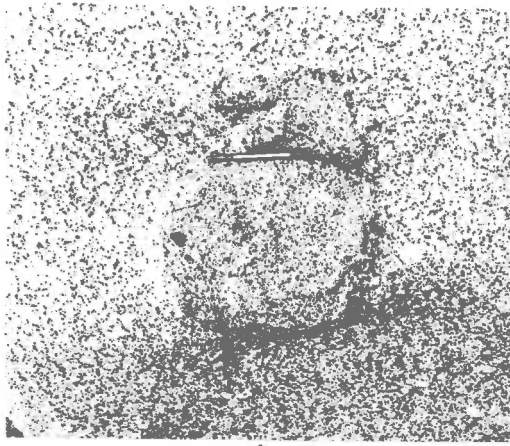
4



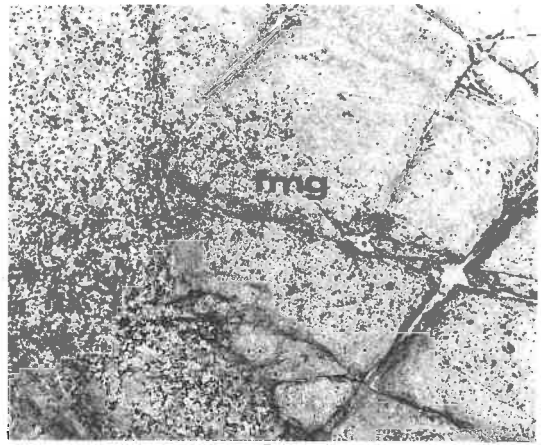
5

PLATE 28

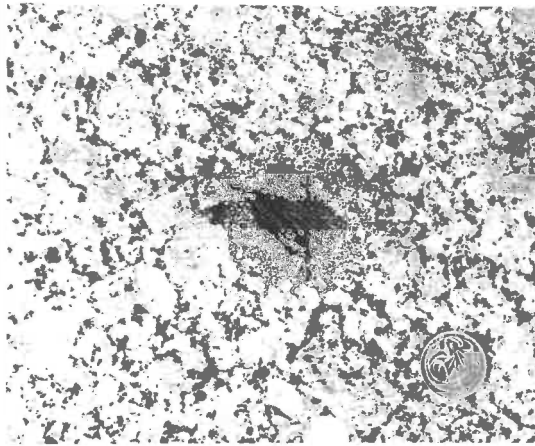
1. Patch of fine grained granophyric-textured leucogranite in inner facies megacrystic granite north-east of Commodore Point, Port Elliot. (Pen is 14cm long).
2. Fine grained megacrystic granite inclusion (fmg) in inner facies megacrystic granite at north-eastern edge of Horseshoe Bay, Port Elliot. Note relatively sharp contact between inclusion and inner facies megacrystic granite host. (Pen is 14cm long).
3. Small layered hornfels xenolith with recrystallised border zone in inner facies megacrystic granite north-east of Commodore Point, Port Elliot. (Coin is 2.1cm in diameter).
4. Xenolith of schist-like material in inner facies megacrystic granite just east of fault contact between inner facies and border facies megacrystic granites near Green Bay, Port Elliot. The schist-like material contains dark coloured biotite-rich clots, and is partly rimmed by massive opalescent blue quartz (q). Dark circle near centre of left mass is a diamond drill hole. (Lens cap is 5.5cm in diameter).
5. Small dark coloured clots of schist-like material within inner facies megacrystic granite on eastern side of rocky cove, about 100m east of Green Bay, Port Elliot. (Lens cap is 5.5cm in diameter).



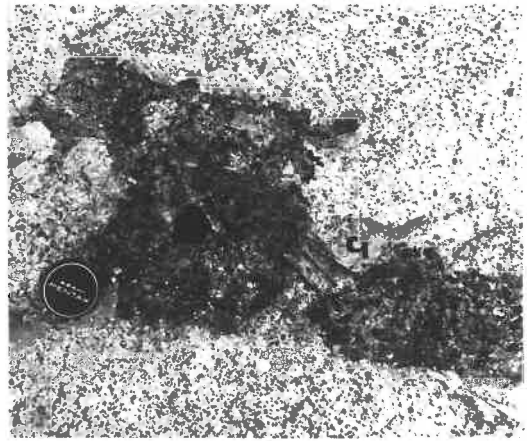
1



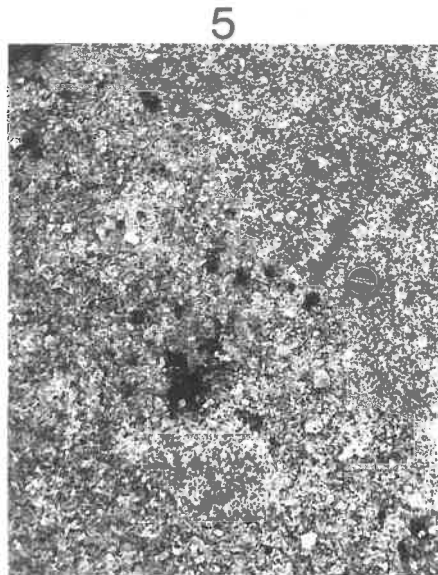
2



3



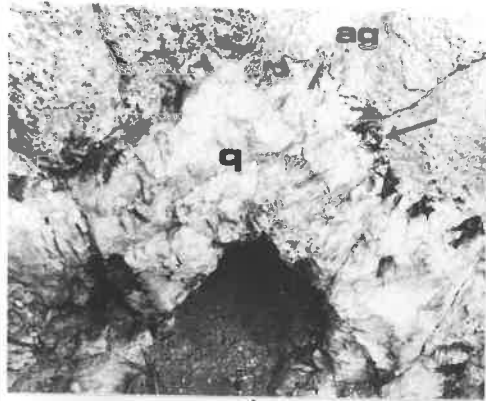
4



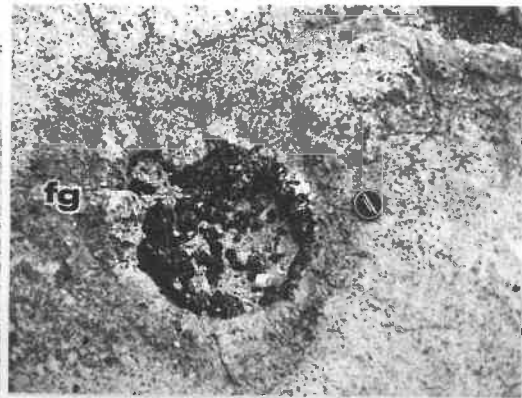
5

PLATE 29

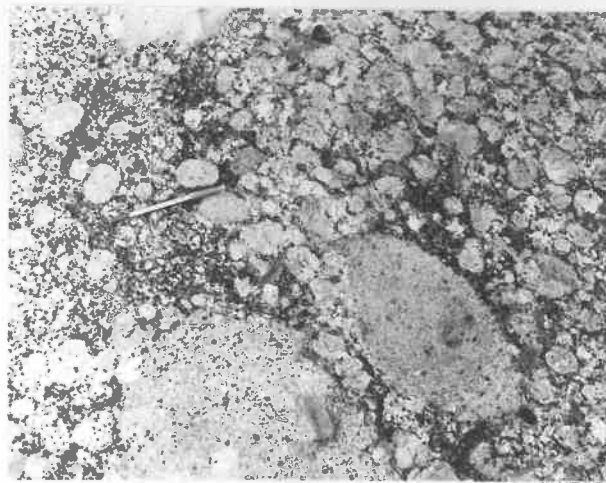
1. Quartz-tourmaline pegmatite at the intersection of two joints within the inner facies megacrystic granite on the eastern side of the rocky cove, about 100m east of Green Bay, Port Elliot. Central core of pegmatite has been eroded away, but may have contained sulphide minerals (suggested by the occurrence of relict goethite and jarosite boxwork structures). Intermediate zone is composed of milky quartz (q). Next is a thin zone of quartz-tourmaline intergrowths (arrowed). This is followed by an outer zone of variable thickness composed of albitised inner facies megacrystic granite (ag). (Milky quartz zone is about 30cm wide).
2. Tourmaline-rich pegmatite pod in inner facies megacrystic granite east of Green Bay, Port Elliot. Tourmaline-rich core (black) is surrounded by zone of feldspathised granite (fg). (Lens cap is 5.5cm in diameter).
- 3 and 4. Zones of accumulation of large potash feldspar megacrysts in association with a variety of hornfels and hybrid granite xenoliths in the border facies megacrystic granite, rock-pile locality, Granite Island. The spaces between the potash feldspar megacrysts shown in 3 are filled mainly with biotite and with small hornfels xenoliths. The potash feldspar megacrysts shown in 4 are packed together to the virtual exclusion of other minerals. (Pen is 14cm long).



1



2



3

4

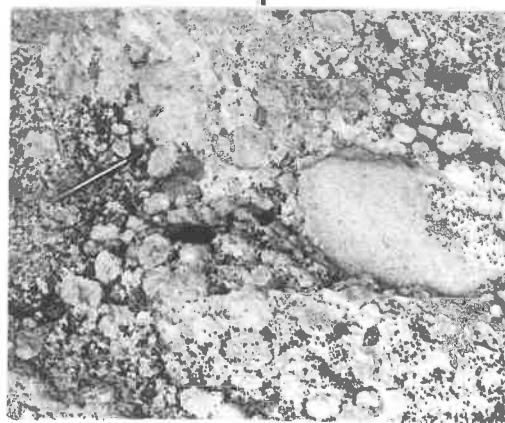


PLATE 30

1. Biotite-rich layers alternating with quartzo-feldspathic layers in a zone within the inner facies megacrystic granite north-east of Commodore Point, Port Elliot. (Hammer is 28cm long).
2. Part of layered zone in 1 showing preferred orientation of two small tabular hornfels xenoliths (arrowed) in the plane of the layers. The alternation of biotite-rich layers and quartzo-feldspathic layers is well displayed in the upper part of the photograph. Comparatively sharp bottom contacts and gradational upper contacts to the biotite-rich layers can be discerned. (Hammer is 28cm long).
3. Biotite-rich layers alternating with quartzo-feldspathic layers (which contain potash feldspar megacrysts, as indicated by the arrow) in the border facies megacrystic granite at the rock-pile locality, Granite Island. Dark area in upper left part of photograph is biotite-rich zone. (Pen is 15cm long).
4. Spiral-shaped zone of biotite layering in border facies megacrystic granite in wave zone, south of rock-pile locality, Granite Island. The layered zone is similar to that shown in 3 except in shape. The biotite-rich layers tend to be split along their length. (Bar scale represents about 1m).

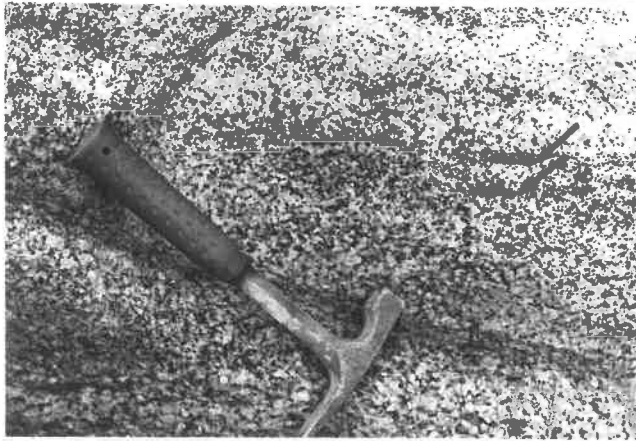
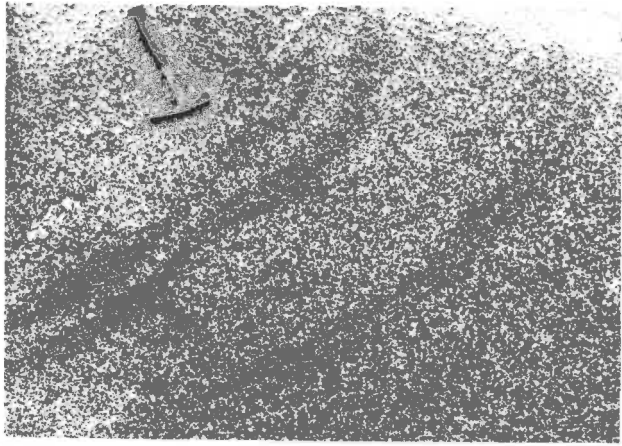
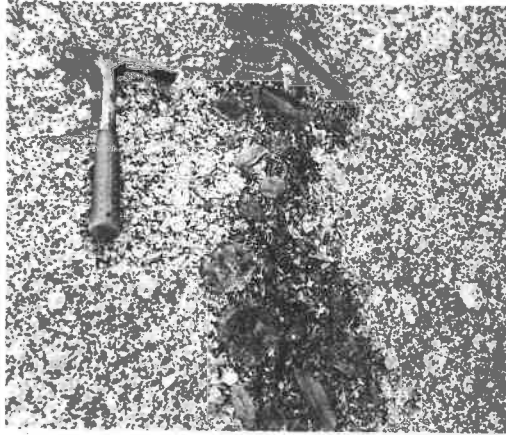


PLATE 31

1. Train of hornfels, metasedimentary rock and hybrid granite xenoliths and a corresponding biotite-rich schlieren in border facies megacrystic granite on south side of Granite Island, about 150m west of Nature's Eye locality. (Hammer is 28cm long).
2. Thin leucogranite bands alternating with inner facies megacrystic granite on northern side of small cove, north-east of Commodore Point, Port Elliot. (Bar scale represents about 1m).
3. Preferential albitisation of potash feldspar megacrysts (white) along joint fracture in border facies megacrystic granite at rock-pile locality, Granite Island. (Pen is 14cm long).
4. Dark coloured bands defining margins of albitised zone adjacent to joint in inner facies megacrystic granite just west of fault near Green Bay, Port Elliot. Note light colour of albitised granite. Pen (arrowed) is 14cm long.

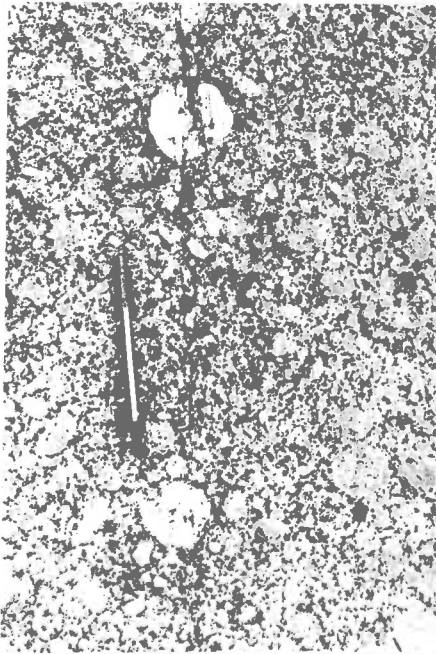
1



2



3



4

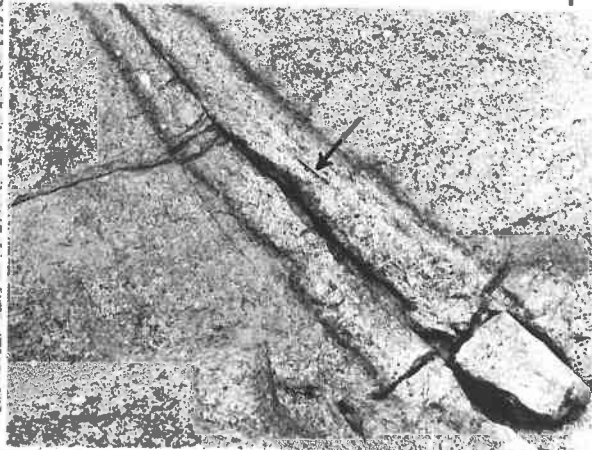


PLATE 32

1. Contact between border facies megacrystic granite (Gr) and the megacrystic albite-chlorite rock (Ab-Ch) on the western end of Granite Island. Quartz is absent in the albite-chlorite rock to the left of the pen (arrowed). The megacrystic granite is strongly fractured near its contact with the albite-chlorite rock, and has been partly albitised up to 1m from the contact. (Pen is 15cm long).
2. Gradational contact (limits partly outlined in ink) between medium even-grained granite (gr) and border facies megacrystic granite (Gr) just east of Knights Beach, Port Elliot. Thin aplite vein can be seen crossing the contact in upper part of photograph. (Hammer is 28cm long).
3. Zones of albitised medium even-grained granite (agr) north-east of Commodore Point, Port Elliot. Contacts between albitised granite and unaltered granite (gr) are defined by dark coloured bands (arrowed). The albitisation has been controlled by the closely spaced vertical joints trending directly away from the camera position. (Bar scale represents about 1m).

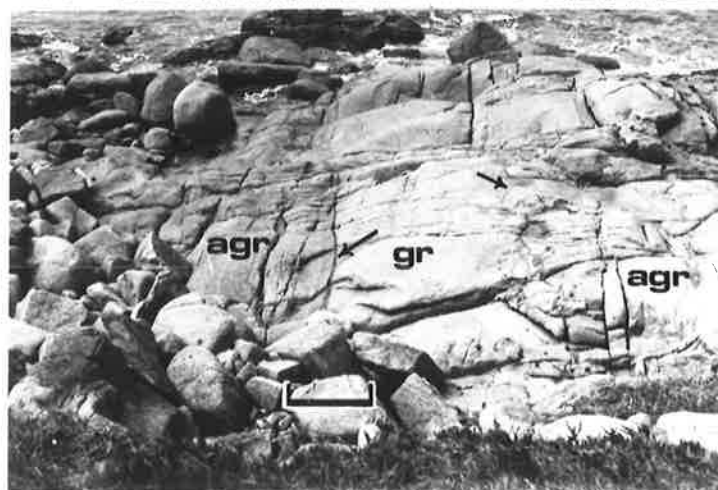
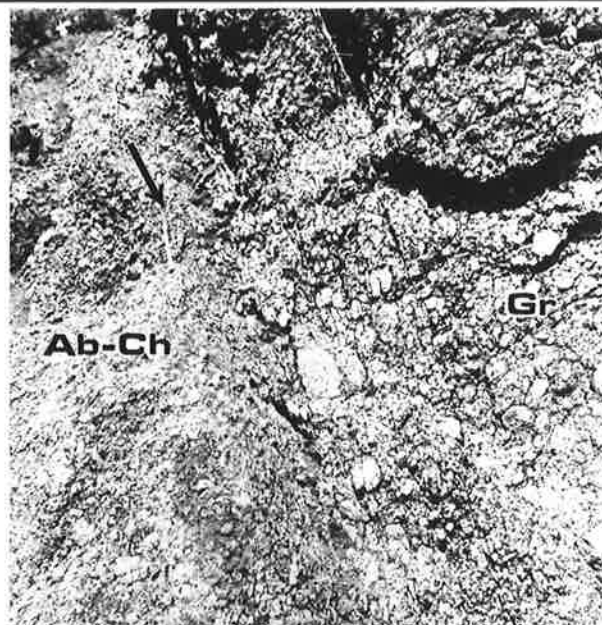


PLATE 33

1. Closely spaced joints in joint-set that has controlled albitisation of the medium even-grained granite north-east of Commodore Point, Port Elliot. Joints have smoothed sides indicative of post-albitisation movement. (Pen is 14cm long).
2. Laminated metasiltstone xenolith in medium even-grained granite just west of fault near Green Bay, Port Elliot. (Coin is 2.1cm in diameter).
3. Rare fine grained leucogranite xenoliths in medium even-grained granite just east of fault near Green Bay, Port Elliot. (Hammer is 28cm long).
4. Pegmatite pod composed of tourmaline-rich core surrounded by feldspathised zone in medium even-grained granite illustrated in 2 and 3. (Lens cap is 5.5cm in diameter).

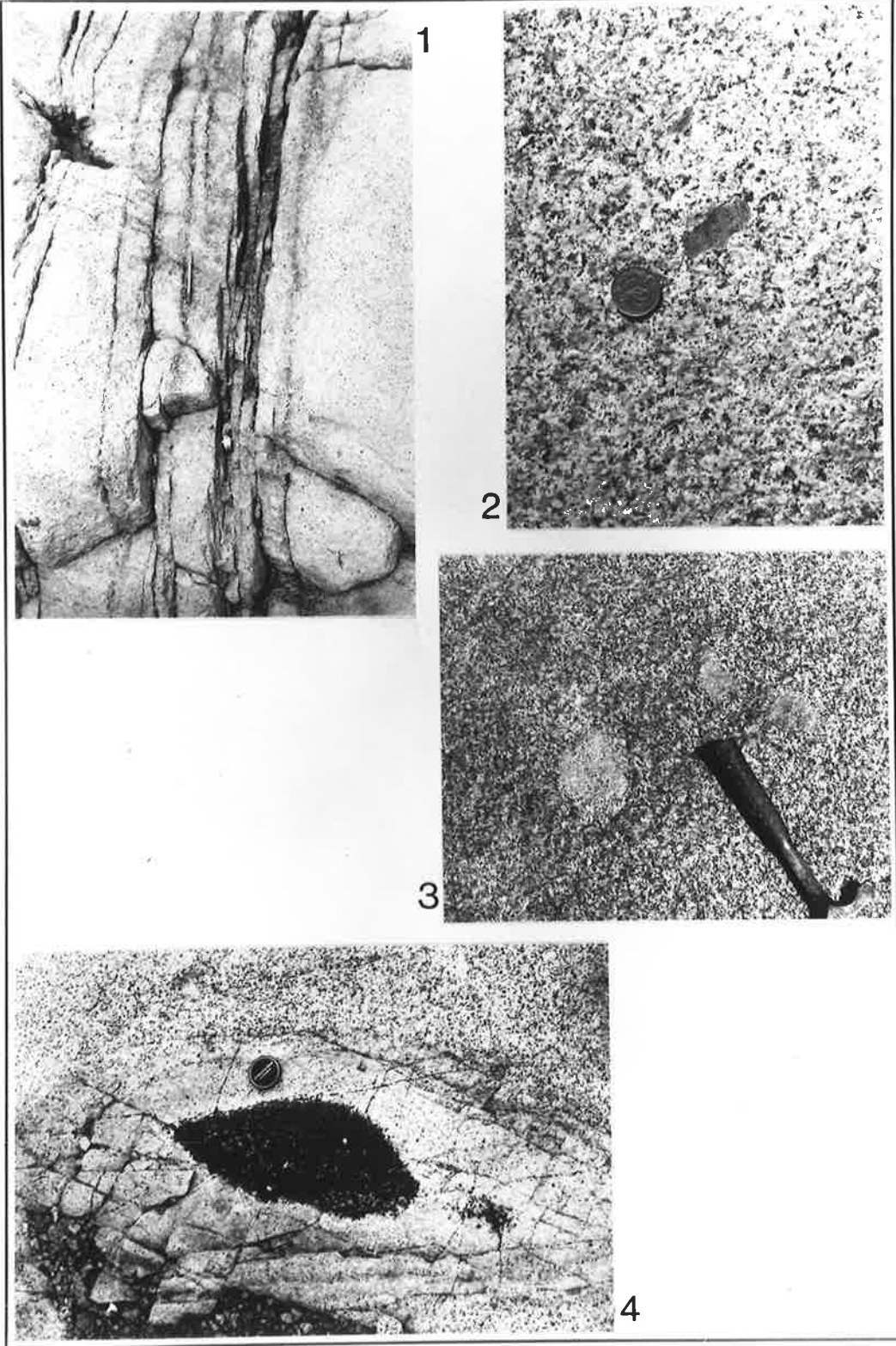
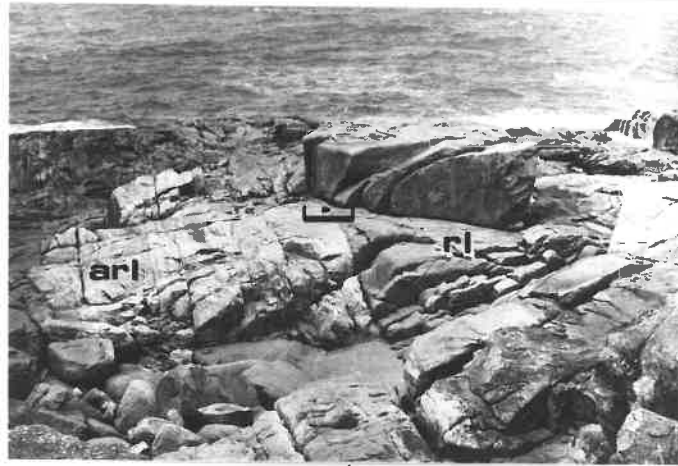


PLATE 34

1. View of albitised red leucogranite (arl) in zone of closely spaced joints on left side of photograph, and unaltered red leucogranite (rl) on right. (Bar scale beneath black camera case near centre of photograph represents 1m).
2. A series of parallel dark coloured bands within an albitised joint zone in the red leucogranite north-east of Commodore Point, Port Elliot. The bands are parallel to the contact between the red leucogranite and the albitised red leucogranite. (Bar scale beneath black lens cap represents 50cm).
3. A series of dark coloured bands around a remnant wedge of red leucogranite (rl) in a zone of albitised red leucogranite (arl). (Bar scale next to black lens cap represents 50cm).



1



PLATE 35

1. Slab of type A hybrid granite (3-15) stained with sodium cobaltinitrite after etching with hydrofluoric acid, showing typical texture. Potash feldspar megacryst (kf) near bottom left of photograph is mantled by plagioclase. Plagioclase megacrysts (pl), quartz megacrysts (q) and biotite/hornblende clots (arrowed) occur in a fine grained groundmass composed mainly of plagioclase, quartz, potash feldspar, hornblende and biotite. (Bar scale represents 1cm).
2. Natural surface of type A hybrid granite at Nature's Eye locality, Granite Island. Hybrid granite contains inconspicuous dark coloured hornfels inclusions (arrowed), as well as poikilitic potash feldspar megacrysts mantled by plagioclase. (Pen is 15cm long).
3. Slab of type A hybrid granite (3-38) stained with sodium cobaltinitrite after etching with hydrofluoric acid. Note layering defined by differences in megacryst abundance. Megacrysts are predominantly plagioclase (white) and quartz, and occur with biotite/hornblende clots. Note also the occurrence of thin dark coloured band outlining what appears to be a fold hinge within megacryst-free layer. (Scale is in millimetres).

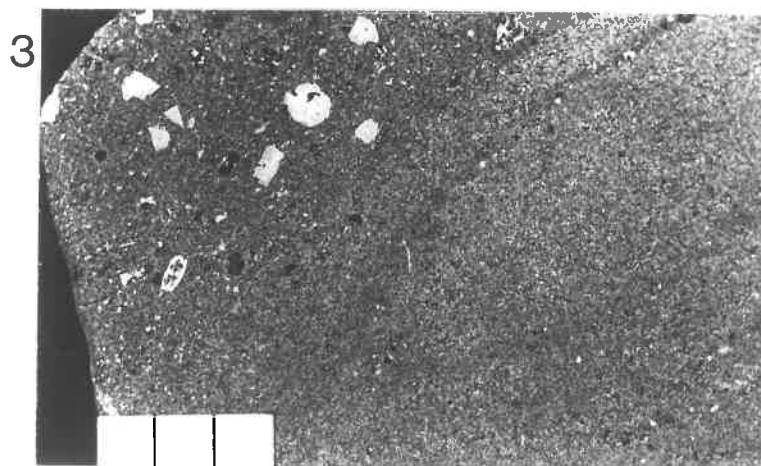
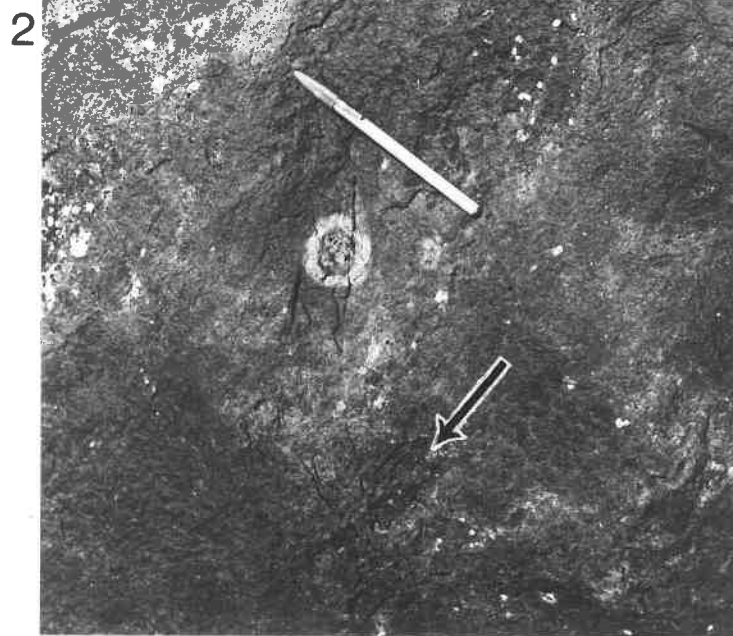
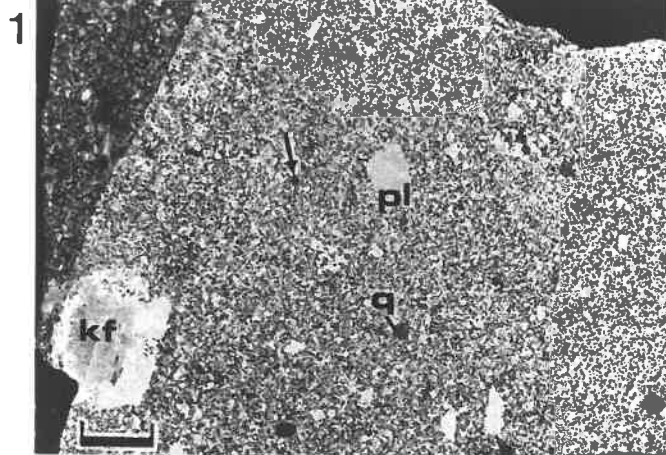
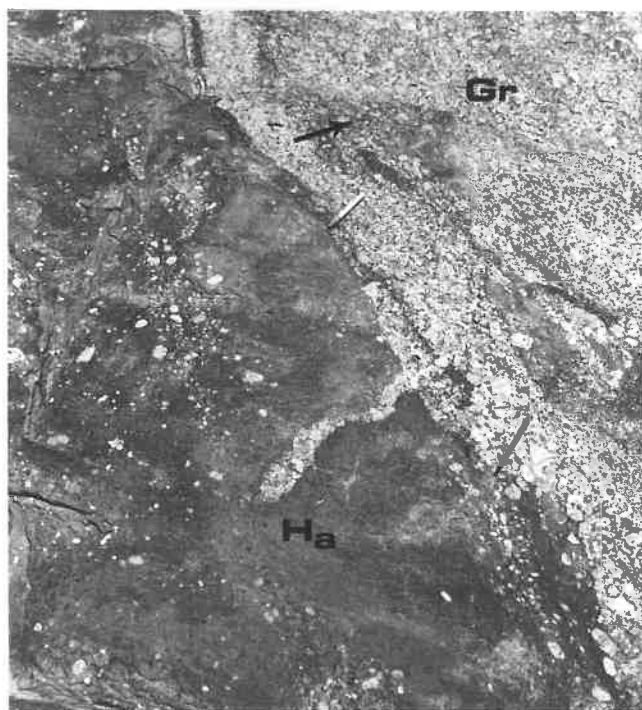


PLATE 36

1. Contact between type A hybrid granite (H_a) and border facies megacrystic granite (Gr) at Nature's Eye locality, Granite Island. Note rafts of hybrid granite and biotite-rich schlieren in megacrystic granite adjacent to contact. Note also streams of potash feldspar megacrysts within hybrid granite, and an irregular tongue of megacrystic granite penetrating hybrid granite. The contact between the megacrystic granite and type A hybrid granite is sharp, except where type B hybrid granite occurs as an intermediate phase (arrows). (Pen is 15cm long).
2. Part of contact zone between type A hybrid granite (H_a) and the border facies megacrystic granite at Nature's Eye locality, Granite Island. Note xenoliths within type A hybrid granite (near top left part of photograph), tongues of megacrystic granite, and irregular zones of type B hybrid granite (H_b) containing conspicuous xenoliths. (Pen is 15cm long).



1

2

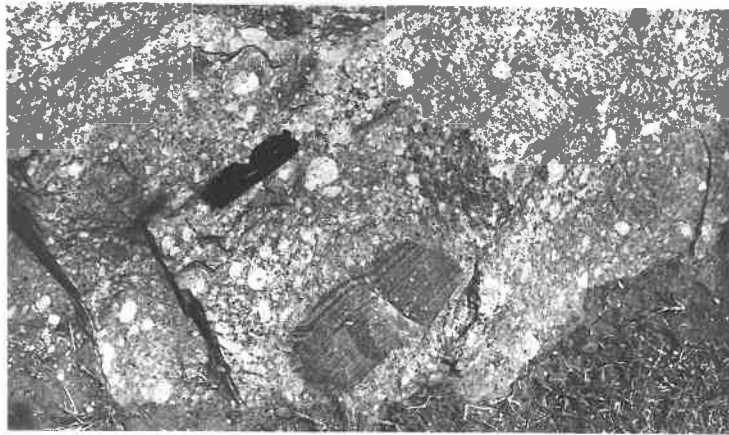


PLATE 37

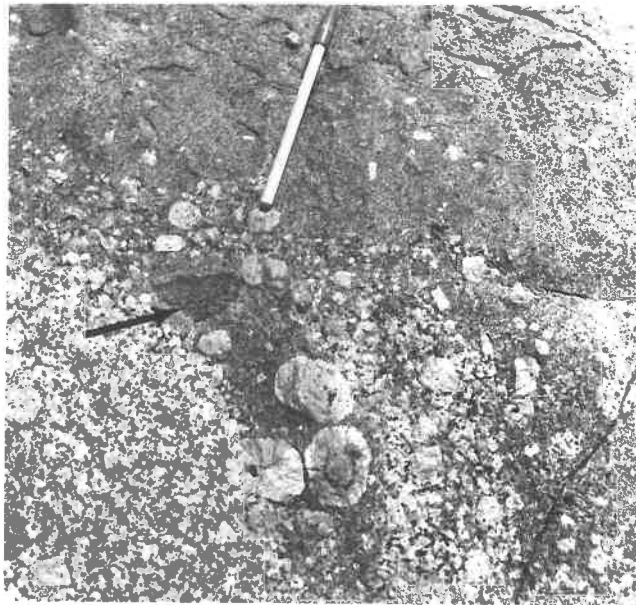
1. Type B hybrid granite containing abundant hornfels xenoliths (layered and non-layered) and conspicuous large potash feldspar megacrysts. About 130m west of Nature's Eye locality, Granite Island. (Pen is 15cm long).
2. Laminated hornfels xenolith in type B hybrid granite along roadway on northern side of Granite Island. Note large potash feldspar megacrysts. (Sunglasses are 14cm long).
3. Large potash feldspar megacrysts (one containing an inner zone of biotite inclusions) straddling the contact between type B hybrid granite and the border facies megacrystic granite at Nature's Eye locality, Granite Island. Type B hybrid granite occurs here as an intermediate phase between type A hybrid granite and the megacrystic granite. Note finely laminated hornfels xenolith (arrowed). (Pen is 14cm long).



1



2



3

PLATE 38

1. Aplite dykes (arrowed) within border facies megacrystic granite in the cliff-face on the western side of Green Bay, Port Elliot.
2. Diagonal fractures (parallel to pen) in quartz veins infilling north-easterly trending joints within inner facies megacrystic granite in small cove north-east of Commodore Point, Port Elliot. The orientation of the fractures suggests differential movement along the quartz-filled joint after crystallisation of the quartz. Note complexly zoned potash feldspar megacryst near bottom of photograph. (Pen is 15cm long).
3. Metadolerite dyke (black) exposed in high cliff-face at the head of a narrow gulch on the seaward side of Rosetta Head. (Top of promontory is about 100m above sea level).

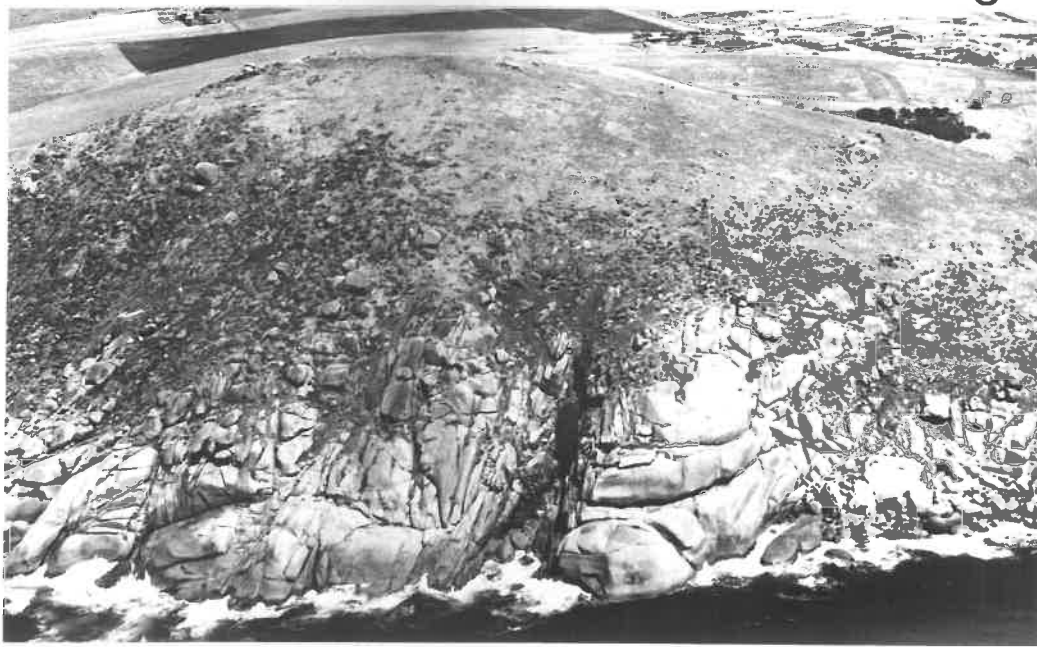
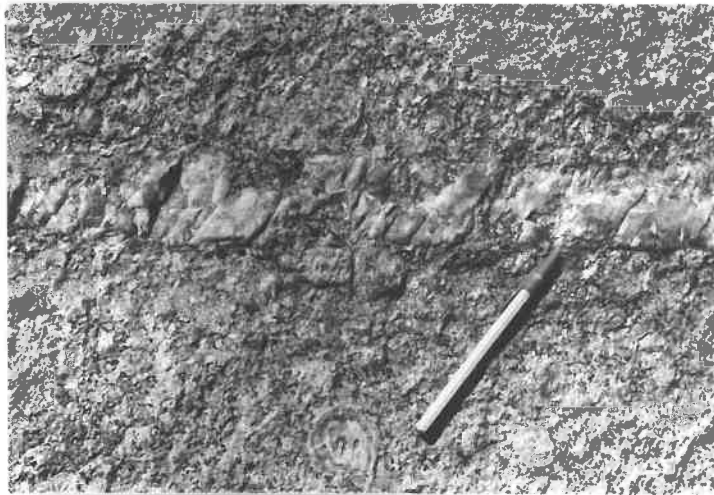
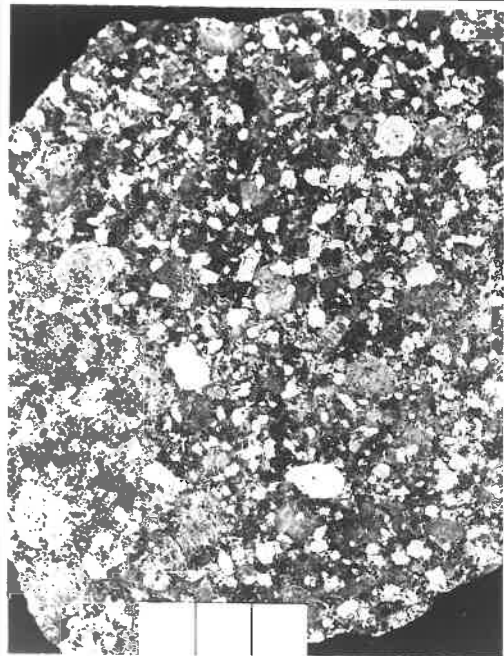


PLATE 39

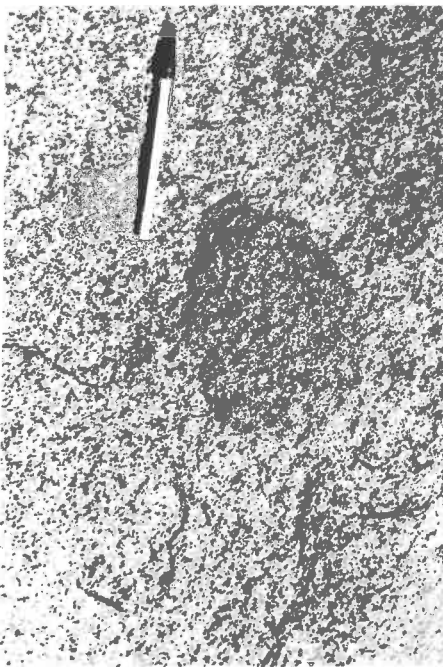
1. Slab of Cape Willoughby megacrystic granite (W9) stained with sodium cobaltinitrite after etching with hydrofluoric acid, showing typical texture. Plagioclase appears white; potash feldspar appears medium-grey; quartz and biotite appear black. The texture of this granite should be compared with the textures of the border facies and the inner facies megacrystic granites shown in Plate 25. (Scale is in millimetres).
2. Laminated metasandstone xenolith in the Cape Willoughby megacrystic granite on coast north-east of light station. (Pen is 15cm long).
3. Recrystallised and metasomatised margins of a laminated metasandstone xenolith has produced a rock-type similar in texture to the type B hybrid granite. Coast north of light station at Cape Willoughby. (Pen is 14cm long).
4. Hornfels xenolith within Cape Willoughby megacrystic granite on coast north of light station. (Pen is 15cm long).



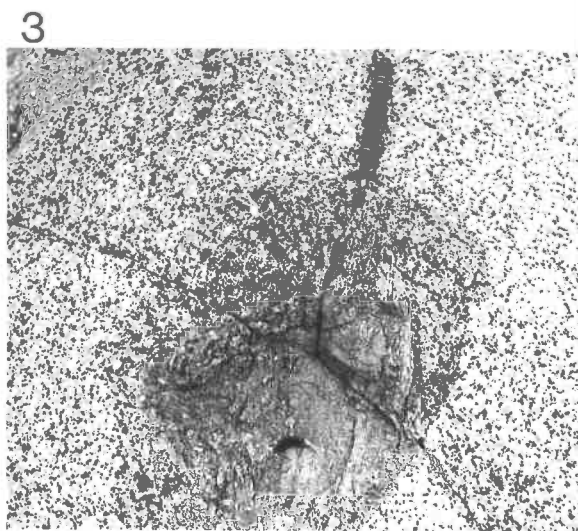
1



2



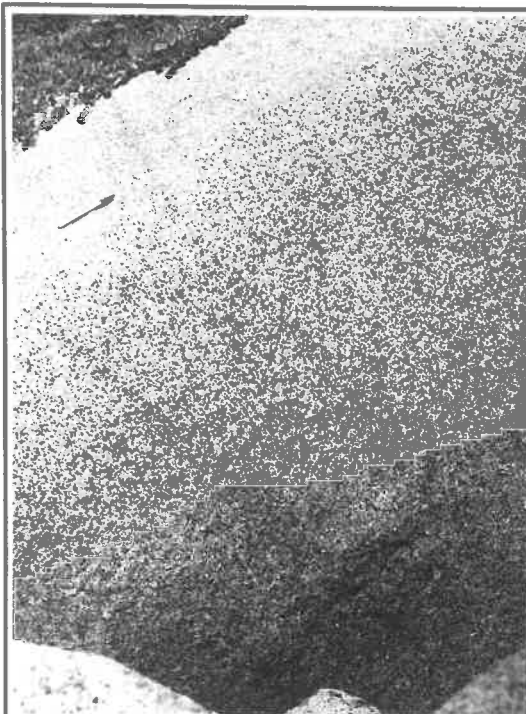
4



3

PLATE 40

1. Diffuse biotite-rich layers in Cape Willoughby megacrystic granite on coast north of light station. (Pen is 15cm long).
2. Series of diffuse biotite-rich layers, some resembling sedimentary cross-stratification, in Cape Willoughby megacrystic granite north of light station. (Hammer is 72cm long).
3. View of red leucogranite (r1), which occurs as a north-westerly plunging sheet-like body within the Cape Willoughby megacrystic granite (Gr) just west of Cannon Hill. Contact between red leucogranite and megacrystic granite has been outlined in ink. Light coloured rocks in background are albitised and greisenised megacrystic granite. Photograph taken from colour transparency.



1



2

3

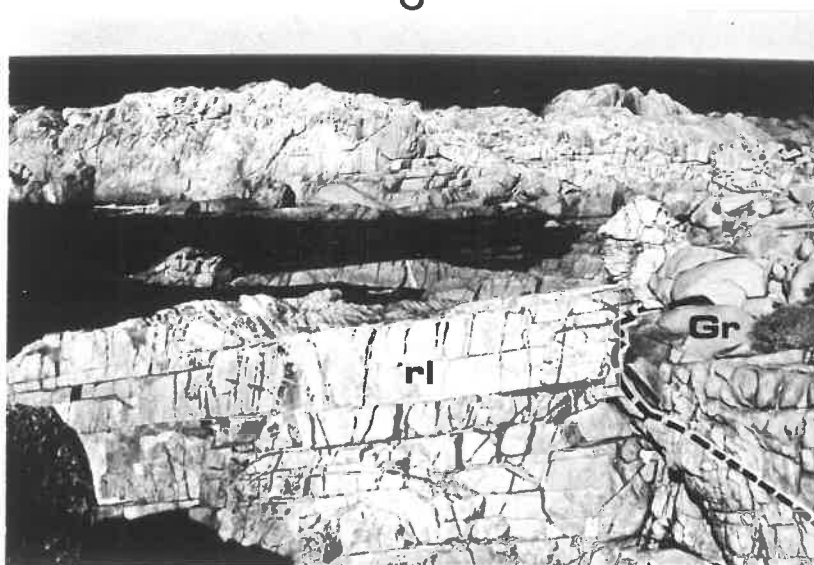


PLATE 41

1. Gradation (outlined in part) between red leucogranite (rl) and border facies megacrystic granite (Gr) at the upper contact of the red leucogranite sheet, just west of Cannon Hill, Cape Willoughby. (Pen is 14cm long).
2. Red leucogranite (rl) interlayered with megacrystic granite (Gr) at the lower contact of the red leucogranite sheet, just west of Cannon Hill, Cape Willoughby. (Pen is 14cm long).
3. Type B hybrid granite containing dark coloured laminated and non-laminated hornfels xenoliths. On coast just south of Pink Bay, Cape Willoughby. (Hammer is 72cm long).
4. Type B hybrid granite containing dark coloured laminated and non-laminated hornfels xenoliths. On coast west of Barn Bluff, Cape Willoughby. (Hammer is 72cm long).



1



2

3



4

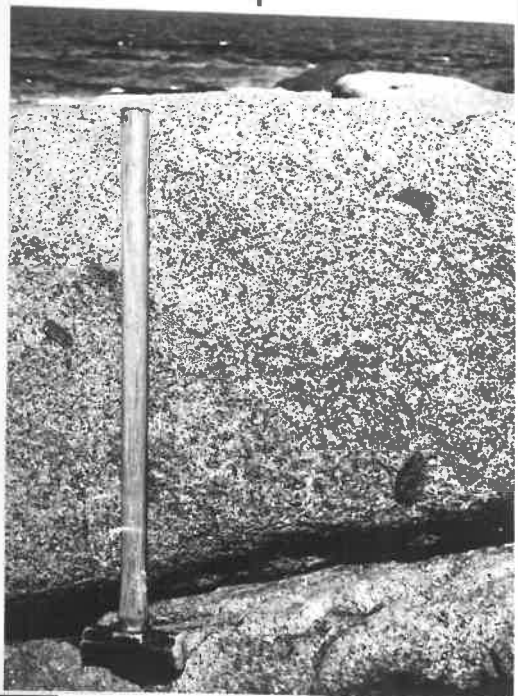
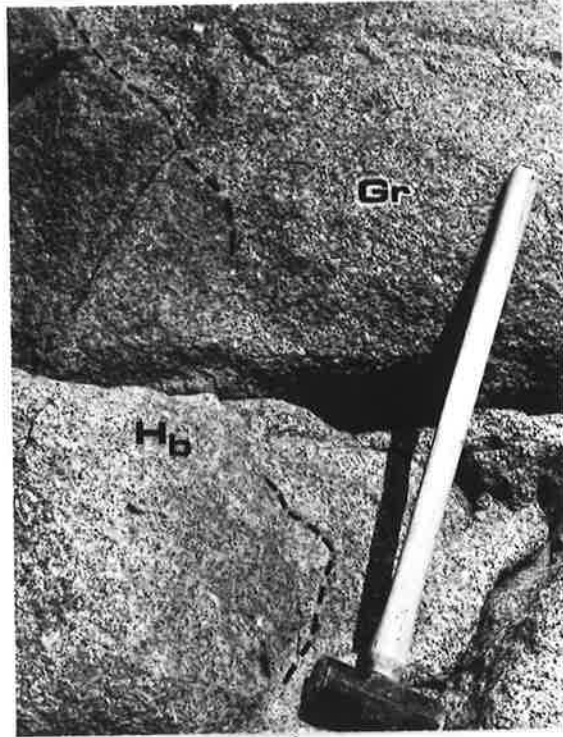


PLATE 42

1. Contact (partly outlined in ink) between type B hybrid granite (H_b) and megacrystic granite (Gr) on coast just south of Pink Bay, Cape Willoughby. The contact is gradational over 1-2cm, and is not a conspicuous feature because of the similar textures of the two rock types. (Hammer is 72cm long).
2. Part of round inclusion of type A hybrid granite (H_a) in megacrystic granite on coastline just north of Pink Bay, Cape Willoughby. Note sharp contact between the two rock types. (Pen is 14cm long).



1

2

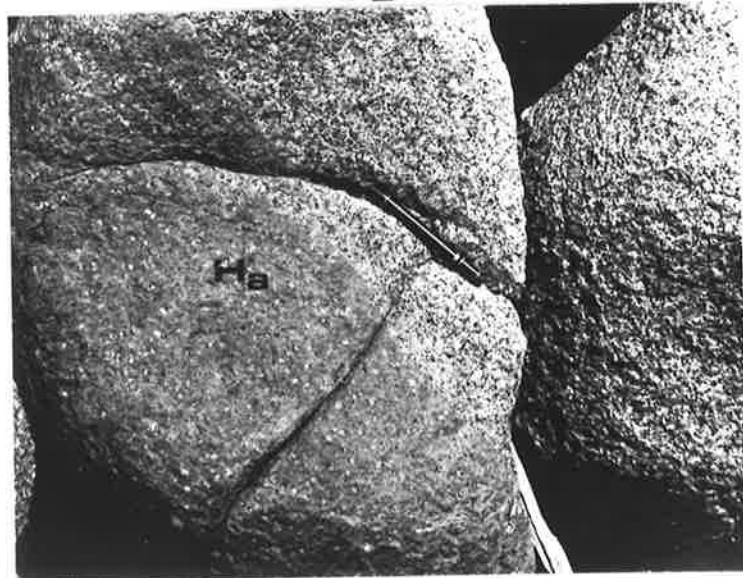


PLATE 43

1. Joints that have controlled greisenisation at Cape Willoughby dip at a shallow angle towards the south-east, as shown in this cliff section north of the light station. (Height of cliff about 25m).
2. Greisenisation of megacrystic granite along shallow-dipping joint exposed on coast north of Cape Willoughby light station. Note dark band marking upper limit of alteration. A similar dark band marks the lower limit of alteration beneath the joint, but can not be seen in this photograph. (Hammer head is 13cm long).
3. Large ovoid-shaped potash feldspar megacryst (kf) in Cape Kersaint granite on coast west of Cape Kersaint. Mica schistosity in granite is approximately horizontal in this photograph, which was copied from a colour transparency. Black elongate objects are biotite-rich xenoliths. (Lens cap is 5.5cm in diameter).
- 4 and 5. Laminated metasedimentary rock xenoliths in Cape Kersaint granite on coast west of Cape Kersaint. Xenolith in 4 is part of a fold of unknown origin. Xenolith in 5 contains fold structures that are not penetrative, and thus may be of sedimentary origin. Both photographs are copies of colour transparencies. (Lens cap is 5.5cm in diameter).
6. Natural surface of outcrop of megacrystic granite similar to Cape Kersaint granite along banks of Stun-Sail-Boom River. Large sub-hedral to round-shaped megacrysts of potash feldspar (white) are conspicuous. (Hammer head is 13cm long).

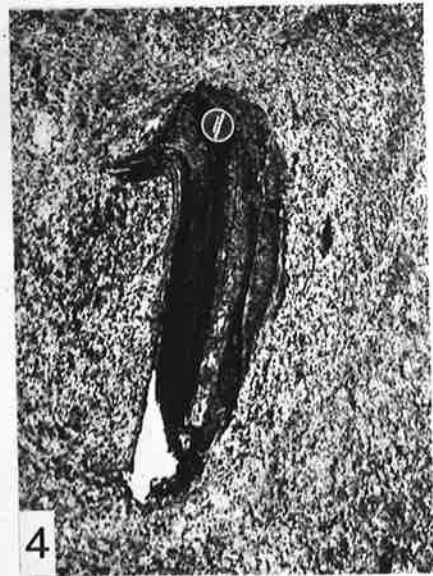
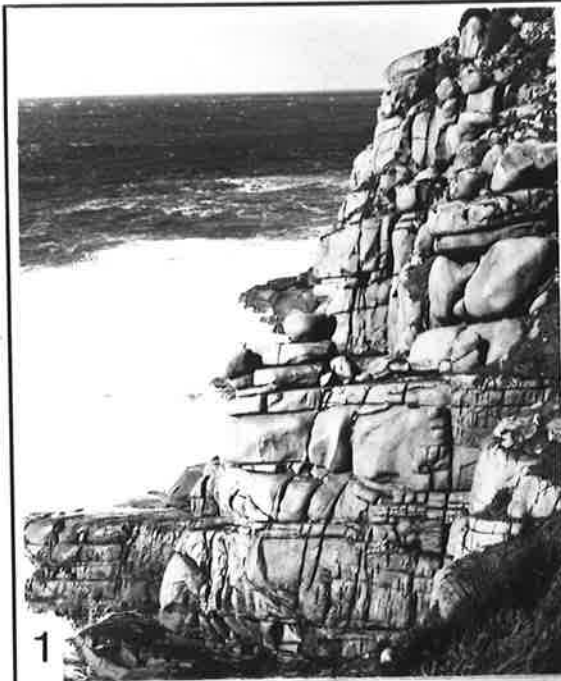


PLATE 44

- 1 and 2. Granophyric intergrowths of quartz and groundmass potash feldspar in thin section of border facies megacrystic granite 4-61. Transmitted light, crossed nicols. (Bar scale represents 0.10mm).
3. Granophyric intergrowth between quartz and potash feldspar bordering euhedral potash feldspar megacryst in thin section of border facies megacrystic granite 4-61. Transmitted light, crossed nicols. (Bar scale represents 0.10mm).
4. Granophyric intergrowth bordering euhedral potash feldspar megacryst in thin section of border facies megacrystic granite 7-9. Transmitted light, crossed nicols. (Bar scale represents 0.10mm).
- 5 and 6. Granophyric intergrowths between quartz and potash feldspar bordering euhedral potash feldspar megacrysts in thin section of feldspar porphyry from Gawler Ranges, South Australia. Transmitted light, crossed nicols. (Bar scales represent 0.20mm).
7. Small anhedral quartz inclusions in cross-hatched portion of potash feldspar megacryst in thin section of border facies megacrystic granite 3-28. Transmitted light, crossed nicols. (Bar scale represents 0.10mm).
8. Angular and embayed quartz inclusion in potash feldspar megacryst in thin section of border facies megacrystic granite 4-55. Transmitted light, crossed nicols. (Bar scale represents 0.05mm).

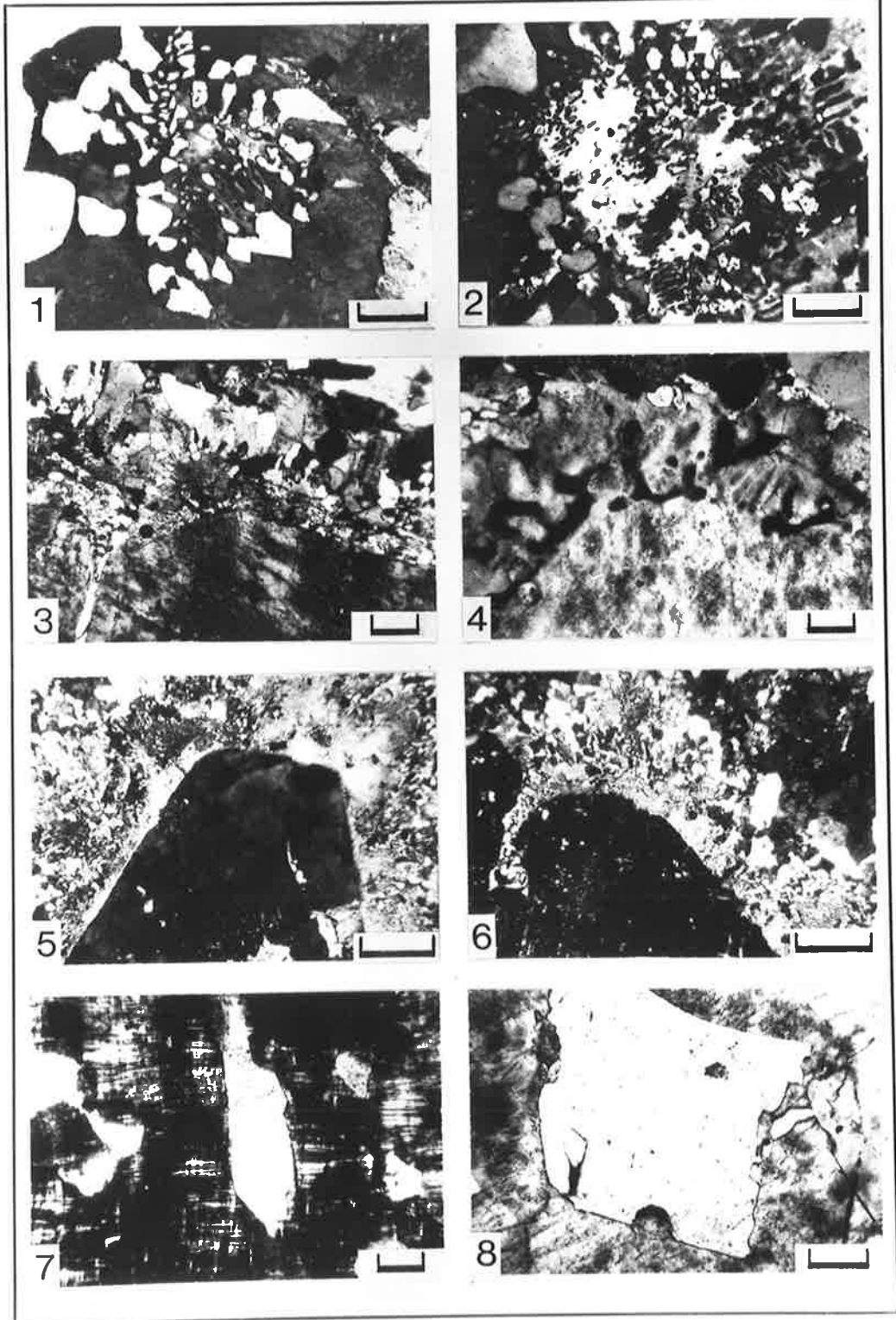


PLATE 45

- 1 and 2. Slabs of border facies megacrystic granite stained with sodium cobaltinitrite after etching with hydrofluoric acid. Note potash feldspar megacrysts (kf) mantled by plagioclase (pl). The round-shaped potash feldspar megacryst in 1 has a plagioclase border of uniform thickness. The potash feldspar megacryst near the centre of photograph 2 has a plagioclase border of variable thickness. Near the bottom right of photograph 2, a potash feldspar megacryst has a thin border zone of fine grained plagioclase crystals. (Bar scale represents 1cm).
3. Film perthite texture in potash feldspar megacryst in thin section of border facies megacrystic granite 7-9. The dark coloured lamellae are composed of albite. Transmitted light, crossed nicols. (Bar scale represents 0.10mm).
4. Vein perthite texture in potash feldspar megacryst in thin section of border facies megacrystic granite 7-39. The irregular sided veins are composed of albite, and exhibit lamellar twinning. Transmitted light, crossed nicols. (Bar scale represents 0.05mm).
5. Patch perthite texture in potash feldspar megacryst in thin section of border facies megacrystic granite 4-55. The lamellar-twinned patches are composed of albite, are optically continuous, and are separated by diffuse patches of potash feldspar. (Bar scale represents 0.10mm).
6. String-like quartz (arrowed) along irregular plane separating two potash feldspar "twin" individuals in potash feldspar megacryst in thin section of border facies megacrystic granite 7-9. The individuals may in fact be separate crystals intergrown in syneusis relationship. Transmitted light, crossed nicols. (Bar scale represents 0.10mm).
7. Complex oscillatorily zoned plagioclase megacryst with fine-scale lamellar twinning (light coloured lamellae near top left part of photograph) in thin section of border facies megacrystic granite 3-33. Transmitted light, crossed nicols. (Bar scale represents 0.10mm).
8. Oscillatorily zoned plagioclase megacryst with band of lamellar twinning in thin section of border facies megacrystic granite 3-26. Transmitted light, crossed nicols. (Bar scale represents 0.10mm).

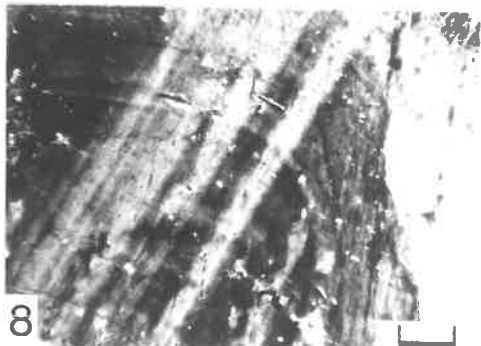
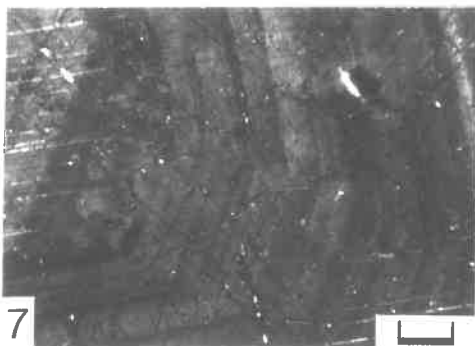
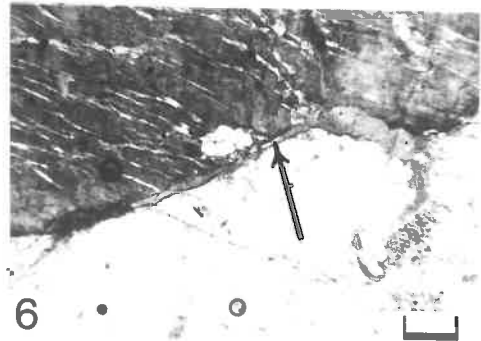
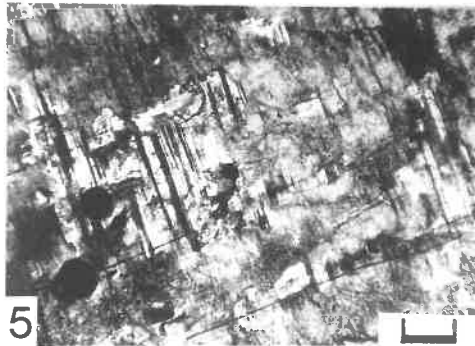
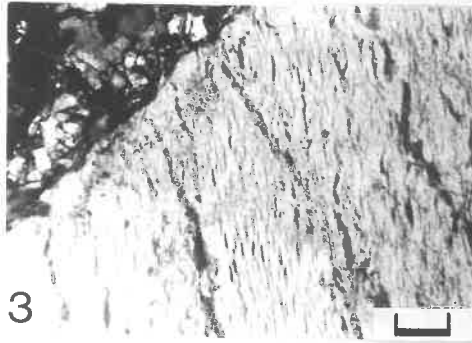
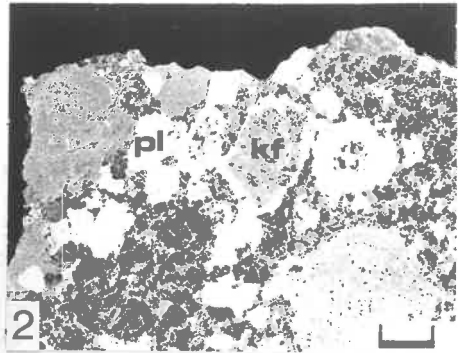


PLATE 46

1. Zone of bleb-like and vermicular quartz surrounding euhedral core in plagioclase megacryst in thin section of border facies megacrystic granite 4-61. This intergrowth closely resembles the granophyric zones surrounding euhedral cores in potash feldspar megacrysts in this granite (see Plate 44: 3 and 4). Transmitted light, crossed nicols. (Bar scale represents 0.10mm).
2. Ovoid megacryst (xenocryst?) of plagioclase consisting of core filled with bleb-like and vermicular quartz inclusions (dark grey to black) with a thin inclusion-free border zone. Slab of border facies megacrystic granite stained with sodium cobaltinitrite after etching with hydrofluoric acid. (Scale is in millimetres).
3. Lamellar-twinned plagioclase with clear albitic border (Ab - in extinction) against potash feldspar crystal (kf). Note irregular boundary of albitic border against potash feldspar. Thin section of border facies megacrystic granite 3-33. Transmitted light, crossed nicols. (Bar scale represents 0.05mm).
- 4 and 5. Potash feldspar (kf) filling interstitial spaces between euhedral quartz crystals in thin section of border facies megacrystic granite 4-61. Transmitted light, crossed nicols. (Bar scale in 4 represents 0.10mm; bar scale in 5 represents 0.05mm).
6. Zonal variation in opalescent blue colour in euhedral quartz megacryst in cut and polished surface of slab of border facies megacrystic granite 4-55. (Length of crystal 1cm).
7. Acicular and lath-like to anhedral ilmenite in cleavage in biotite crystal in polished section of border facies megacrystic granite 4-55. Incident plane polarised light, oil immersion. (Bar scale represents 0.04mm).
8. Lath-like ilmenite parallel to cleavage in biotite crystal (outline of crystal can just be discerned). Note euhedral zoned zircon inclusion. Polished section of border facies megacrystic granite 4-55. Incident plane polarised light, oil immersion. (Bar scale represents 0.04mm).

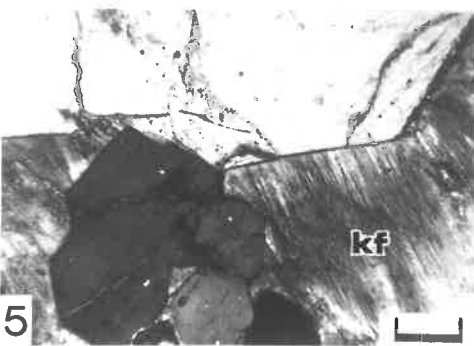
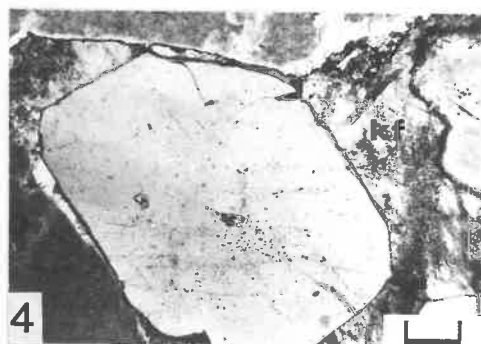
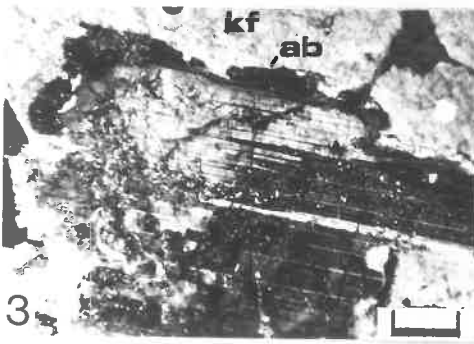
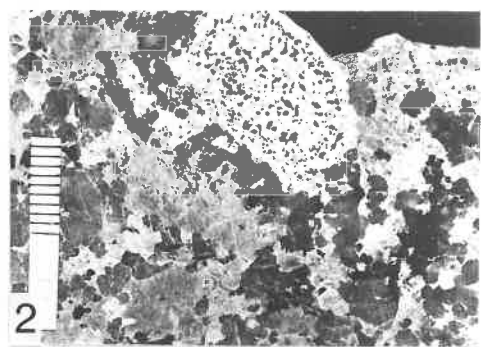
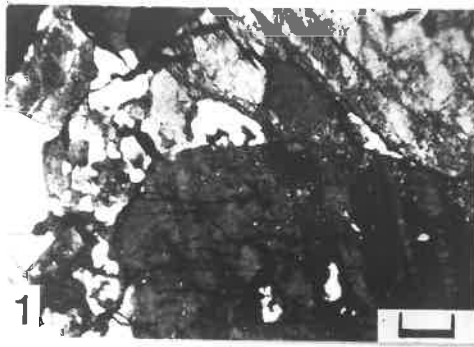


PLATE 47

1. Small pyrrhotite crystals (po) replaced by marcasite (ma) around their margins. Polished section of border facies megacrystic granite 4-55. Incident plane polarised light, oil immersion. (Bar scale represents 0.04mm).
2. Euhedral pyrite crystal (py) with small anhedral pyrrhotite crystal (po) partly replaced by marcasite (ma). Polished section of border facies megacrystic granite 4-55. Incident plane polarised light, oil immersion. (Bar scale represents 0.04mm).
3. Chess-albite (ca) pseudomorphing interstitial potash feldspar in thin section of albitised border facies megacrystic granite 7-55. Chess-albite is distinguished by a characteristic development of lamellar twinning resulting in a complex pattern of short alternating twin lamellae that do not pass through the entire crystal. Transmitted light, crossed nicols. (Bar scale represents 0.10mm).
4. Chess-albite (ca) pseudomorphing interstitial potash feldspar in thin section of albitised border facies megacrystic granite 7-55. Chess-albite texture is well displayed. Albitised plagioclase crystal has retained lamellar twinning. Transmitted light, crossed nicols. (Bar scale represents 0.05mm).
5. Albitised plagioclase crystal displaying well developed kink bands and spindle-shaped lamellar twins. Thin section of albitised border facies megacrystic granite 7-7. Transmitted light, crossed nicols. (Bar scale represents 0.10mm).
6. Aggregate of fine grained biotite/phlogopite crystals in thin section of albitised border facies megacrystic granite 7-55. The biotite crystals contain numbers of small rutile inclusions which can not be distinguished in this photograph. Transmitted plane polarised light. (Bar scale represents 0.10mm).
7. Phlogopite (with colourless muscovite lath) containing abundant small dark coloured rutile granules aligned in the phlogopite cleavage planes. Large zircon inclusion is also present. Thin section of albitised border facies megacrystic granite 7-1. (Bar scale represents 0.02mm).
8. Chlorite littered with fine rutile granules and rods. Thin section of albitised border facies megacrystic granite 7-17. Transmitted plane polarised light. (Bar scale represents 0.05mm).

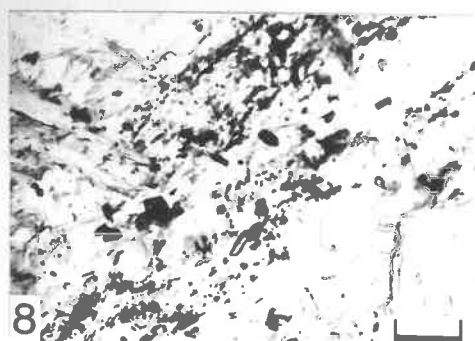
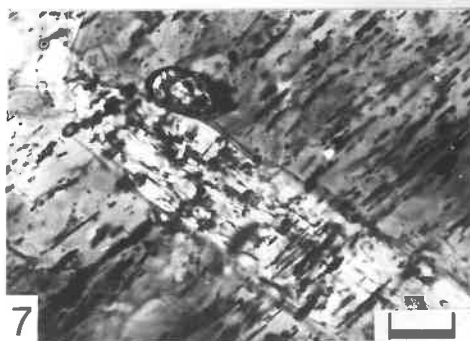
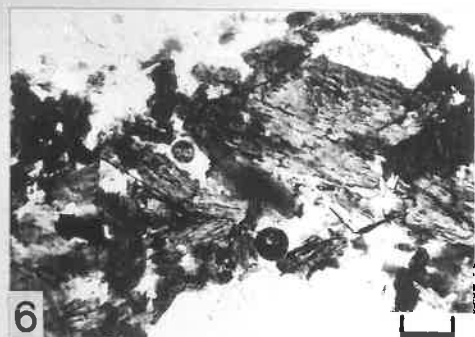
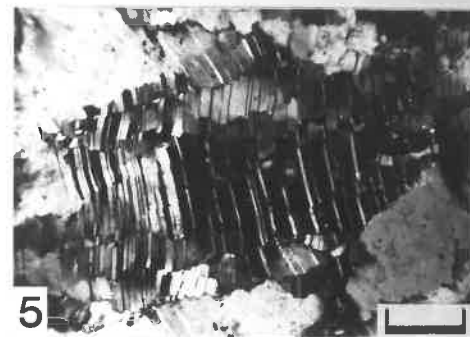
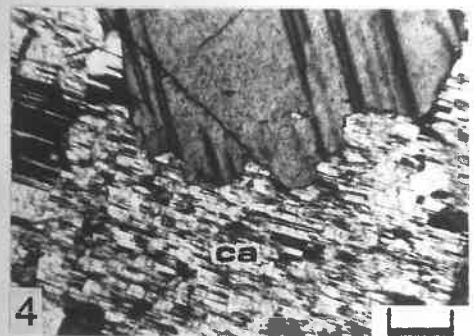
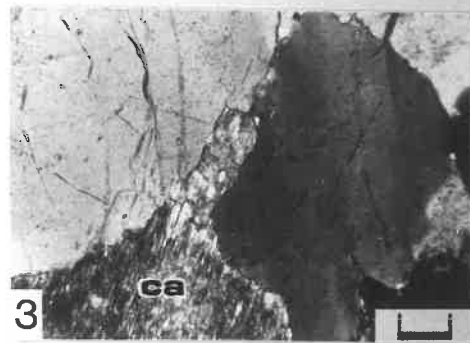
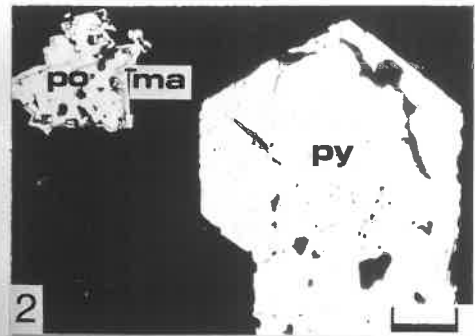
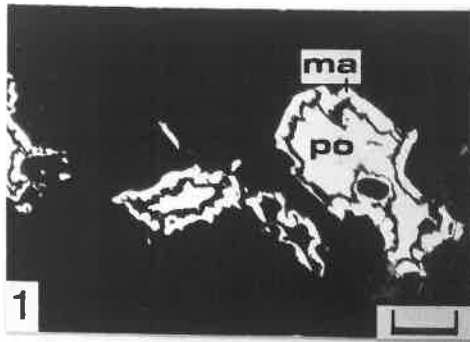


PLATE 48

1. Quartz grain partly replaced by chess-albite in thin section of megacrystic albite-chlorite rock 3-40. Note peculiar structure resulting from projection of albite twin lamellae (white) into unreplaced quartz. Transmitted light, crossed nicols. (Bar scale represents 0.05mm).
2. Coarse-scale patch perthite texture in potash feldspar. The patches are lamellar-twinned and are composed of albite. Thin section of medium even-grained granite 4-10. Transmitted plane polarised light, crossed nicols. (Bar scale represents 0.10mm).
3. Potash feldspar partly replaced by skeletal muscovite (white in centre of photograph, dark grey near bottom right corner). Thin section of medium even-grained granite 4-11. Transmitted plane polarised light, crossed nicols. (Bar scale represents 0.05mm).
4. Marked sub-grain development in quartz crystal in thin section of medium even-grained granite 4-15 due to post-crystallisation deformation. Transmitted plane polarised light, crossed nicols. (Bar scale represents 0.10mm).
5. Interfingering contact between lamellar-twinned plagioclase and cross-hatched microcline crystals interpreted as the result of corrosion of plagioclase by microcline. Thin section of medium even-grained granite 4-10. Transmitted light, crossed nicols. (Bar scale represents 0.05mm).
6. Biotite with zircon (z), muscovite (white lath) and ilmenite (black) inclusions in medium even-grained granite 4-10. Note ilmenite inclusions concentrated along the contact between the two biotite crystals, and also forming rim around zircon inclusion. Transmitted plane polarised light. (Bar scale represents 0.05mm).
7. Quartz (q), lamellar-twinned albite and chess-albite (ca) in thin section of albitised medium even-grained granite 4-13. Note corroded boundaries of quartz in contact with chess-albite, suggesting replacement of quartz by chess-albite. Transmitted light, crossed nicols. (Bar scale represents 0.10mm).
8. Lamellar-twinned albite, chess-albite (ca) and quartz (q) in thin section of albitised medium even-grained granite 4-13. Chess-albite occurs as an interstitial phase and appears to have replaced interstitial potash feldspar. Transmitted light, crossed nicols. (Bar scale represents 0.10mm).

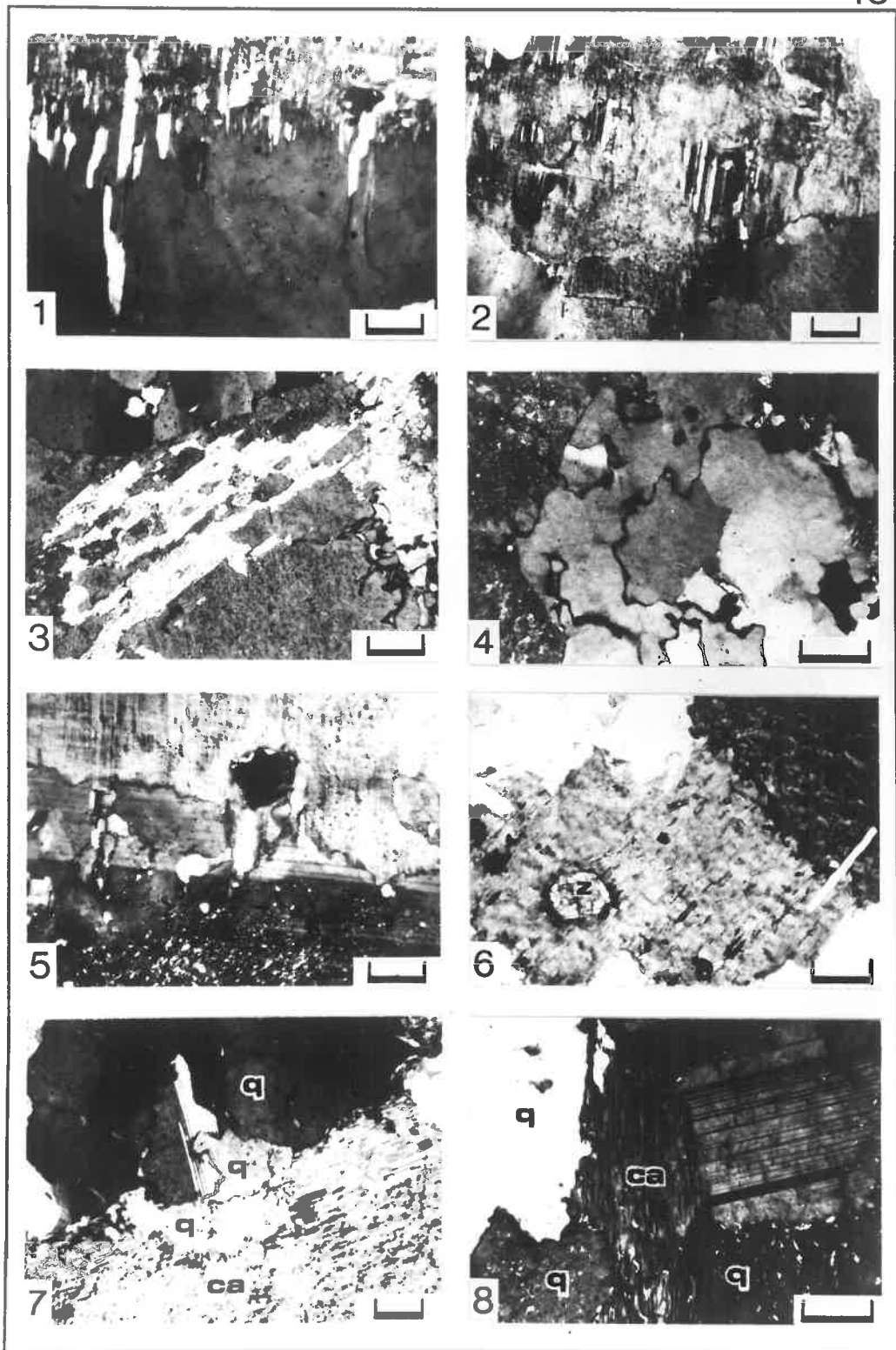


PLATE 49

1. Chess-albite (in extinction) replacing quartz (light coloured) in skeletal fashion in thin section of albitised medium even-grained granite 4-13. Transmitted light, crossed nicols. (Bar scale represents 0.10mm).
2. Granophyric intergrowth rimming quartz crystal (in extinction) in thin section of the red leucogranite W26C. Light coloured mineral at top right part of the photograph is potash feldspar. Transmitted light, crossed nicols. (Bar scale represents 0.10mm).
3. Granophyric intergrowth bordering euhedral potash feldspar megacryst in thin section of red leucogranite W26C. Transmitted light, crossed nicols. (Bar scale represents 0.10mm).
4. Granophyric intergrowth which nearly obscures host potash feldspar crystal. Thin section of red leucogranite W26C. Transmitted light, crossed nicols. (Bar scale represents 0.10mm).
5. Part of "granophyric" intergrowth between quartz (dull grey) and muscovite (bright grey) in thin section of miarolitic granophyre 4-66B. Muscovite has replaced potash feldspar in original granophyric intergrowth adjacent to miarolitic cavity. Black areas are holes due to removal of muscovite during preparation of the thin section. Transmitted light, crossed nicols. (Bar scale represents 0.10mm).
6. Anhedral quartz (q) replacing potash feldspar (kf) and lamellar-twinning plagioclase adjacent to miarolitic cavity in thin section of miarolitic granophyre 4-66B. Note also the presence of muscovite (m) replacing potash feldspar. Transmitted light, crossed nicols. (Bar scale represents 0.10mm).
7. Oscillatorily zoned plagioclase megacryst in thin section of type A hybrid granite 3-8. Note euhedral zone outlines and the large number of zones present. Transmitted light, crossed nicols. (Bar scale represents 0.10mm).
8. Plagioclase megacryst displaying sausseritised calcic core and albitic rim typical of normal zoning, as well as oscillatory zoning. Thin section of type A hybrid granite 3-8.

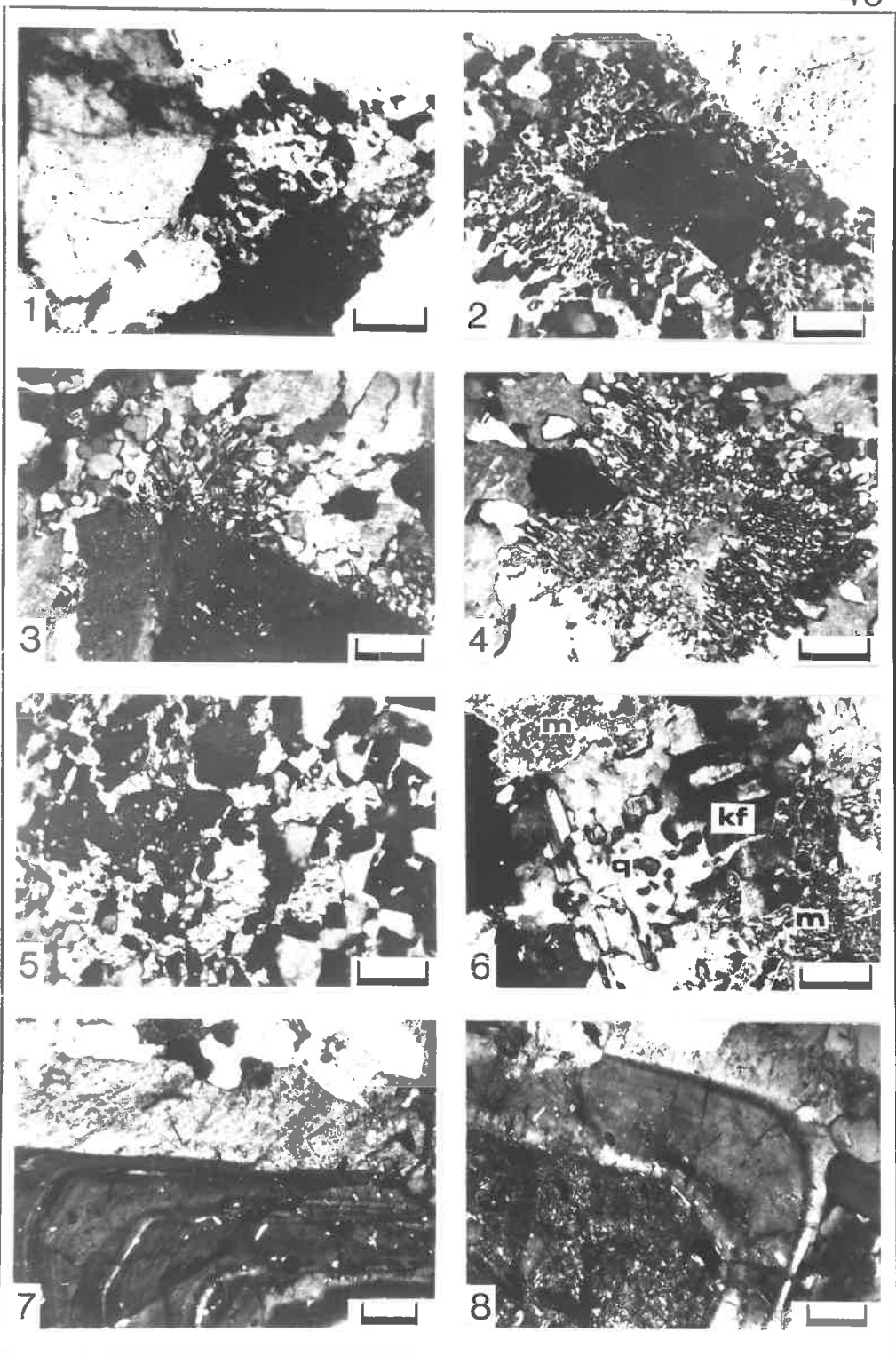
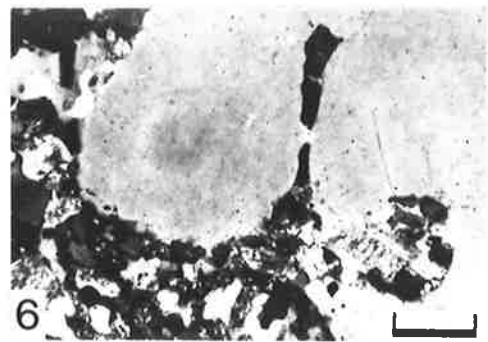
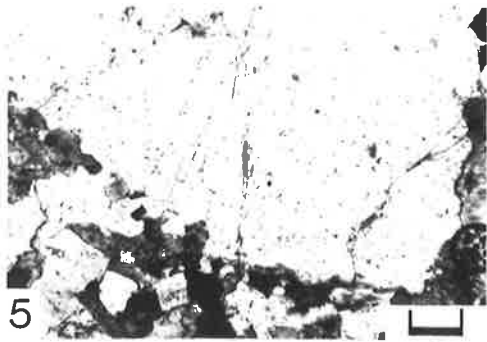
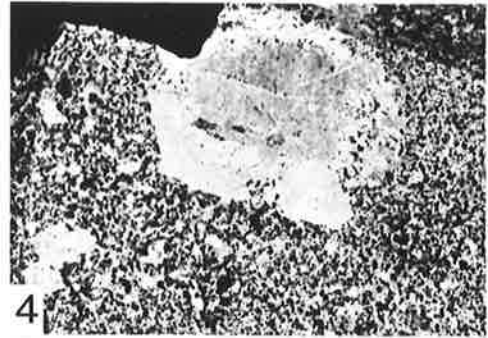
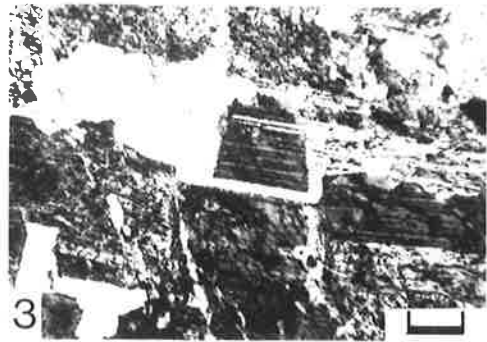
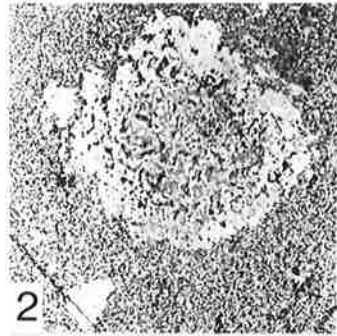
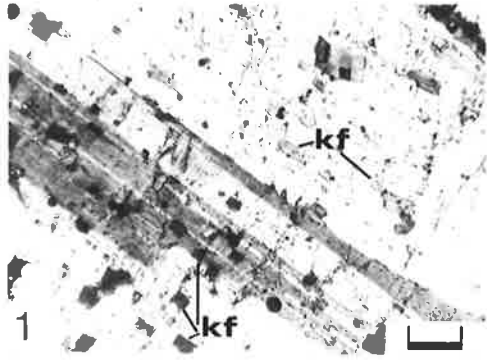


PLATE 50

1. Lamellar-twinning plagioclase megacryst with small rectangular inclusions of potash feldspar (kf). Thin section of type A hybrid granite 3-8. Transmitted light, crossed nicols. (Bar scale represents 0.10mm).
2. Poikilitic megacryst in type A hybrid granite 3-29. Megacryst is composed of a poikilitic potash feldspar core surrounded by plagioclase. The inner part of the plagioclase mantle is poikilitic whereas the outer part tends to be inclusion-free. Slab stained with sodium cobaltinitrite after etching with hydrofluoric acid. (Megacryst is about 2cm in diameter).
3. Part of patch-work texture characteristic of poikilitic megacrysts shown in 2. Lamellar-twinning plagioclase crystallite is rimmed by anhedral quartz (white). The potash feldspar components of the megacryst appears clouded with alteration products in this photograph. Thin section of type A hybrid granite 3-29. Transmitted light, crossed nicols. (Bar scale represents 0.10mm).
4. Megacryst composed of potash feldspar core comparatively free of inclusions, and plagioclase border zone. Abundant inclusions occur near the contact between the potash feldspar and the plagioclase. Note also embayments of the groundmass into the margins of the plagioclase border. Slab of type A hybrid granite 3-15 stained with sodium cobaltinitrite after etching with hydrofluoric acid. (Megacryst is about 1.5cm long).
5. Quartz megacryst in thin section of type A megacrystic granite 3-38. Note serrated borders of megacryst due to embayment by groundmass minerals. Transmitted light, crossed nicols. (Bar scale represents 0.10mm).
6. Margin of quartz megacryst embayed by groundmass minerals in thin section of type A hybrid granite 3-38. The minerals filling these embayments are generally dominated by potash feldspar, which commonly forms rims around the quartz megacrysts. Transmitted light, crossed nicols. (Bar scale represents 0.10mm).
7. Granophyric intergrowth within simple-twinning groundmass potash feldspar crystal in thin section of type B hybrid granite 3-27. The granophyric intergrowth partly outlines an euhedral core. Transmitted light, crossed nicols. (Bar scale represents 0.10mm).



Daily, B. and Milnes, A.R. (1971). Stratigraphic notes on Lower Cambrian fossiliferous metasediments between Campbell Creek and Tunkalilla Beach in the type section of the Kanmantoo Group, Fleurieu Peninsula, South Australia. *Transactions of the Royal Society of South Australia Inc.*, v.95(4), 199-214.

NOTE: This publication is included in the print copy of the thesis held in the University of Adelaide Library.

Milnes, A.R. and Bourman, R.P. (1972). A Late Palaeozoic glaciated granite surface at Port Elliot, South Australia. *Transactions of the Royal Society of South Australia Inc.*, v.96(3), 149-155.

NOTE: This publication is included in the print copy of the thesis held in the University of Adelaide Library.

Daily, B. and Milnes, A.R. (1972). Revision of the stratigraphic nomenclature of the Cambrian Kanmantoo Group, South Australia. *Journal of the Geological Society of Australia*, v.19(2), 197-202.

NOTE: This publication is included in the print copy of the thesis held in the University of Adelaide Library.

It is also available online to authorised users at:

<http://dx.doi.org/10.1080/14400957208527880>

PRECAMBRIAN BLOCKS AND ARCUATE TECTONIC TRENDS
IN SOUTH AUSTRALIA AND TASMANIA

B. Daily, J.B. Jago and A.R. Milnes

B. Daily Department of Geology and Mineralogy, University
of Adelaide.

J.B. Jago Department of Applied Geology; South Australian
Institute of Technology.

A.R. Milnes CSIRO Division of Soils, Glen Osmond, S.A.

Submitted to NATURE PHYSICAL SCIENCE
(Now in press)

NOTE

Published article is titled:
'Large-scale horizontal displacement within
Australo-Antarctica in the Ordovician'.

PRECAMBRIAN BLOCKS AND ARCuate TECTONIC TRENDS IN
SOUTH AUSTRALIA AND TASMANIA

Recently, Crawford and Campbell¹ (p.11) postulated that the southern continental margin of Australia between longitude 131°E and 143°E 'is the relic of a major shear which in Early Ordovician time extended still farther across what is now Tasmania, and that dextral movement of at least 300 km occurred'. We believe that this hypothesis is without foundation and that the curvature of the southern portion of the Adelaide Orogen and the curvilinear pattern of the Mount Road Volcanics in Tasmania, which were cited to support their arguments, can be explained without invoking¹ (p.12) 'fault-drag on an immense scale' on opposite sides of the postulated shear (see line ABC in Fig. 1).

The Precambrian crystalline Gawler Block is the largest and most stable tectonic element in South Australia. Its eastern margin is delimited by the Terrens Lineament, a fracture zone or hinge line which controlled sedimentation throughout much of the long depositional history of the Adelaide "Geosyncline"². The lineament separates the thin platform cover of flat to gently deformed Late Precambrian and/or Cambrian sediments on the ^{ea}western side of the block from the thicker and more highly deformed rocks of the same ages within the Adelaide Orogen to the east of the lineament. However, records from bores to the east and north of the exposed orogen indicate that both weakly and strongly folded rocks of the same ages occur beneath the Late Palaeozoic, Mesozoic and Cainozoic deposits of the western part of the Great Artesian Basin and Murray Basin. Indeed, evidence indicates that the Adelaide 'Geosyncline' and the Amadeus Basin in the Northern Territory were linked below the cover of the western Great Artesian Basin and that they formed part of a single basin of deposition during the Late

Precambrian^{3,4} and Early Cambrian^{5,6,7}. Under the western part of the Murray Basin metasediments of the same general ages occur. Along the Padthaway Ridge they are intruded by Early Ordovician granites⁸.

It has been argued¹ that the sigmoidal nature of the Mt. Lofty-Olary arc⁹, which stretches between Kangaroo Island and the Willyama Block, was formed by fault-drag along postulated mega-shears during the Early Ordovician. This thesis can be refuted on several grounds.

Within the orogen the basement and its cover were folded sympathetically, for it has been demonstrated⁹⁻¹⁵ that the basement inliers are the eroded axial culminations of anticlinal structures. At the southern end of the Mt. Lofty-Olary arc folds within the cover adjacent to the inliers tend to be overturned towards the Gawler Block, but in stratigraphically younger strata more remote from the basement the folds are more open and upright. Thrusting, frequently associated with the overturned limbs, is also directed towards the block. On the inner margin of the arc the north-south Torrens Lineament or hinge zone (Fig. 2) makes a broad sweep to the west¹⁴ instead of continuing south to meet the Cygnet Fault as is shown on the recent tectonic map of Australia¹⁵. There this deflected fault zone forms the southern margin of the Gawler Block, which in places, for example on the heel of Yorke Peninsula, is covered by virtually flat-lying fossiliferous basal Cambrian sandstones and dolomites overlain unconformably by Middle Cambrian limestones and clastics¹⁶. Although Late Precambrian sediments are unknown on this part of the block, they occur¹⁷ below the metasediments of the Early Cambrian¹⁸ Normanville Group¹⁵ and the overlying and very thick Karamntoo Group (Cambrian) which outcrop on Kangaroo Island south of the Cygnet Fault thus proving the continuation of the Precambrian sediments beyond the postulated limits as formerly believed. North of the Cygnet Fault less

metamorphosed and fossiliferous Lower Cambrian clastics are folded against the Gawler Block.

Geophysical evidence¹⁹ suggests that the east-west trending belt of Kanmantoo Group and Precambrian rocks on Kangaroo Island swings to the north-west beneath the floor of the offshore Dumetron Basin which follows the southern margin of the Gawler Block. This basin probably connects with the Polda Trough. Gently dipping sandstones and conglomerates of unknown age occur on Mt. Wedge on the eastern margin of the trough and are lithologically similar to Cambrian rocks on the north coast of Kangaroo Island and Yorke Peninsula and may be Cambrian in age. In the Mallabie Depression to the north-west, sediments that have been provisionally equated with the Observatory Hill Beds²⁰ in the little known Officer Basin, have been encountered in Mallabie No. 1 Bore. Although fossils are unknown in Observatory Hill Beds in their type section north-west of the Gawler Block, this sequence has been tentatively correlated with the Lake Frome Group of Middle Cambrian to ?Early Ordovician age²¹. However, it is suggested that the Observatory Hill Beds and a similar sequence at Mt. Johns²² in the north-east extremity of the Officer Basin may be the equivalent of the Lower Cambrian Billy Creek Formation of the Flinders Ranges. Whichever opinion is accepted, it seems likely that Cambrian clastics were deposited in a more or less continuous belt around the Gawler Block. It is well to note also that during the Late Precambrian, there was an interconnection between the Officer Basin and the Adelaide 'Geosyncline' at least around the northern part of the Gawler Block. This is indicated by similar stratigraphic sequences and the identification²³ of the Late Precambrian Ediacara Fauna in both basins.

Thus we would argue that the arcuate belt of mainly Kanmantoo Group meta-sediments which outlines the southern-most segment of the Mt. Lofty-Olary arc

is but a small portion of the probable Cambrian sediments circumscribing the Gawler Block. Moreover this southern segment of the arc owes its shape to compression against the virtually unyielding Gawler Block whose margin, bounded by the Torrens Lineament, is curved in the same sense.

In order to explain the curvature of the orogen in the Olary region Crawford and Campbell¹ (p.13) postulated that the Willyama Block 'was torn off the Mt. Painter Block and rotated' clockwise, the movement inducing the widespread diapirism^{24,25} in the Flinders Ranges and creating the Frome Embayment. Crawford and Campbell¹ (p.13) further argued that if their hypothesis was correct 'Cambrian rocks would be absent, stretched or fragmented' within the Frome Embayment. However, this hypothesis is untenable because bore information combined with seismic data²⁶ and unpublished palaeontological studies by one of us (B.D.) have revealed that a virtually undeformed fossiliferous Lower and Middle Cambrian platform sequence is extensively developed within the embayment. The cover indicates that a relatively stable block underlies the Frome Embayment and that the Mt. Painter and Willyama Blocks are basement fragments peripheral to this relatively stable block and were involved in the Early Palaeozoic orogeny referred to in the southern part of the orogen as the Delamerian Orogeny²⁷. The earlier views that the Mt. Painter and Willyama Blocks are axial culminations within the fold belt and were themselves folded during this time are upheld.

In Tasmania there is no evidence for a mega-shear trending north-west to south-east across north-eastern Tasmania as postulated by Crawford and Campbell¹. Such a shear is essential to their hypothesis which argues for a clockwise drag on a formerly trending north-south Dundas Trough. However, as is indicated by Corbett et al.²⁸ (p.10), 'there may have been an almost continuous Cambrian belt around the Tyennan nucleus'. Thus the supposed¹ (p.12) 'turn eastward across the

north-central part of the island' is seen to be only the northern segment of a probably once almost continuous belt of Cambrian sediments and volcanics which extended around the Tyennan Geanticline (Fig. 3). Corbett²⁹ has reported the occurrence of fossiliferous Upper Cambrian in the Denison Range area on the south-east side of the geanticline.

As seen in Fig. 3, probable Cambrian sediments occur near O'Connors Peak³⁰ on a south-easterly trend continuous with the Cambrian of the Deloraine area³¹. This trend swings south-eastwards out from the postulated margin of the geanticline. Finally, we note that in Tasmania fossiliferous Cambrian sediments and volcanics³⁰ occupy north-south trends in far north-western Tasmania and also in the central part of the north coast in the Port Sorell area³². Neither area appears to be affected by drag.

Thus we conclude that there is no evidence to support the hypothesis advanced by Crawford and Campbell of large scale horizontal displacement across the southern part of the Australian continent. Rather, we would envisage that during the Late Precambrian and Cambrian within the region shown in Fig. 1 there was a mosaic of crystalline blocks the number and distribution of which, particularly in the east, is still conjectural. Within the western part of the region basins of varying subsidence lay between the blocks, and sediments, some of which were derived from the erosion of the exposed parts of blocks, were laid down. Transgressions onto blocks gave rise to platform sediments with facies often of the same general aspect as the generally thicker basinal deposits. Frequent unconformities, particularly within the platform cover, point to regressive phases, both local and regional, which can generally be related to minor tectonic episodes.

Strong folding of the Adelaide 'Geosynclinal' sediments was effected adjacent

to the Musgrave Block with the onset of the Petermann Range Orogeny³³ just before the end of the Precambrian. The main phase of this orogeny is post-Ediacaran and prior to the initial Cambrian transgression, the latter synchronous in both the Amadeus Basin and the Adelaide 'Geosyncline'.¹⁶ The age of the orogeny has recently been set at about 580 million years³⁴. If correct, it will have important implications for the dating of the base of the Cambrian. Elsewhere within the orogen tectonism leading to final cratonisation is believed to be Late Cambrian to Ordovician in age, the folding being directed against the surrounding more stable blocks resulting in the arcuate fold trends seen today.

In Tasmania the Cambrian was folded by the ^{Julesian} Tyennan Movement, believed to be latest Cambrian in age. Its effects are most obvious adjacent to the Tyennan Geanticline³⁰ around which conglomerates were deposited in latest Cambrian and early Ordovician times.

Department of Geology and Mineralogy
University of Adelaide
Adelaide
South Australia 5001

B. DAILY

Department of Applied Geology
South Australian Institute of Technology
Adelaide
South Australia 5000

J.B. JAGO

C.S.I.R.O. Division of Soils
Glen Osmond
South Australia 5064

A.R. MILNES

REFERENCES

1. Crawford, A.R., and Campbell, K.S.W., Nature Physical Science, 241, 11(1973).
2. Sprigg, R.C., in Sir Douglas Mawson Anniv. Vol., 153 (Univ. Adelaide, 1953).
3. Noakes, L.C., in Rept. 20th Internat. Geol. Cong., Mexico 1956. El sistema Cambrico su Paleogeografía Y el Problema de su Base 2, 213(1956).
4. Mawson, D., Aust. J. Sci., 19, 152(1957).
5. Madigan, C.T., Trans. R. Soc. S. Aust., 56, 71(1932)
6. Opik, A.A., Rept. 20th Internat. Geol. Cong., Mexico 1956. El sistema Cambrico su Paleogeografía Y el Problema de su Base 2, 239(1956)
7. Daily, B., Rept. 20th Internat. Geol. Cong., Mexico 1956. El sistema Cambrico su Paleogeografía Y el Problema de su Base 2, 91(1956).
8. Thomson, B.P., Trans. R. Soc. S. Aust., 94, 193(1970).
9. Campana, B., J. geol. Soc. Aust., 2, 47(1955).
10. Campana, B., and King, D., S. Aust. geol. Surv. Bull. 34, 133(1955).
11. Glaessner, M.F., and Parkin, L.W., J. geol. Soc. Aust., 5(2), 163(1956).
12. Talbot, J.L., Geol. Assoc. Canada Spec. Pap. 5, 59(1969).
13. Daily, B., and Milnes, A.R., Trans. R. Soc. S. Aust. 97 (in press).
14. Stuart, W.J., and von Sanden, A.T., J. Aust. Petroleum Explor. Ass. 12(2), 9(1972).
15. Geological Society of Australia, Tectonic Map of Australia and New Guinea 1:5,000,000 (1971)
16. Daily, B., Centre for Precambrian Research, Univ. Adelaide, Spec. Pap. 1, 13(1972).
17. Daily, B., and Milnes, A.R., Search, 2, 431(1971).
18. Daily, B., and Milnes, A.R., Search, 3, 89(1972).
19. Smith, R., and Kamerling, P., J. Aust. Petroleum Explor. Ass., 9(2), 60(1969).
20. Wopfner, H., Trans. R. Soc. S. Aust., 93, 169(1969).
21. Daily, B., and Forbes, B.G., Aust. N.Z. Assoc. Adv. Sci., Geol. Excursions Handbook, Section 3, 23(Adelaide, 1969).

22. Kreig, G., J. Aust. Petroleum Explor. Ass., 9(2), 8(1969).
23. Daily, B., Trans. R. Soc. S. Aust., 90, 199(1966).
24. Coats, R.P., Rep. Invest. Geol. Surv. S. Aust., 26, (1964).
25. Dalgarno, C.R., and Johnson, J.H., Am. Assoc. Petroleum Geologists Mem., 8, 301(1968).
26. Wopfner, H., Am. Assoc. Petroleum Geologists Bull., 54, 2595(1970).
27. Thomson, B.P., Handbook of South Australian Geology, 263(Geol. Surv. S. Aust., 1969).
28. Corbett, K.D., Banks, M.R., and Jago, J.B., Nature Physical Science, 240, 9(1972).
29. Corbett, K.D., Sedimentology, 19, 99(1972).
30. Banks, M.R., J. geol. Soc. Aust., 9, 127(1962).
31. Department of Mines, Tasmania, Geol. Atlas, 1-mile series, Quamby Sheet (1969).
32. Department of Mines, Tasmania, Geol. Atlas, 1-mile series, Beaconsfield Sheet (1971).
33. Wells, A.T., Forman, D.J., Ranford, L.C., and Cook, F.J., Bull. Miner. Resour. Aust. Bull., 100, 222(1970).
34. Thomson, B.P., Ann. Rept. (1971-72) Director Mines, Dept. Mines, S. Aust., 64(1972).

Figures have not been reproduced.

8 6.77

STRATIGRAPHY, STRUCTURE AND METAMORPHISM OF THE KANMANTOO
GROUP (CAMBRIAN) IN ITS TYPE SECTION EAST OF TUNKALILLA
BEACH, SOUTH AUSTRALIA

by

B. Daily and A.R. Milnes

B. Daily. Department of Geology and Mineralogy, University of
Adelaide.

A.R. Milnes. CSIRO Division of Soils, Glen Osmond, South Australia.

SUBMITTED TO TRANSACTIONS OF THE ROYAL SOCIETY OF SOUTH AUSTRALIA

(Now in press)

Daily, B. and Milnes, A.R. (1973). Stratigraphy, structure and metamorphism of the Kanmantoo Group (Cambrian) in its type section east of Tunkalilla Beach, South Australia. *Transactions of the Royal Society of South Australia Inc.*, v.97(3), 213-242.

NOTE: This publication is included in the print copy of the thesis held in the University of Adelaide Library.

Figures have not been reproduced because of their bulk.

Daily, B. and Milnes, A.R. (1972). Significance of Basal Cambrian metasediments of Andalusite Grade, Dudley Peninsula, Kangaroo Island, South Australia. *Search*, v.3(3), 89-90.

NOTE: This publication is included in the print copy of the thesis held in the University of Adelaide Library.

Daily, B. and Milnes, A.R. (1971). Discovery of Late Precambrian Tillites (Sturt Group) and Younger Metasediments (Marino Group) on Dudley Peninsula, Kangaroo Island, South Australia. *Search*, v.2(11/12), 431-433..

NOTE: This publication is included in the print copy of the thesis held in the University of Adelaide Library.